# Investigation of α-aryl substituted 3-indolylethanones as potential antiplasmodial agents

A thesis submitted in fulfilment of the

requirements for the degree of

**Master of Science (Pharmacy)**

Of

Rhodes University

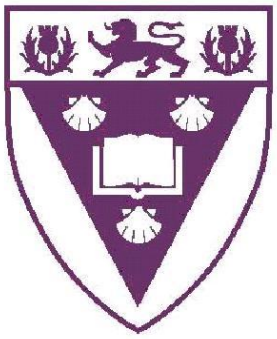

by

Archibald Lesley Svogie

December 2015

**Abstract**

According to the World Health Organisation (WHO), deaths attributed to *Plasmodium falciparum* exceeded 584 000 in 2013, with 198 million new cases of malaria being reported. One contributing factor to these alarming figures is the emergence of drug resistance against available antimalarial agents. Therefore, there is a pressing need to develop new therapeutic antimalarial drugs with novel mechanisms of action in order to curb the increasing spread of malaria. The indole scaffold is often associated with biologically active compounds, recently exemplified by the antimalarial agent NITD609, which is currently in phase 1 clinical trials. Based on the biological evaluation of a small series of indolyl-3-amides and esters which showed moderate antimalarial activity, coupled to significant toxicity, we were prompted to investigate the synthesis of a series of indolyl-3-ethanone-α-amines (**3.37** and **3.41**), ethers (**3.39** and **3.44**) and thioethers (**3.42**, **3.43**, **3.40**, **3.45** – **3.73**), where the carbonyl moiety and respective heteroatom were separated by a methine spacer. We further investigated these compounds for *in vitro* biological activity against *P. falciparum* and a human HeLa cell line. Our study explored the synthetic pathway of a three-step procedure toward our target compounds, with the initial Friedel-Crafts acetylation of indole, followed by α-bromination of the respective 3-acetylindoles. Finally, the halogen of the α-bromo ketone was substituted with an appropriate nucleophile, to yield our desired compounds. Various reagents were explored to optimise the nucleophilic displacement step, including potassium carbonate and various silver containing compounds. While many of the silver salts were found to assist in nucleophilic substitution, none were superior to the addition of potassium carbonate.

The majority of compounds, chiefly the thioethers, displayed promising antimalarial activity, against the chloroquine sensitive 3D7 *P. falciparum* strain, with two thioethers in particular (**3.54** and **3.65**) inhibiting *P. falciparum* in the low nanomolar range. Additionally, active compounds were generally found to be non-toxic against HeLa cells, indicating that indolyl-3-thioethers are selective for the malaria parasite. These findings allowed us to begin hypothesising a structure activity relationship of this class, as well as elucidating the possible pharmacophore.

In a speculative attempt to uncover the possible mechanism of action of these active compounds, *in silico* docking studies were conducted against *Staphylococcus aureus* HPPK (PDB ID: 4CRJ), which is an enzyme that immediately precedes DHPS in the microbial folate biosynthesis. Inhibition of folate biosynthesis is a validated selective antimalarial pathway and HPPK also exists in *P. falciparum*. Results from these docking studies suggested that our inhibitors bound well in the HPPK ATP pocket and were supportive of our hypothesized structure activity relationship.

**Table of Contents**

**List of Figures**

**List of schemes**

Page

**List of tables**

Page

**List of abbreviations**

| | |
|---|---|
| Å | Angstrom |
| AcOH | Acetic acid |
| $Ac_2O$ | Acetic anhydride |
| AIDS | Acquired immunodeficiency syndrome |
| aq. | Aqueous |
| ATP | Adenosine triphosphate |
| $^{13}C$ NMR | Carbon-13 Nuclear Magnetic Resonance |
| °C | Degrees Celsius |
| DCM | Dichloromethane |
| Calcd | Calculated |
| conc. | Concentrated |
| CQ | Chloroquine |
| δ | Chemical Shift |
| d | Doublet |
| dd | Doublet of doublets |
| DDT | Dichloro-diphenyl-trichloroethane |
| DHPS | Dihydropteroate synthase |
| DMF | *N,N*-dimethyl formamide |

| | |
|---|---|
| DMSO | Dimethyl sulfoxide |
| EtOAc | Ethyl acetate |
| EtOH | Ethanol |
| g | Gram |
| h | Hour |
| HMBC | Heteronuclear Multiple Bond Correlation |
| HRESMS | High resolution electrospray mass spectrometry |
| HSQC | Heteronuclear Single Quantum Correlation |
| HTS | High throughput screening |
| $IC_{50}$ | 50% Inhibitory Concentration |
| IR | Infra-red spectroscopy |
| *J* | Spin-Spin Coupling Constant |
| K | Kelvin |
| lit | Literature |
| m | Multiplet |
| Me | Methyl |
| $MeNO_2$ | Nitromethane |
| MeOH | Methanol |
| mg | Milligram |

| | |
|---|---|
| MHz | Megahertz |
| MIC | Minimum inhibitory concentration |
| min | Minute |
| ml | Millilitre |
| mmol | Millimolar |
| mol | Moles |
| mp | Melting point |
| MRSA | Methicillin-resistant *Staphylococcus aureus* |
| nM | Nanomolar |
| NMR | Nuclear Magnetic Resonance |
| Ph | Phenyl |
| PK | Pyruvate kinase |
| ppm | Parts per million |
| r.t. | Room temperature |
| s | Singlet |
| SAR | Structure activity relationship |
| sat | Saturated |
| t | Triplet |
| TB | Tuberculosis |

| | |
|---|---|
| *tert* | Tertiary |
| TLC | Thin layer chromatography |
| µg | Microgram |
| µL | Microlitre |
| µM | Micromolar |
| WHO | World Health Organization |

“Put your heart, mind, and soul into even your smallest acts. This is the secret of success.”

-Swami Sivananda-

Dedicated to my brothers, Adrian and Anvet Svogie.

**Acknowledgements**

First and foremost I would like to thank the Lord Almighty for blessing me with the good health and well-being which was necessary to complete this work.

I would like to thank my two supervisors Dr C. G. L Veale and Dr S. D Khanye for the proper guidance, advice, patience and constant encouragement throughout this project. Their supervision and unique set of skills benefited me a lot during the time of research, preparation for conferences and writing of this thesis.

I would also want to extend my gratitude to the following people who contributed to the success of my work: Professor Heinrich Hoppe and Michelle Isaacs for assisting with biological activity assays and Sally and Dave Morley for technical support.

I'm also grateful to Professor R. Walker, Dr C. Oltmann and the rest of the Faculty of Pharmacy staff members for the support they provided me during the downfall moments of my research life.

I also thank my fellow lab mates Dr Maynard Chiwakata, Dr Jameel Fakee, Emanuel Olawade, Tafadzwa Mutsvairo, Mohammed Adams, Chiko Chakaingesu, Theoneste Umumararungu, Ayanda Zulu, Oliver Darrell and Faith Magwenzi for team support and happy moments that we shared together in the laboratory.

Special thanks goes to these special awesome people; Benhilda Jaji, Ranga Simon Chamwadoro, Sandile Dube, Pritchard Ndebele and Faith Nhunge. Your love, support and motivation is greatly cherished.

Last but not the least, I would like to thank my parents (**Bessie** and **Ezekiel Svogie**) and to my brothers (**Adrian** and **Anvet Svogie**) for the unconditional love, care, encouragement and belief in me. May the Lord Jesus Christ continue blessing you.

# Chapter One

## Introduction and literature review

### 1.1 General overview: Malaria

Malaria is a deadly parasitic disease which claims scores of human lives globally.[1–3] According to the World Health Organisation (WHO), deaths attributed to *P. falciparum* exceeded 584 000 in 2013, with 198 million cases of malaria being reported. It is estimated that *P. falciparum* kills one child every 30 seconds in Africa.[4] Malaria is caused by protozoa of the *Plasmodium* genus, with five species responsible for the disease in humans, namely *P. falciparum*, *P. vivax*, *P. malariae* and *P. ovale* and *P. knowlesi*.[1,5] Of the four species, *P. falciparum* and *P. vivax* are the major cause of most human malarial infections and they are responsible for the majority of deaths in Africa and South East Asia.[6,7] Malaria is transmitted to humans when an infected female *Anopheles* mosquito feeds on a human subject.[1] This process is colloquially referred to as 'biting'.

The development of malaria is linked with numerous factors such as delayed diagnosis, pregnancy and infections including human immunodeficiency virus (HIV), acquired immunodeficiency syndrome (AIDS) and tuberculosis (TB).[8,9] Since both malaria and TB are endemic tropical infectious diseases, the co-infection with these two pathogens is common.[9] The high malaria burden especially in Africa, is a major cause for concern compounded by resistance to commercially available antimalarials.[8,10,11] Non-compliance to the prescribed antimalarial regimen and supply of counterfeit antimalarial drugs are amongst the leading causes of antimalarial drug resistance.[10,12]

**1.2 The life cycle of the parasite**

The malaria parasite has a complex life cycle that involves both a human host for asexual reproduction and a vector host for sexual reproduction. The life cycle of the malaria parasite shown in **Figure 1.1** begins with the pre-erythrocytic sporozoite inoculation stage, where the infected female mosquito injects sporozoites into the skin of the human host during feeding on blood. The infecting sporozoites then cross the endothelium of the capillaries in the skin and enter into the blood circulation.

Through the circulation system, sporozoites reach the liver and mature into schizonts after incubating for about 10 days. Within the liver hepatocytes, the schizonts increase in number 40 000 fold and differentiate into merozoites.[13] At this stage, malaria is symptomless resulting in infected individuals being unaware that they are infected. The rupture of hepatocyte derived vesicles referred to as merosomes results in the release of the merozoites into the bloodstream and marks the beginning of the symptomatic asexual blood stage of the malarial life cycle. Over a series of 48 hour cycles, merozoites multiply within the erythrocytes and result in their destruction, which may manifest as clinical presentations. The clinical symptoms may include headache, fever and lethargy. The life cycle of the malaria parasites in the human hosts is completed when the asexual blood-stage parasites differentiate into male and female gametocyctes that are taken up in a mosquito's blood meal. The last stage of the sexual cycle occurs in the mosquito midgut where fertilisation of male and female gametes occurs to form the ookinetes that cross the midgut epithelium and differentiate into sporozoites. The sporozoites then invade the salivary glands of the mosquito and this completes the malaria parasite's life cycle in the mosquito host [1,8,13,14]

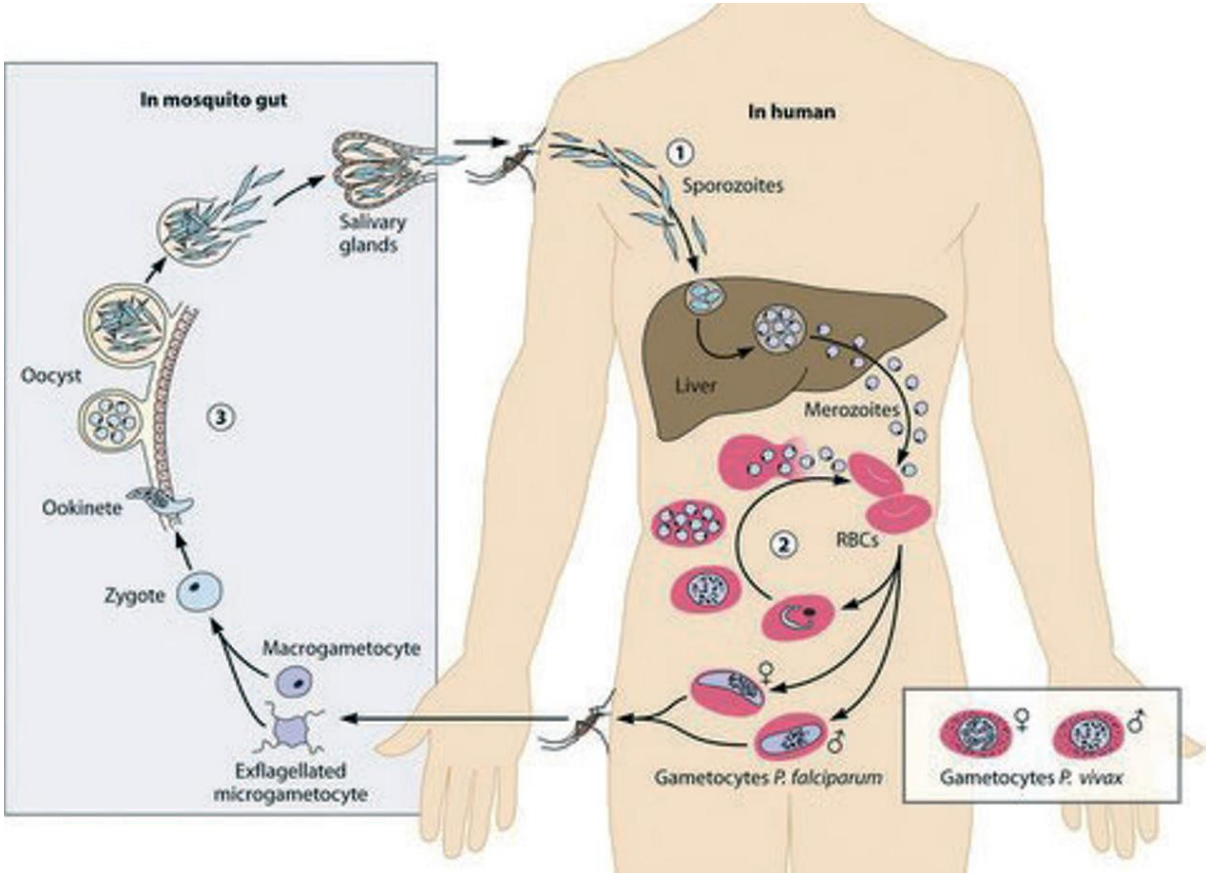


**Figure 1.1** Malaria parasite life cycle stages. Image reproduced with permission from the authors[14]

## 1.3 Malaria diagnosis

Early diagnosis forms the basis of an early malaria treatment plan which could manage the spread of malaria infection.[5,11] Diagnostic blood tests are more reliable and accurate than both the clinical features and physical signs in the diagnosis of malaria.[11] Microscopic examination of blood films is a definitive diagnostic test for the *Plasmodium* species.[5] The major limitation is the management and maintenance of the quality microscopes which may also not be accessible in some regions of Africa.[1]

Alternative methods includes the antigen-capture tests, rapid tests, polymerase chain reaction analysis and the quantitative buffy coats.[1,5] Their limitations include cost and

nonspecific factors such as a false-positive results that could be obtained in a healthy person with parasitaemia due to living in a highly malaria-endemic area.[1,5]

### 1.4 Vector control of malaria

Prophylaxis at the pre-infection stage is considered one of a number of various approaches to the control and management of malaria. This strategy involves 'bite' prevention, primarily through the use of mosquito nets[11] and vector control from Insecticide-treated mosquito nets (ITNs) and indoor residual house-spraying using the insecticide dichloro-diphenyl-trichloroethane (DDT).[1] Studies have been conducted which demonstrate the success of malaria prevention using the vector control approach.[1,4] However, limitations of this approach includes the limited number of available insecticides and rising cases of insecticide resistance.[15]

### 1.5 Vaccine control of malaria

Despite the recent approval of the RTS,S/AS01 vaccine for children by the WHO in 2015, there is still no available preventative vaccine for adults.[16] Currently, studies are on-going to produce vaccines that will provide immunity against malaria by avoiding the asexual blood stage through inhibiting the transformation of the sporozoites into merozoites.[17] In addition to the non-availability of vaccines for adults[16], progress on vaccines is also being hindered by financial constraints and the challenges of finding the optimum parasite antigen from which to make the vaccines.[14]

### 1.6 Rationale for finding new antimalarial drugs

The small collection of antimalarial drugs which were once used to effectively treat malaria have been significantly compromised by the spread of drug-resistant parasites.[4] These include the traditional drugs such as chloroquine (**1.1**), pamaquine (**1.2**), mefloquine (**1.3**) and artemisinin (**1.4**).[18]

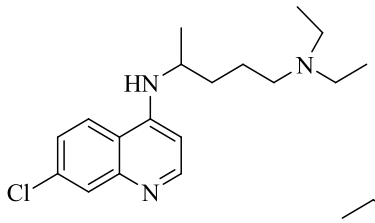


**1.1 Chloroquine**

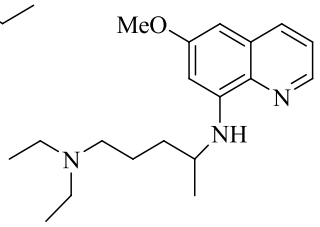


**1.2 Pamaquine**

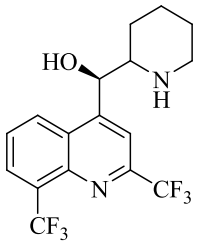


**1.3 Mefloquine**

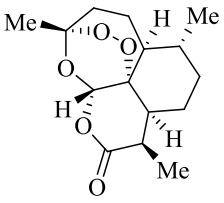


**1.4 Artemisin**

The widespread resistance of the *Plasmodium* parasites to the known antimalarial agents has posed a major threat in the treatment of malaria.[19–21] In resource poor settings, the utility of antimalarial drugs is limited by factors which include high costs, poor adherence/ compliance, low efficacy and poor safety as well as toxicity and undesirable side effects.[22,23] In addition to the resistance of the malaria parasites to the previously widely used drugs such as CQ (**1.1**) and the resistance of mosquitoes to the pesticides also poses as a major challenge.[22] Temporary solutions to overcome the emerging drug resistance have been attempted through the use of various drug combinations with independent modes of action.[22] Therefore, there is an urgent need for researchers to develop novel and potent antiplasmodial agents which are also affordable to control and eventually eradicate malaria.[24]

# Chapter Two

## The indole scaffold and its derivatives in drug discovery

### 2.1. Indoles: General overview in drug discovery

Indoles represent some of nature's most privileged heterocyclic compounds.[25] They are found in a wide range of pharmaceutical products including indomethacin (**2.1**), vinblastine (**2.2a**), vincristine (**2.2b**), pindolol (**2.3**), sumatriptan (**2.4**) and the naturally occurring hallucinogen dimethyltryptamine.[26,27] Tryptamine, serotonin and 5-methoxytryptamine are amongst some of the indole containing endogenous hormones which act as ligands to one or more polyamine binding sites in the body, e.g. the brain.[28] It is also built into proteins in the form of the essential amino acids tryptophan.[29,30]

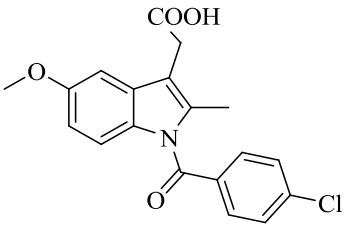


**2.1. Indomethacin**

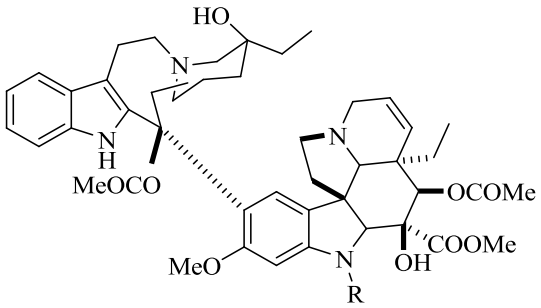


**2.2a :** R = Me
**2.2b :** R = CHO

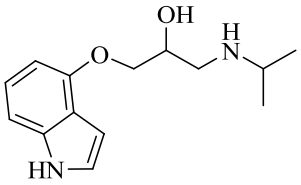


**2.3. Pindolol**

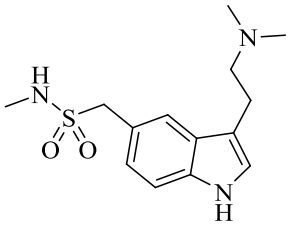


**2.4. Sumatriptan**

The indole scaffold consists of an aromatic heterocyclic fused ring structure, with a non-basic nitrogen atom which acts as an H-bond donor, as well as a hydrophobic benzene portion.[25,30]

The pi excessive heterocyclic portion is nucleophilic, particularly the C-3 position, while the benzene side is susceptible to electrophilic attack, making it useful for various chemical modifications (**Fig 2.1**).[25]

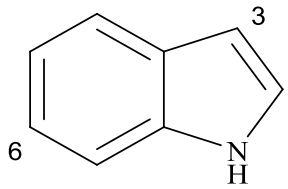


**Figure 2.1** General structure of the indole scaffold

More importantly, the indole scaffold exhibits a broad spectrum of biological properties.[26–30] Below (see section **2.2**), we will discuss the utility of indoles in medicinal chemistry through a selection of examples which have been reported in literature.

## 2.2 Medicinal chemistry and biological activity of indole containing compounds

### 2.2.1. Antibacterial activity

In the quest for inhibitors active against the enzyme enoyl acyl carrier protein reductase (FabI), Seefeld *et al*.[31] prepared a series of 2,9-disubstituted 1,2,3,4-tetrahydropyrido[3,4-*b*]indole analogues as inhibitors of FabI.[31] FabI plays a major role in the synthesis of bacterial fatty acid which makes it to be a good inhibitory target for antibacterial activity.[32] Of the

compounds prepared for this study, **2.5** was found to be the most potent inhibitor of the FabI enzyme in both *E. coli* and *S. aureus*.[31]

A series of 2-aryl-2,5-dihydro-3(3*H*)-oxo-pyridazino[4,3-*b*]indole-4-carboxylic acid analogues were assayed *in vitro* against a wide range of bacteria cell lines.[33] Compound **2.6** displayed a broad antibacterial spectrum against Gram-positive bacteria, *E*. *coli* ATCC 8739, *K*. *pneumoniae*, *A*. *calcoaceticus* a1 and a4 and *P*. *aeruginosa*.[33]

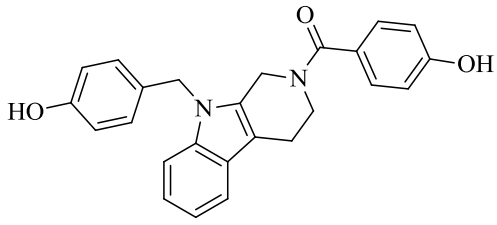

**2.5**

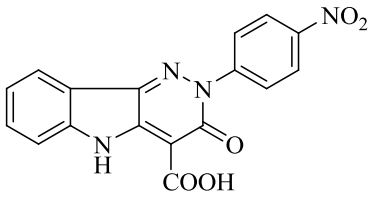

**2.6**

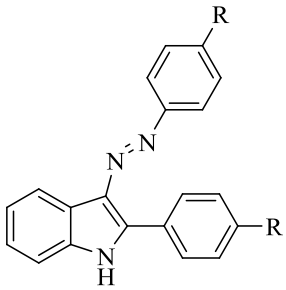

**2.7a :** R = Cl
**2.7b :** R = Br
**2.7c :** R = F
**2.7d :** R = OMe

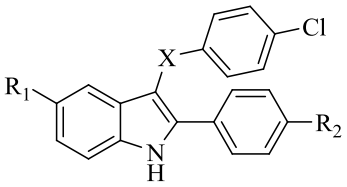

**2.8a :** X = O, $R_1$ = Cl, $R_2$ = Cl
**2.8b :** X = S, $R_1$ = H, $R_2$ = Cl
**2.8c :** X = S, $R_1$ = H, $R_2$ = Br
**2.8d :** X = S, $R_1$ = Cl, $R_2$ = Cl

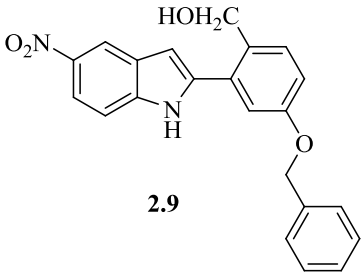

**2.9**

Daly *et al*.[34] synthesised a series of azo-containing heterocycles **2.7a – d** and evaluated them as antibacterial agents against hospital acquired infections including methicillin-resistant *Staphylococcus aureus* (MRSA) and vancomycin-resistant *Enterococcus faecalis* (VRE).[34]

However, the stability of the azo functionality under physiological conditions was of major concern, which led Daly *et al.* explore the bioisosteric replacement of the azo-functionality

with sulfur and oxygen atoms.[34] From this approach, a promising series of compounds (**2.8a – d**) with antibacterial activity against Gram-positive organisms was synthesised. The aryloxyindole **2.8a** displayed superior activity compared to its analogues containing the sulfur (**2.8b – d**) and azo groups.[34] Additionally, the antibacterial inhibitory activity of **2.8a** was comparable to the clinically used antibiotics vancomycin and penicillin G.[34]

2-Aryl-5-nitro-1*H*-indole derivatives were synthesised and their potential antibacterial activity assessed through the inhibition of the NorA multidrug resistance pump in the bacterium *S. aureus*.[35] The NorA protein extrudes antimicrobials from the bacteria conferring resistance to the antibacterial drug agents.[36] The NorA inhibitory activity was assayed on *S. aureus* K1758 and K2361 strains.[35] Compound **2.9** exhibited the highest inhibitory activity against the *S. aureus* strains and synergistically potentiated the actions of other antibiotics such as ciprofloxacin.[35]

The indole derivatives **2.10a – d** were investigated *in vitro* for their antibacterial activity against *S. aureus* and *P. aeruginosa* by the agar well diffusion method with ciprofloxacin used as a reference drug.[37] The bacterial strains were collected from sputum and urine samples of patients with different infectious status who had no prior exposure to any antibacterial drug for a period of at least 2 weeks.[37] The greatest inhibition zone was afforded by **2.10d** which displayed inhibitory activity similar to the reference drug.[37]

Quantitative evaluations for the antimicrobial activity of a series of simple 3-aryl substituted indoles were made through determining MIC values against Gram-positive (*S. aureus* and *Bacillus cereus*), and Gram-negative (*E. coli* and *K. pneumoniae*) bacterial strains.[38] The synthesised analogues displayed poor activity against the Gram-negative strains while **2.11**,

**2.12a** and **2.12b** exhibited the highest antibacterial activity against the two Gram-positive strains.[38]

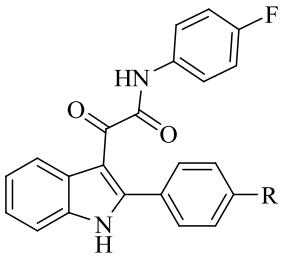

**2.10a :** R = Br
**2.10b :** R = Cl
**2.10c :** R = F
**2.10d :** R = Me

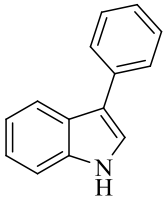

**2.11**

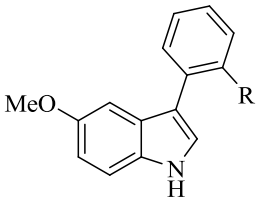

**2.12a :** R = H
**2.12b :** R = Me

Upon screening a library of indole-containing compounds, Yamamoto *et al*.[39] identified an interesting class of coumarin and quinolone containing compounds (**2.13 – 2.15**). Although compound **2.13** was found to be inactive against Gram-negative bacteria, it showed encouraging activity against Gram-positive bacteria including MRSA and VRE.[39] In an attempt to investigate the SAR and to improve the activity of **2.13** against Gram-positive bacteria, a series of analogous compounds related to **2.13** was synthesised including **2.14** and **2.15**, which were potent against MRSA, VRE, *S. aureus* and *E. faecium* displaying greater activity than the standard drugs vancomycin and linezolid.[39]

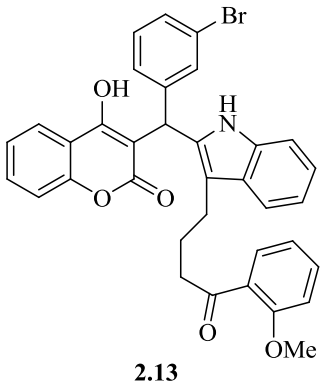

**2.13**

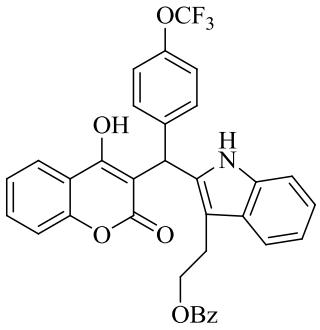

**2.14**

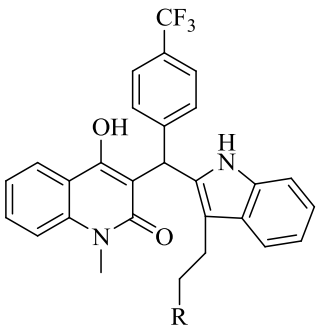

**2.15a :** R = OC (O)– 
**2.15b :** R = NHCON(Me)Ph

In an attempt to find new antimicrobial agents, Singh *et al*.[40] synthesised a series of N-1, C-3 and C-5 substituted bisindoles.[40] The activity was tested against an ampicillin resistance gene encoded plasmid of *E. coli* .[40] Compounds **2.16**, **2.17a** and **2.17b** were found to be the most active antibacterial agents. More importantly, they exhibited comparable inhibition zone diameters to the reference drugs apalcillin and piperacillin.[40] Molecular docking studies conducted on compounds **2.16**, **2.17a** and **2.17b** suggested that these compounds bound well in the active sites of lanosterol demethylase, dihydrofolate reductase and topoisomerase II enzymes.[40]

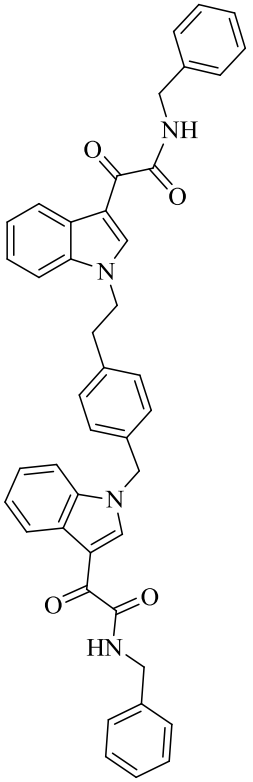

**2.16**

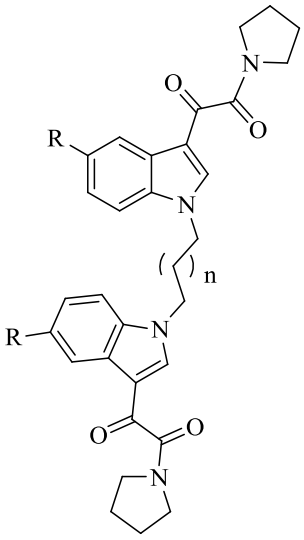

**2.17a :** R = H, n = 2
**2.17b :** R = Br, n = 1

In light of the emerging threat from MRSA, Zoraghi *et al*.[41] utilized a target based drug discovery approach to uncover inhibitors of MRSA pyruvate kinase (PK). MRSA PK is an evolutionary conserved highly connected hub protein which is crucial for the survival of the MRSA bacterium.[41] A screen of natural product analogues revealed bisindole alkaloids *cis*-

3,4-dihydrohamacanthin B (**2.18**) and bromodeoxytopsentin (**2.19**) to be potent and selective inhibitors of MRSA PK. This led to the development of several pseudo symmetrical deoxytopsentin analogues as inhibitors of MRSA PK.[42]

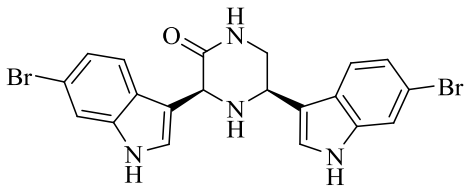

**2.18 *cis*-3,4-dihydrohamacanthin B**

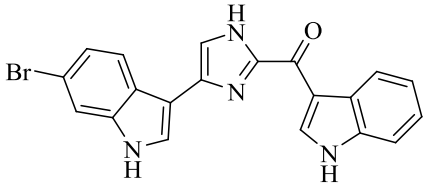

**2.19 bromodeoxytopsentin**

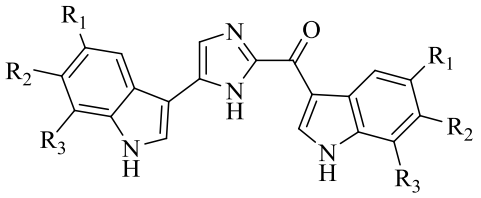

**2.20a :** $R_1 = R_2 = R_3 = H$
**2.20b :** $R_1 = R_3 = H$, $R_2 = Br$
**2.20c :** $R_1 = R_3 = H$, $R_2 = F$
**2.20d :** $R_1 = R_3 = H$, $R_2 = Cl$
**2.20e :** $R_1 = Br$, $R_2 = R_3 = H$
**2.20f :** $R_1 = R_3 = H$, $R_2 = I$
**2.20g :** $R_1 = R_2 = H$, $R_3 = Cl$

The synthesised analogues were assayed for their ability to inhibit enzymatic activity against purified recombinant MRSA and human PKs.[42] While compound series **2.20b – f** displayed potent activity and high selectivity towards the MRSA PK than the human PK, **2.20a** and **2.20g** showed significantly reduced activity.[42] It is worth noting that **2.20b** and **2.20d** exhibited greater inhibitory activity than **2.19** with comparable activity to **2.18**, coupled to a marked increase in selectivity.[42]

3-(1-(1*H*-indol-3-yl)-2-oxo-2-phenylethyl)indolin-2-one derivatives were prepared and their activity tested against the Gram-positive strains of *Bacillus subtilis*, *S. aureus*, *S. epidermidis* and the Gram-negative organisms of *E. coli*, *P. aeruginosa*, and *K. pneumonia*.[43] Moderate

activity was noted for the synthesised derivatives with **2.21a – d** displaying significant activity against *P*. *aeruginosa* although non superior to the standard drugs penicillin and streptomycin.[43]

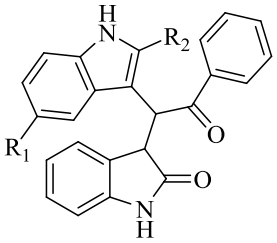

**2.21a :** $R_1$ = H, $R_2$ = H
**2.21b :** $R_1$ = $NO_2$, $R_2$ = H
**2.21c :** $R_1$ = Cl, $R_2$ = H
**2.21d :** $R_1$ = H, $R_2$ = Ph

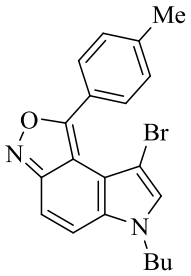

**2.22**

In an attempt to combine the isoxazole moiety with the indole motif to enhance antibacterial activity, 8-bromo-6-alkyl-1-aryl-6*H*-isoxazolo[4,3-*e*]indole derivatives were synthesised as antibacterial agents.[44] Screening was done against *E*. *coli*, *S*. *aureus* pathogens [(MRSA) and methicillin-susceptible *S. aureus* (MSSA), *P*. *aeruginosa* and *B*. *subtilis*].[44] The MIC was determined through the dilution test tube method and the results were compared to the MIC values of cephalexin and erythromycin.[44] The synthesised derivatives showed activity against Gram-positive bacteria with **2.22** displaying the best inhibitory activity against MRSA and MSSA.[44]

### 2.2.2 Anticancer activity

Indole containing vinblastine (**2.2a**) and vincristine (**2.2b**) are amongst the most commonly used antimitotic agents in the clinic.[45,46] Factors such as emerging drug resistance, severe side effects and low bioavailability have highlighted the need to develop new potential anticancer drug.[45]

Due to the diversity of biologically active indole-based compounds, a vast number of different indoles have been used as pharmacophores in the quest for new anticancer drugs.[45,47,48]

The indole motif is present in several tubulin polymerisation inhibitors.[48,49] These compounds bind in the colchicine-binding site and inhibit α/β-tubulin polymerisation thereby inhibiting microtubule formation, resulting in cell arrest at the G2/M phase of the cell cycle.[48,49] The selenoxide containing compound **2.23**, was synthesised and tested *in vitro* for its antiproliferative activity against three human cancer cell lines namely SGC7901, KB and HT1080.[47] Additional *in-vitro* tubulin polymerisation inhibition studies and immunofluorescence experiments demonstrated that **2.23** was a potent anticancer agent, which inhibited the tubulin assembly process during mitosis.[47] Benzimidazole carbamate bearing indole moieties linked *via* either a sulfur or selenium atom were evaluated as antiproliferative and antitubulin drug agents against three human cancer cell lines (SGC-7901, A-549 and HT-1080). The seleno-ether **2.24** exhibited good antiproliferative activity which was similar to the reference drug nocodazole.[50]

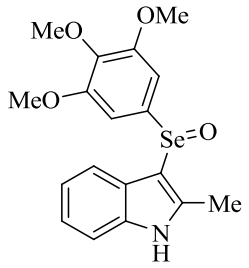


**2.23**

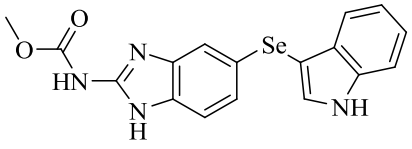


**2.24**

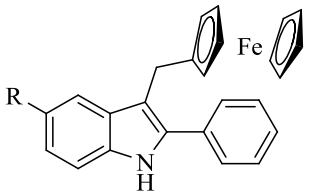


**2.25a:** R = OMe
**2.25b:** R = $NO_2$

The aromaticity, aqueous stability and redox behaviour properties of ferrocene [51–53] prompted Quirante *et al*.[48] to introduce the ferrocene moiety at the C-3 position of various 2-phenylindole derivatives with the primary aim of achieving compounds with increased

cytotoxicity.[48] In comparison to their organic parent compounds, ferrocene-indole hybrids **2.25a** and **2.25b** showed improved *in vitro* activity against the A549 carcinoma cell line.[48]

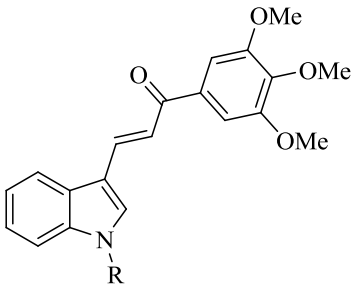

**2.26a:** R = H
**2.26b:** R = Me

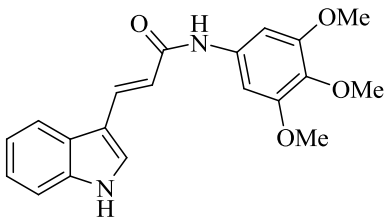

**2.27**

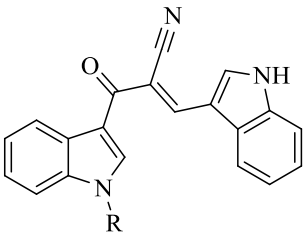

**2.28a:** R = Me
**2.28b:** R = H

A series of indole based chalcones were assessed as potential antitumor agents against A-549, PaCa-2, and PC-3 cancer cell lines in comparison to combretastatin A-4 where compounds **2.26a** and **2.26b** were found to be potent as anticancer agents.[54] Similarly, a series of *trans* indole-3-acrylamides were evaluated as anticancer agents with compound **2.27** emerging as a potent antiproliferative agent against HL-60 and Raji cell lines.[49] The observed activity was attributed to the inhibition of tubulin polymerase thus preventing metastasis of the growth of cancer cell lines.[49] Furthermore, novel indole–acrylonitrile hybrids were evaluated as anticancer agents with compounds **2.28a** and **2.28b** displaying greater cytotoxicity than Paclitaxel against the Paclitaxel resistant BEL-7402 cell line.[55]

Gali *et al*.[56] synthesized a series of indole containing thiazolylcoumarins *via* a one pot multi-component methodology.[56] *In vitro* growth inhibition activity performed against a panel of tumour cell lines led to discovery of **2.29** as a promising antitumour agent and displayed activity against leukaemia, lung, colon, central nervous system (CNS), melanoma, ovarian, renal, prostate and breast cancer cell lines.[56]

Lai *et al*.[57] performed the synthesis of 1-aryl and 1-heteroarylindoles as anticancer agents. These compounds were identified as a potent new class of microtubule destabilising agents.[57] The destabilising agents resulted in mitotic cell arrest through binding at the cholchicine binding site on the microtubules.[57]

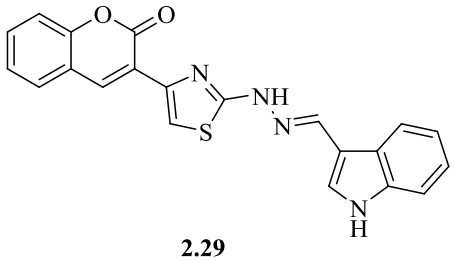

**2.29**

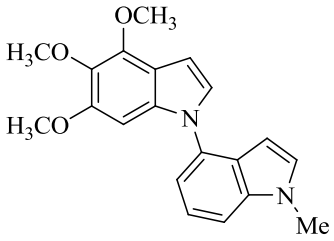

**2.30**

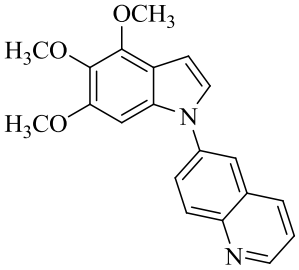

**2.31**

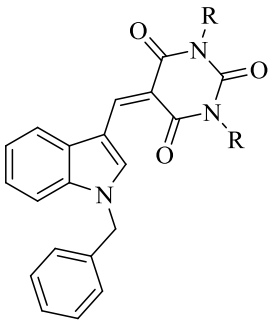

**2.32a :** R = H
**2.32b :** R = Me

The most potent agents, **2.30** and **2.31** were both bi-heterocycles of 1-indolylindole and 1-quinolinylindole respectively.[57] More importantly, these compounds showed superior potency as anticancer agents compared to the reference compound combretastatin A-4 (CA4) against five human cancer cell lines.[57]

Hybrid compounds consisting of the indole moiety and barbituric acid, both known to possess anticancer activity were evaluated for their potential anticancer activity against 60 cancer cell lines.[58] Compounds **2.32a** and **2.32b** exhibited enhanced tumour activity compared to the reference drug 5-fluorouracil.[58] In addition, docking studies conducted at the active site of ribonucleotide reductase, an enzyme involved in the tumour growth

activity of cancer, revealed that their anticancer activity was likely due to the inhibition of this enzyme.[58]

Niemyjska *et al*.[59] synthesised the methylene linked bisindoles **2.33** and **2.34** which were found to be potent anticancer agents. These compounds exhibited enhanced growth inhibition of melanoma UACC-62, renal CAKI-1 and breast cancer T-47D cell lines compared to the respective untreated control cells.[59] The substitution at the N atom by the phenyl sulfonyl group resulted in **2.34** possessing better anticancer activity than **2.33**.[59]

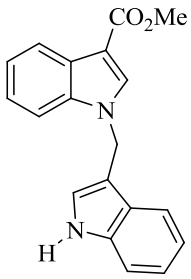


**2.33**

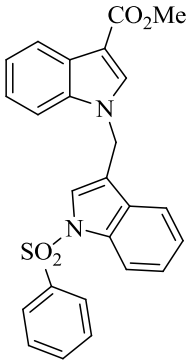


**2.34**

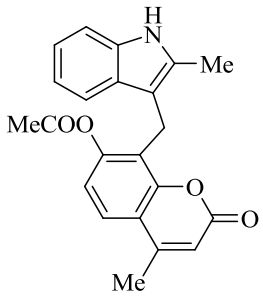


**2.35**

The related bis-indole (**2.35**) was selected from a series of 18 unsymmetrical methylene derivatives which were evaluated *in vitro* for their potential anticancer activity against the MCF7 and MDA-MB-231 breast cancer cell lines. Compound **2.35** exhibited the best antiproliferative activity which was superior compared to the reference indole-3-carbinol.[60]

A series of hybrid indole-pyrimidine, indole-indolinone and indole-pyrazole analogues were investigated for tumour growth inhibitory activities against 60 human tumour cell lines. This study led to the discovery of two promising compounds **2.36a** and **2.36b**. Further SAR analysis of these hits aided the design of indole-oxindoles (**2.37** and **2.38**), which displayed good inhibitory tumour growth activity comparable to the standards 5-fluorouracil, indomethacin and celecoxib.[61]

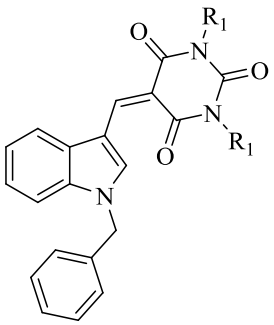

**2.36a :** $R_1$ = H
**2.36b :** $R_1$ = Me

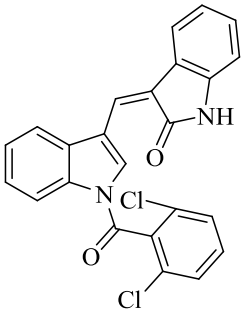

**2.37**

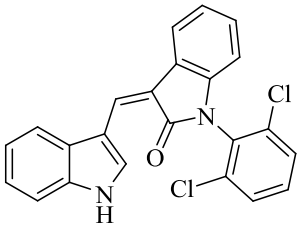

**2.38**

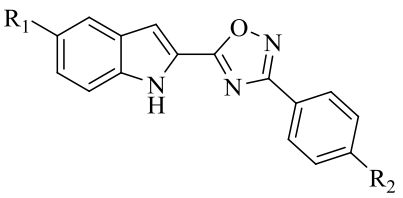

**2.39a :** $R_1$ = $NO_2$, $R_2$ = Cl
**2.39b :** $R_1$ = Cl, $R_2$ = OMe

Based on their original study which identified 3,5-diaryl-1,2,4-oxadiazole derivates, **2.39a** and **2.39b** as pro-apoptotic antitumor agents[62], Tohid *et al*.[63] synthesised a series of 3,5-diarylisoxazole derivatives which included compounds **2.40a** and **2.40b**.[63] These compounds were the most active in the series which was evaluated against colon and lung cancer cell lines and had no impact on the cell viability of the human bronchial smooth muscle cells.[63]

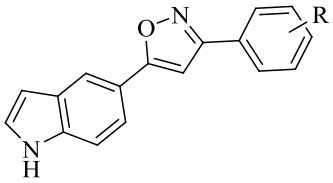

**2.40a :** R= 4-OMe
**2.40b :** R= 3,4,5-tri-OMe

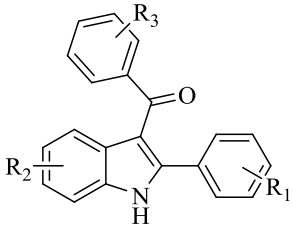

**2.41a :** $R_1$ = 3`-OH, 4`-OMe, $R_2$ = 6-OMe, $R_3$ = 3``,4``,5``-tri-OMe
**2.41b :** $R_1$ = 4`-OMe, $R_2$ = 6-OMe, 7-OH, $R_3$ = 3``,4``,5``-tri-OMe
**2.41c :** $R_1$ = 3`-OH, 4`-OMe, $R_2$ = 6,7-di-OMe, $R_3$ = 3``,4``,5``-tri-OMe

The initial discovery of **2.41a**, a potent inhibitor for both tubulin assembly and cell growth, led to the synthesis of a small series of 2-aryl-3-aroyl indole-based analogues as anticancer agents.[64] *In vitro* cytotoxicity activity evaluated against the SK-OV-3, NCI-H460 and DU-145 human cancer cell lines uncovered two further analogues, **2.41b** and **2.41c** which displayed anticancer activity comparable with **2.41a**.[64]

Celastrol is a quinone methide triterpenoid which has been proven clinically to possess anticancer activity.[46] In a study to explore the C-6 position of celastrol, a series of C-6 substituted indole derivatives were synthesised.[46] The *in vitro* antiproliferative activity study was conducted on human hepatocellular carcinoma Bel7402 and human glioblastoma cell line H4.[46] The synthesised derivatives **2.42a** and **2.42b** displayed the best anticancer activity against Bel7402 cancer cell line with similar activity to the celastrol.[46]

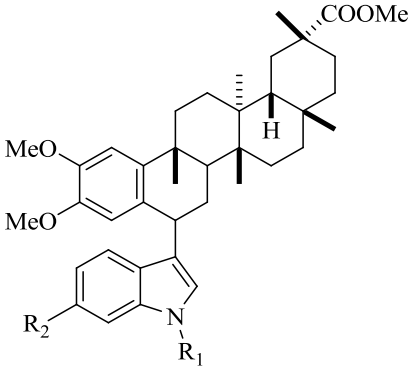


**2.42a :** $R_1$ = H, $R_2$ = Me
**2.42b :** $R_1$ = Me, $R_2$ = Cl

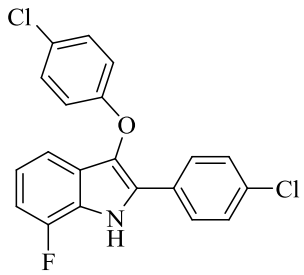


**2.43**

In an attempt to synthesise 2,3-disubstituted indoles as antiproliferative agents against apoptosis-resistant cancer cells, Magedov *et al*.[65] explored the diversity of different substituents at position C-3 of the indole moiety.[65] The substituents which were at the C-3 positions included either the ether, thioether, amide, pyrazole and dithiocarbamate moieties.[65] *In vitro* evaluation against apoptosis-resistant cancers cell lines showed that the C-3 ether and thioether indoles were potent anticancer agents.[65] Based on the $GI_{50}$ values, the ether indole **2.43** was found to be the most potent anticancer agent.[65]

### 2.2.3 Antifungal activity

Given the broad biological spectrum of biological activity of indoles, substituted-10-methyl-1,2,3,4-tetrahydropyrazino[1,2-*a*]indole derivatives were investigated for their potential

activity against four pathogenic fungal strains namely *Aspergillus fumigatus*, *A. flavus*, *A. niger* and *Candida albicans*.[66] Within the series, compound **2.44** displayed the greatest *in vitro* antifungal activity with an encouraging cytotoxicity profile despite its lower activity than the reference drug amphotericin B (**2.45**).[66]

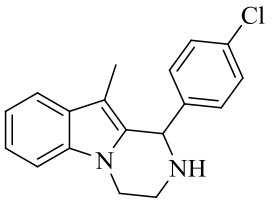

**2.44**

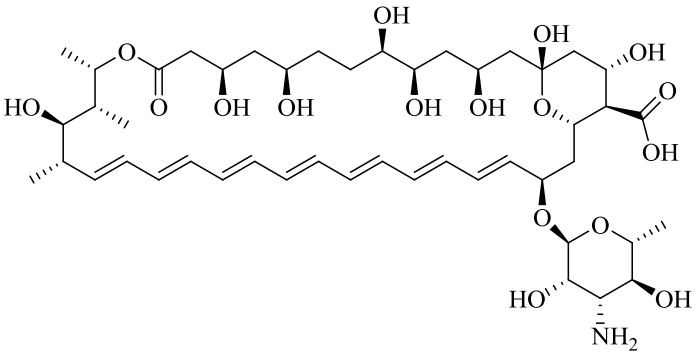

**2.45**

A series of triazole containing compounds inspired by fluconazole (**2.46**) including 1-[(1*H*-indol-5-ylmethyl)amino] derivatives were evaluated against *C. albicans* and *A. fumigatus* strains.[67] Compound **2.47** emerged as a potent antifungal agent with superior activity to that of fluconazole (**2.46)** against fluconazole-resistant species.[67] In a related study, another series of indole containing triazoles were investigated against *C. albicans*, *C. neoformans*, *A. fumigatus* and *C. krusei* strains.[68]

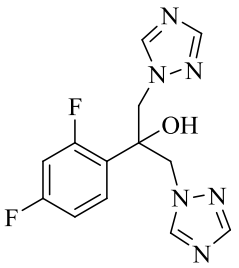

**2.46**

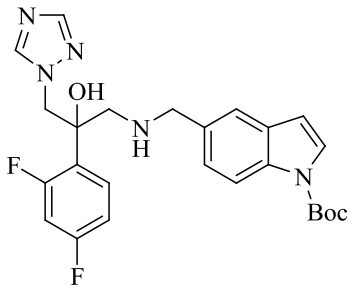

**2.47**

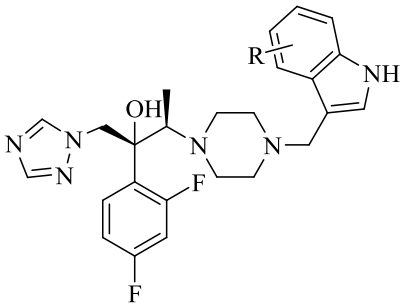

**2.48a :** R = 5,6-Cl
**2.48b :** R = 4,5,6,7-F
**2.48c :** R = 6-$N_3$
**2.48d :** R = 7-CN

Interestingly, most of the compounds pursued, including **2.48a** and **2.48b**, exhibited higher antifungal activity against *C. albicans* compared to the positive control drugs **2.45** and **2.46**.[68] This led to the conclusion that the antifungal activity of these analogues against *Candida* species was enhanced by the introduction of an indole moiety to the triazole pharmacophore.[68] In contrast, *C. neoformans* was less sensitive to the synthesised indole derivatives whilst **2.48c** and **2.48d** displayed comparable activities against *A. fumigatus*.[68]

A separate study investigated the *in vitro* activity of a series of differentially substituted 4-arylthiosemicarbazide derivatives against *Candida* species.[69] The data obtained revealed that **2.49a** and **2.49b** were the most potent compounds against *C. albicans* ATCC 10231, *C. albicans* ATCC 90028 and *C. parapsilosis* ATCC 22019 species.[69] Relatively simple 2- and 3-aryl substituted indoles were also investigated as potential antifungal agents with compound **2.50a**, **2.50b** and its regioisomer **2.51** all displaying similar encouraging activity against *C. neoformans.*[38]

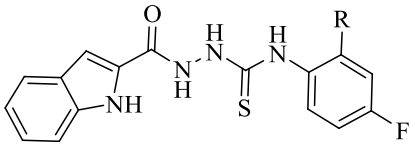

**2.49a :** R = H
**2.49b :** R = F

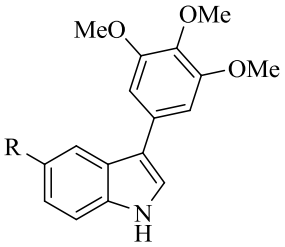

**2.50a :** R = H
**2.50b :** R = OMe

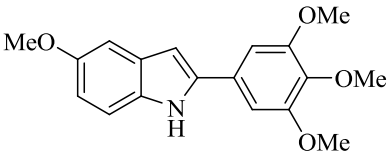

**2.51**

From the aerial parts of *Alstonia rupestris Kerr*, a plant of the family Apocynaceae, Zhang *et al*.[70] extracted and isolated alkaloids **2.52a – c** which exhibited significant activity against the fungi species *Alternaria alternata* and *Phytophthora capsici*.[70] 3-(1-(1*H*-indol-3-yl)-2-oxo-2-phenylethyl)indolin-2-one analogues were evaluated against *C. albicans*, *Saccharomyces cerevisiae*, *Rhizopus oryzae* and *A. niger* with compound **2.53** displaying good activity as an

antifungal agent.[43] Further investigation of other potential indole-based antifungals had also led to the synthesis and *in vitro* biological evaluation of 2-(indole-3-yl)-thiochroman-4-ones.[71] Of the synthesised compounds, **2.54a – d** were identified as the most active compounds and displayed better activity against a panel of fungal strains in comparison with standard antifungal agents **2.45** and **2.46**.[71]

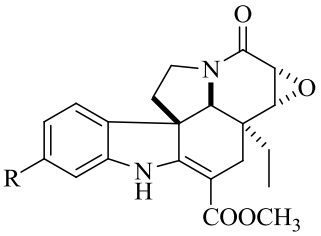

**2.52a :** R = H
**2.52b :** R = OAc
**2.52c :** R = OH

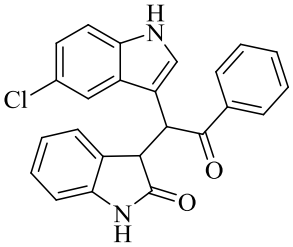

**2.53**

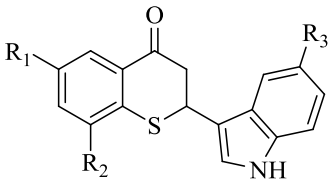

**2.54a :** $R_1$ = Cl, $R_2$ = H, $R_3$ = Cl
**2.54b :** $R_1$ = H, $R_2$ = F, $R_3$ = H
**2.54c :** $R_1$ = H, $R_2$ = F, $R_3$ = Cl
**2.54d :** $R_1$ = H, $R_2$ = F, $R_3$ = OH

### 2.2.4 Anti-HIV activity

A significant number of indole-based compounds have been investigated for potential use in the treatment of HIV viral infections. A typical example includes the drug Delavirdine (**2.55**), a non-nucleoside reverse transcriptase inhibitor (NNRTI), which is used clinically for the treatment of human immunodeficiency virus (HIV).[72,73] The structural analogue of **2.55**, Atevirdine (**2.56**) is currently in clinical trials as a non-nucleoside reverse transcriptase inhibitor for HIV treatment.[73]

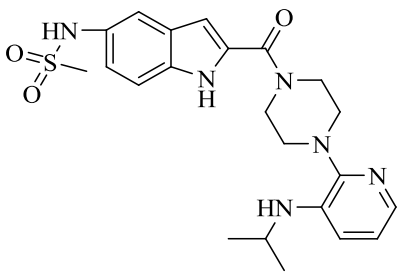

**2.55. Delavirdine**

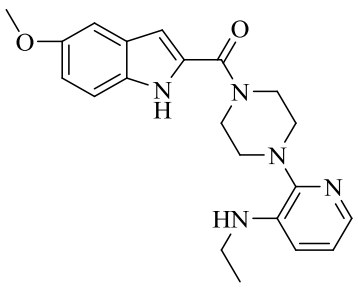

**2.56. Atevirdine**

As part of an on-going SAR study around their active HIV attachment inhibitor **2.57**, Yeung *et al*.[74] synthesised a series indole-7-carboxamide analogues with compounds **2.58** and **2.57** showing encouraging activity.[74] More importantly, preliminary *in vivo* pharmacokinetic studies in rats showed that the oral bioavailability of **2.58** was higher than **2.57**.[74] A series of related compounds were also developed by Wang *et al*.[75] and compounds **2.59a – c** were found to inhibit HIV-1 attachment.[76]

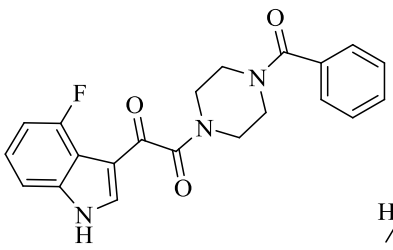

**2.57**

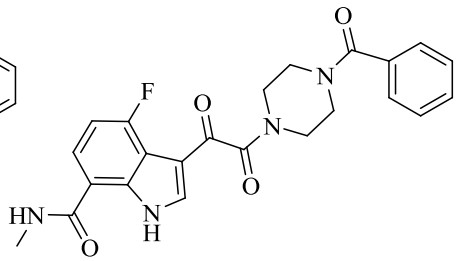

**2.58**

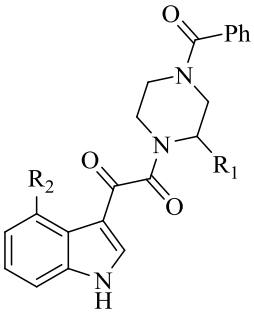

**2.59a :** $R_1$ = H, $R_2$ = F
**2.59b :** $R_1$ = H, $R_2$ = OMe
**2.59c :** $R_1$ = Me, $R_2$ = F

With the hope of finding promising compounds with potential anti-HIV activity, indolylarylsulfone derivatives consisting of a heterocyclic tail joined to indole through the C-2-carboxamideswere were designed as potential NNRTI's.[77] Antiviral activity was assessed based on the potential of these derivatives to inhibit cell death induced by the mutant HIV-1 strain.[77] Compounds **2.60 – 2.62** effectively inhibited the K103N HIV-1 mutant strain in the lymphoid MT-4 cell line.[77] In addition, **2.62** also inhibited the clinically relevant Y181C mutant in MT-4 cells.[77] The (*R*)-enantiomer of indolylarylsulfone **2.63** displayed remarkable potency against a panel of viral strains, and showed better antiviral activity compared to the reference drugs nevirapine (NVP) and efavirenz (EFV) against the HIV-1 WT, K103N and L100I mutant strains respectively.[77] Inspired by IDX-899 (**2.64**), which is an NNRTI in phase 2 of the clinical trials, Pelly and co-workers utilized a molecular modelling guided design

approach in order to rationalise a series of cyclopropyl containing indole derivatives as potent HIV-1 NNRTI's.[78] Of their cohort, they identified compounds **2.65a** and **2.65b** as lead compounds which displayed similar activity to the reference drug NVP.[78] Further investigation yielded compounds **2.66a** and **2.66b**, which displayed improved activity than NVP.[79] Further refinement led to the design of the methoxy derivative (**2.67**), which displayed potent low nanomolar activity in phenotypic assays.[79]

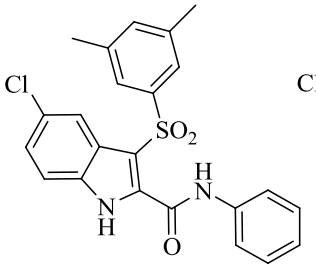

**2.60**

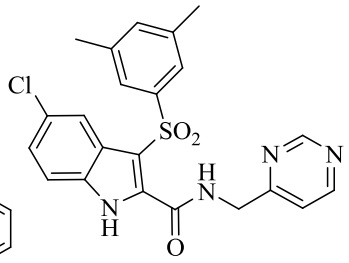

**2.61**

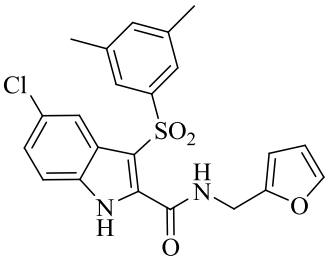

**2.62**

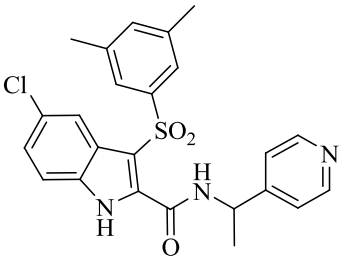

**2.63**

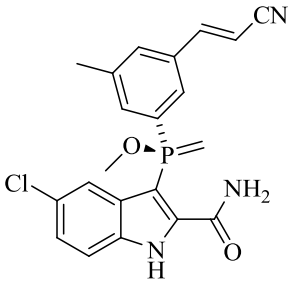

**2.64. IDX-899**

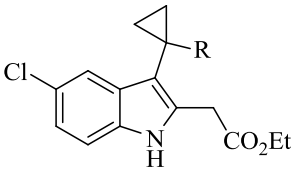

**2.65a :** R = Ph
**2.65b :** R = 2-thiophenyl

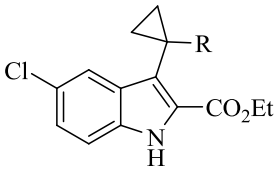

**2.66a :** R = Ph
**2.66b :** R = Thiophene

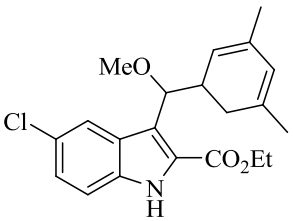

**2.67**

Indole-3-sulfonamide derivatives were evaluated as NNRTIs against the problematic HIV reverse transcriptase mutants K103N and Y181C.[80] Pyrrolidine sulfonamide analogues featuring various substituents at position C-2 (**2.68a**, **2.68b** and **2.69**) displayed encouraging activity against the K103N, and Y181C strains.[80]

Using the structural and biological data of raltegravir and another known potent integrase strand transfer inhibitor, a series of 1H-benzylindole derivatives were generated leading to

compound **2.70** which was active as an inhibitor for the HIV-1 integrase.[81] Utilizing the structure of HIV envelope glycoprotein gp41 complex, Zhou *et al*.[82] rationally designed a series of indole-based derivatives as inhibitory agents against HIV-1 entry across cell membranes.[82] Compound **2.71** displayed promising antiviral activity against HIV-1 fusion in cell culture assays.[82]

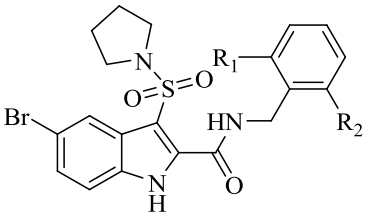

**2.68a :** $R_1$ = Cl, $R_2$ = F
**2.68b :** $R_1$ = H, $R_2$ = OH

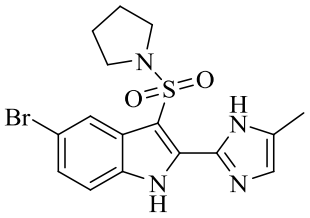

**2.69**

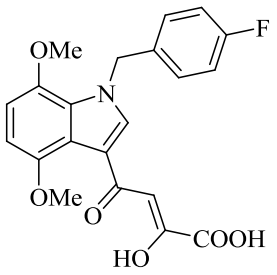

**2.70**

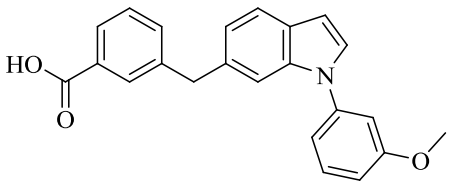

**2.71**

### 2.2.5 Antimalarial activity

The scourge of malarial infections and rising cases of multidrug resistance against clinically approved drugs has prompted an urgent search for new scaffolds. Recently discovered scaffolds include NITD609 (**2.72)**, an antimalarial compound currently in phase 1 clinical trials, which has been found to be as effective as artesunate against *P. falciparum.*[83] This compound bears an indole template endowed with broad biological properties as has been discussed in previous sections. A racemic mixture of spiroazepineindole **2.73** was identified in HTS against whole cell *P*. *falciparum* where it exhibited moderate activity against wild type (NF54) and chloroquine resistant (K1) strains.[84] Expansion of the spiroazepineindole

series led to the discovery of compound **2.74**, which displayed comparable activity to chloroquine and artesunate.[84] Further lead modification finally afforded the potent compound, NITD609.

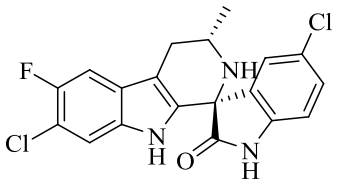


**2.72. NITD609**

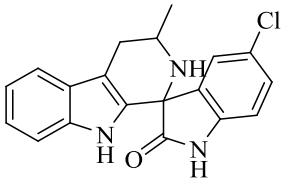


**2.73**

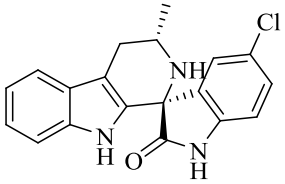


**2.74**

The indole containing hormone melatonin (**2.75**) has been reported to play a crucial role in the malaria parasite replication process.[85] Schuck *et al*.[85] utilized this endogenous ligand to design a series of melatonin antagonists as putative antimalarial agents focusing on the methoxy, carboxamide and amide functionalities present on the indole C-3 position leading to compounds **2.76a**, **2.76b** and **2.77** which showed more potent antimalarial activity than **2.75** in a *P. falciparum* culture.[85]

*Geissospermum vellosii* is one of the most commonly used medicinal trees.[86] Four indole alkaloids were isolated from the stem bark and their antimalarial activity tested *in vitro* against the chloroquine-sensitive strain of *P*. *falciparum* (D10).[86] Geissolosimine (**2.78**) exhibited the best antiplasmodial activity amongst the isolated alkaloids although it was inferior to chloroquine.[86] Encouragingly, compound **2.78** was found to be non-toxic to mammalian cells in the Chinese Hamster Ovarian (CHO) cell line assay.[86] Nugroho *et al*.[87] reported the isolation of indole alkaloids from the bark of *Hunteria zeylanica* as antiplasmodial agents.[87] With the isolation of three indole alkaloids having been reported earlier[88], a total of five indole alkaloids were tested against *P*. *falciparum* (3D7), where CQ was used as a standard drug.[87] Of the five isolated indole alkaloids, Nicalaterine A (**2.79**) displayed the highest antimalarial activity.[87]

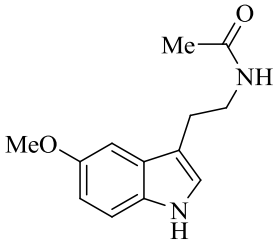

**2.75. Melatonin**

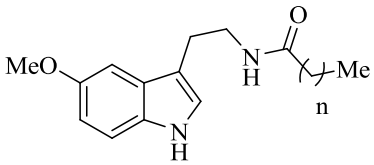

**276a :** n = 2
**2.76b :** n = 4

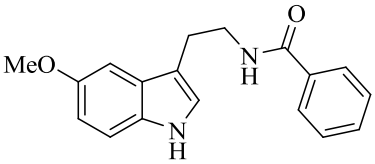

**2.77**

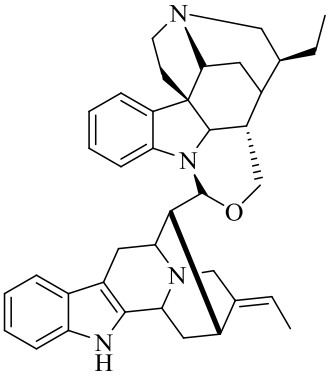

**2.78**

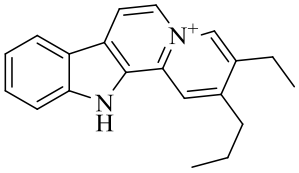

**2.79**

The antimalarial compounds pyrimethamine (**2.80**) and apicidin (**2.81**)[89–91] inspired the design of a series of hybrid indole derivatives as potential antimalarial agents.[92] Compounds **2.82a – f** displayed more potent antimalarial activity than the reference pyrimethamine against the *P. falciparum* NF-54 strain.[92]

In an attempt to discover new antimalarial agents, 6-trifluoromethyl-1,2,4-triazino[5,6-*b*]- and 5*H*-1,2,4-triazolo[10,50,2,3]-1,2,4-triazino-[5,6-*b*] indole derivatives were synthesised.[93] These derivatives were evaluated *in vitro* against the CQ-sensitive (D10) and CQ-resistant (RSA11) strains of *P. falciparum*.[93] Within the series, **2.83a – c** which had a trifluoromethyl group at position 6, and these compounds showed excellent *in vitro* activities against RSA11 strain of *P. falciparum*.[93]

van Schalkwyk *et al*.[94] synthesised a library of indole derivatives based on the active structural constituents of bafilomycin $A_1$, an inhibitor of V-type $H^+$-ATPase enzyme.[94] This

enzyme is important during the intra-erythrocytic stage of *P. falciparum*.[94] While **2.84** and **2.85** were the most potent *in vitro* derivatives, none of the selected inhibitors showed the reduction of the parasitaemia on mice infected with *P. vinckei*.[94]

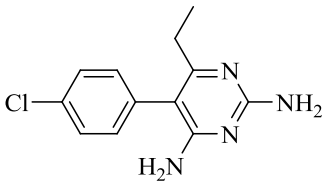

**2.80**

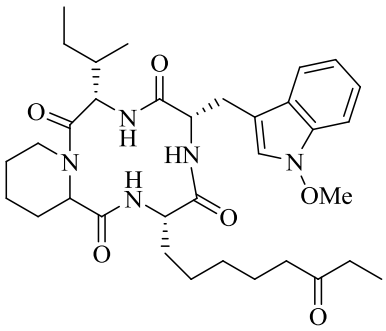

**2.81**

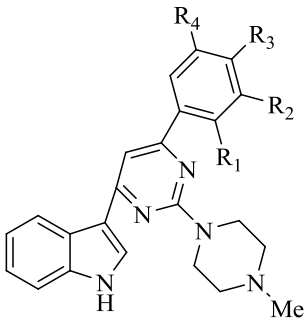

**2.82a :** $R_1$ = H, $R_2$ = H, $R_3$ = H, $R_4$ = H
**2.82b :** $R_1$ = H, $R_2$ = H, $R_3$ = Me, $R_4$ = H
**2.82c :** $R_1$ = H, $R_2$ = H, $R_3$ = OMe, $R_4$ = H
**2.82d :** $R_1$ = H, $R_2$ = OMe, $R_3$ = OMe, $R_4$ = H
**2.82e :** $R_1$ = OMe, $R_2$ = H, $R_3$ = H, $R_4$ = OMe
**2.82f :** $R_1$ = H, $R_2$ = H, $R_3$ = Cl, $R_4$ = H

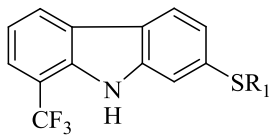

**2.83a :** $R_1$ = Me
**2.83b :** $R_1$ = Et
**2.83c :** $R_1$ = 

Davis *et al*.[95] undertook a HTS on a pre-fractionated natural product extract library.[95] They identified one fraction derived from the sponge *Ancorina* sp. (Ancorinidae) which showed parasitic growth inhibition in the antimalarial imaging assay.[95]

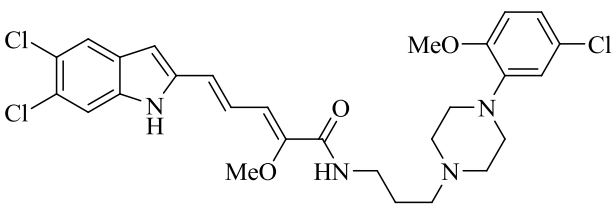

**2.84**

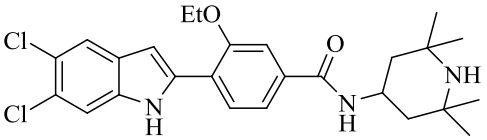

**2.85**

Purification of this fraction led to the isolation of the β-carboline alkaloid, (+)-7-bromotrypargine (**2.86**) and 6-bromotryptamine (**2.87**).[95] Compound **2.86** showed activity against CQ-resistant (Dd2) and CQ-sensitive (3D7) *P. falciparum* strains, whereas compound

**2.87** was not active.[95] More importantly, these compounds showed no toxicity effects against the human embryonic kidney cell line (HEK293).[95]

Another HTS screening by the group of Teguh *et al*.[96] led to the identification of an *N*-acetylated analogue of quinolium **2.88** as a potent antimalarial agent.[96] In an effort to explore the SAR of **2.88**, they synthesised different derivatives for possible antimalarial activity.[96] The activity of the synthesised derivatives was evaluated against CQ-sensitive and resistant strains (3D7 and K1) respectively.[96] The selectivity indices of the derivatives for *P. falciparum* were determined based on comparison to the mammalian cells (HEK293).[96] Of the synthesised derivatives, none were superior to the activity of **2.88** against both the 3D7 and K1 strains.[96] The hit compound **2.88** also displayed reasonable selectivity for *P. falciparum*.[96]

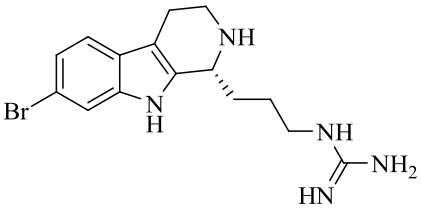


**2.86**

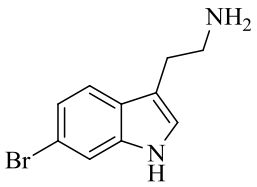


**2.87**

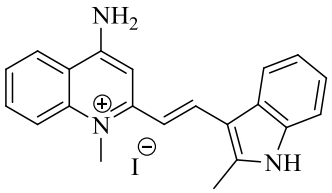


**2.88**

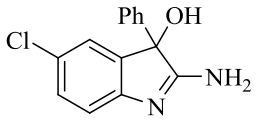


**2.89**

A separate screening campaign of 104 compounds led to the identification of 2-amino-5-chloro-3-hydroxy-3-phenylindole (**2.89**), which displayed potent *in vivo* activity against in a *P. berghei* mouse model.[97] Furthermore, this compound caused a decrease in parasitaemia with no adverse side effects. The good activity prompted Urgaonkar *et al*.[97] to explore and

optimise the compound class of **2.89**. The synthesised 2-amino-3-hydroxy-indoles derivatives were active against the drug-sensitive (3D7) and drug-resistant (Dd2) parasitic strains.[97] However, the racemate of **2.89** was found to be more potent than the separate enantiomers (*S*)-**2.89** and (*R*)-**2.89**.[97]

**2.3 Aim and objectives of the thesis**

In conclusion, the examples discussed above show that the indole scaffold is a critical part of many medicinally important compounds, displaying a variety of biological activities, including antimalarial activity. Its unique blend of chemical characteristics, as well its natural abundance, makes it an excellent starting point for a medicinal chemistry campaign. Therefore the primary objective of this study is to investigate indolyl-3-ethanone-α-amines, ethers and thioethers, collectively referred to as α-aryl substituted 3-indolylethanones as potential antiplasmodial agents. The rationale of these compounds stems from previous work conducted in our laboratory where a small series of indolyl-3-amides and esters displayed moderate antimalarial activity against a chloroquine-sensitive malarial strain (NF54), coupled to significant toxicity.[98] We were curious as to whether introducing a methine carbon between the carbonyl and heteroatom would have a positive effect on the biological activity of the lead compound. As part of our primary objective, several secondary objectives were identified as follows:

- Optimize our synthetic route to the target indolyl-3-ethanone-α-amines. In particular, optimization of a key coupling step will be essential. (Chapter 3).

- Use SAR investigations to inform further design and synthesis of more analogues (Chapter 4).
- Explore the possible mode of action of synthesised compounds through computational modelling experiment analysis of our ligands against the *S. aureus* HPPK binding site (Chapter 4).

# Chapter Three

## Synthesis of α-aryl substituted 3-indolylethanones

### 3.1 Introduction

In this chapter we describe the synthesis and characterisation of novel α-aryl substituted 3-indolylethanones as potential antimalarial agents. A previous study that was done in our research group led to the synthesis of indolyl-3-amides exemplified by compound **3.1**.[98] The preliminary biological investigation of this class of compounds revealed that the indolyl-3-amides exhibited moderate antimalarial properties, albeit coupled to significant toxicity.

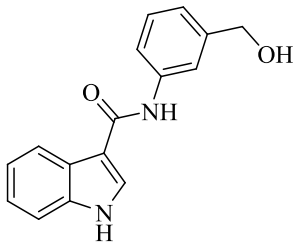


**3.1**

In light of this preliminary data, the current work was undertaken in order to further expand the SAR of this class of compounds as potential antiplasmodial agents. **Figure 3.1** illustrates the design of target molecules which bear the indole scaffold including the proposed regions for structural modifications.

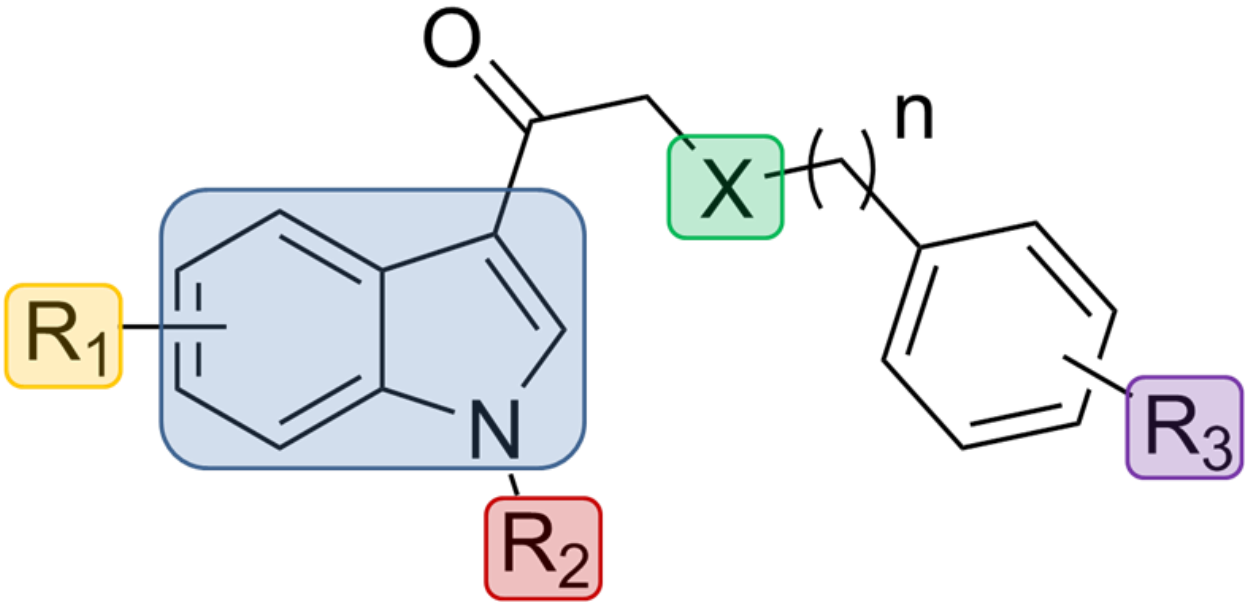


**Figure 3.1**: Proposed chemical modifications as part of a wider SAR investigation, with the indole scaffold highlighted in blue. 'X' highlighted in green represents either an NH, O or S atom. Modifications at $R_1$ will include variable halogen substituents, whose role will be to explore relevant chemical space, as well as the role of lipophilicity to the overall SAR. Similarly, $R_2$ will feature a small number of alkyl substituents, which will explore possible chemical space, as well as determine the relative importance of the H-bond donating indole N-H. The role of $R_3$ will be to optimise hit compounds through various diverse substitutions.

## 3.2 Results and discussion

### 3.2.1 Retrosynthetic analysis of target α-aryl substituted 3-indolylethanones

**Scheme 3.1** details our proposed retrosynthesis for our desired compounds. We reasoned that **3.2** could be acquired through nucleophilic displacement of an appropriate α-halogenated ketone, such as **3.3** with a relevant aniline, phenol or thiophenol respectively. We aimed at synthesizing compound **3.3** from a Friedel-Crafts, derived 3-acetyl indole (**3.4**) over two steps rather than directly from indole (**3.5**) for reasons which will be discussed below. Due to possible alterations of the electronic environment of indole, we opted to introduce the $R_2$ substituents after acetylation.

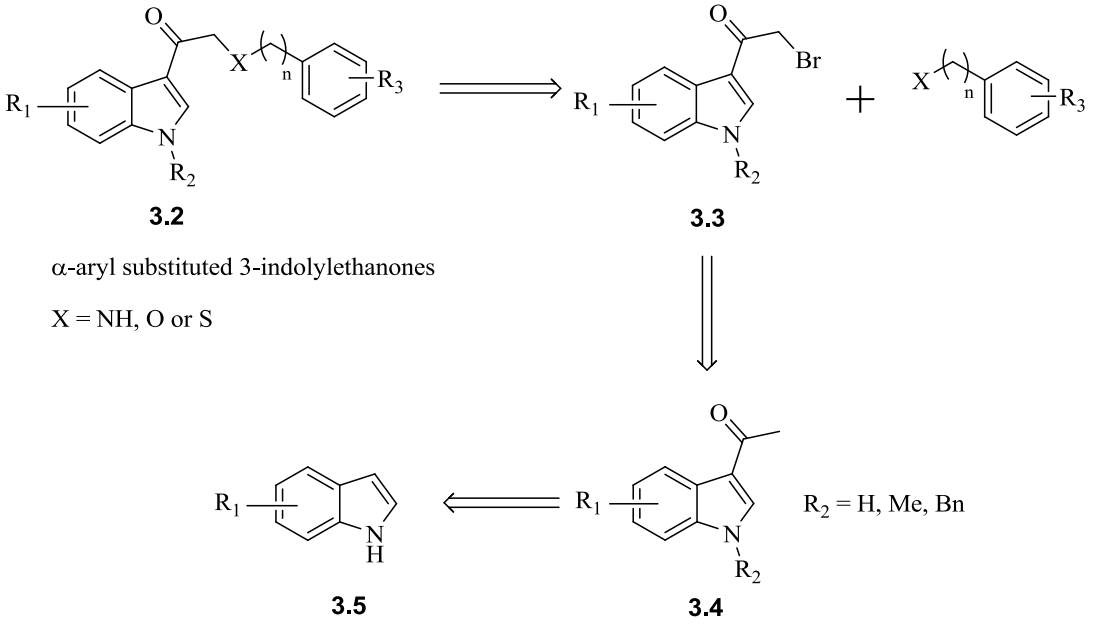


**Scheme 3.1** Retrosynthesis of α-aryl substituted 3-indolylethanones

### 3.2.2 Synthesis of 3-acylindoles

Having reasoned our retro synthetic pathway, our first step was to prepare the relevant α-haloketones from the corresponding 3-acetylindole, which if not available would be prepared from Friedel-Crafts acetylation. Ottoni *et al.*[99] had previously reported a single step method toward the synthesis of α-haloketones **3.8a** and **b** from indole (**3.7**) using either of three acylating agents α, β or γ (**Scheme 3.2**).

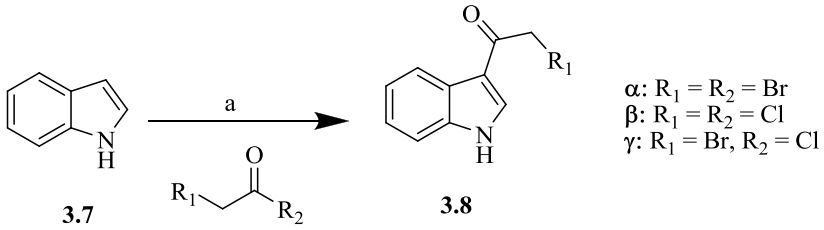


**Scheme 3.2** a) $SnCl_4$, $CH_2Cl_2$, $CH_3NO_2$, Ar 0 $^oC$ to rt

Previous attempts in our lab to repeat this method were however unsuccessful.[100] This lack of success was mirrored in a recent report by Pedersen and co-workers, who investigated this reaction, and were unable to repeat several similar indole acylations.[101]

We therefore resolved to prepare our desired intermediates through acetylation of indole, followed by selective bromination. Friedel-Crafts acetylation of indole often suffers from low yields due to the competitive formation of 1-acylated and/or 1,3-diacylated products and other side reactions including self-polymerisation of indole. In the same study discussed above, Ottoni *et al.*[99] prepared 3-acetylindoles from indole through the use of $SnCl_4$ and a dichloromethane/ nitromethane co-solvent system. In our hands, our group had previously adapted this method to generate a series of 3-acetylindoles[42] in moderate to good yield. Accordingly, we applied this method to prepare acetylated dihalogenated compounds **3.9** and **3.10** (**Scheme 3.3**) in acceptable yields, without any noticeable side products.

The remaining 3-acetylindoles **3.11 – 3.15** were readily available in our laboratory, and it was therefore not necessary to resynthesize them for this medicinal chemistry study.

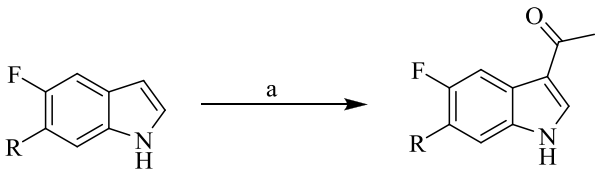


**3.9:** R = Cl 68%
**3.10:** R = Br 55%

**Scheme 3.3** Synthesis of **3.9** and **3.10**

a) $SnCl_4$, $CH_2Cl_2$, $CH_3NO_2$, AcCl, $N_2$ 0 $^oC$ to rt

### 3.2.2.1 Characterisation of compounds 3.9 and 3.10

The successful acetylation of the substituted indoles was confirmed through NMR spectroscopic analysis. For example, the $^{1}$H-NMR spectrum of compound **3.9** (**Figure 3.2**), showed a chemical shift at δ 2.44 ppm integrating for 3 protons, which we attributed to the equivalent methyl protons of acetyl moiety. Similarly, we were confident that acetylation had not occurred at position 1, due to the presence of the NH signal (δ 12.13 ppm) in the $^{1}$H-NMR spectroscopic spectrum. The $^{13}$C-NMR spectrum of **3.9** corroborated the $^{1}$H NMR data and featured the characteristic signals of the methyl group (δ 27.8 ppm) and the carbonyl carbon (δ 193.4 ppm). Additionally, these characteristic signals matched those observed in 3-acetyl indoles **3.10 – 3.15**.

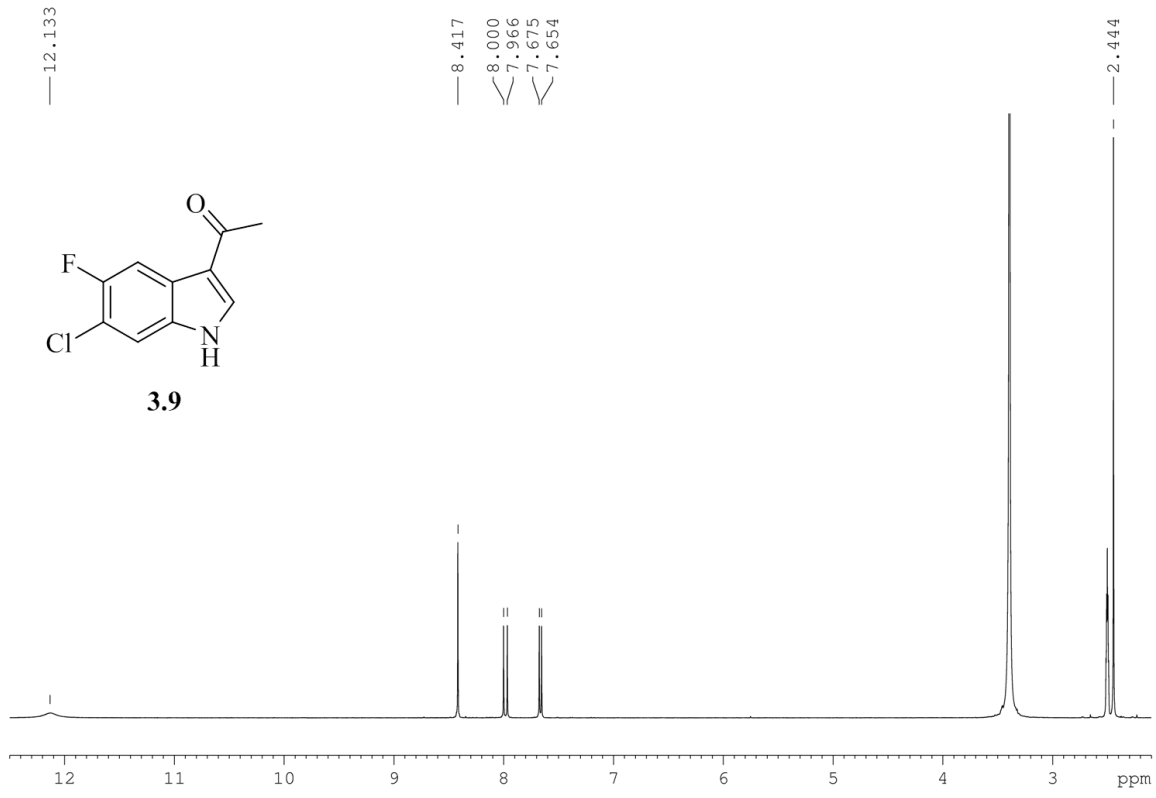


**Figure 3.2**: $^{1}$H NMR spectrum (300 MHz, DMSO-$d_6$) for compound **3.9**

### 3.2.3 Synthesis of *N*-modified 3-acetylindoles

Compounds **3.16** and **3.17** were synthesized from commercially available **3.15**, with the aid of iodomethane and benzylbromide respectively as per a previously reported method (**Scheme 3.4**).[102] While the yields of this step were disappointingly low, we were satisfied that we had sufficient product on hand to continue with our study.

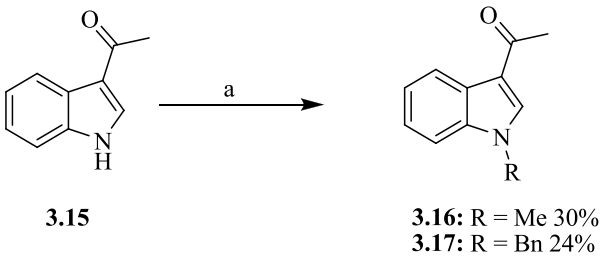


**3.15** **3.16:** R = Me 30%
**3.17:** R = Bn 24%

**Scheme 3.4** Synthesis of **3.16** and **3.17**

a) DMF, NaH, 0 $^{o}$C

#### 3.2.3.1 Characterisation of compounds **3.16** and **3.17**

The $^{1}$H-NMR spectrum of compound **3.16** revealed a characteristic *N*-methyl chemical shift at δ 3.83 ppm integrating for 3 protons, in addition to the disappearance of the N-H proton signal observed for the indole starting material (**Figure 3.3**).

A similar absence of the NH signal was observed for compound **3.17**, a new singlet appeared at δ 5.36 ppm integrating for 2 protons, while additional aromatic signals consistent with the benzyl moiety could be observed. This data was again supported by the $^{13}$C NMR

spectrum, which featured the characteristic signals of the *N*-methyl group (δ 34.3 ppm) for **3.16** and methylene group (δ 50.9 ppm) for **3.17**.

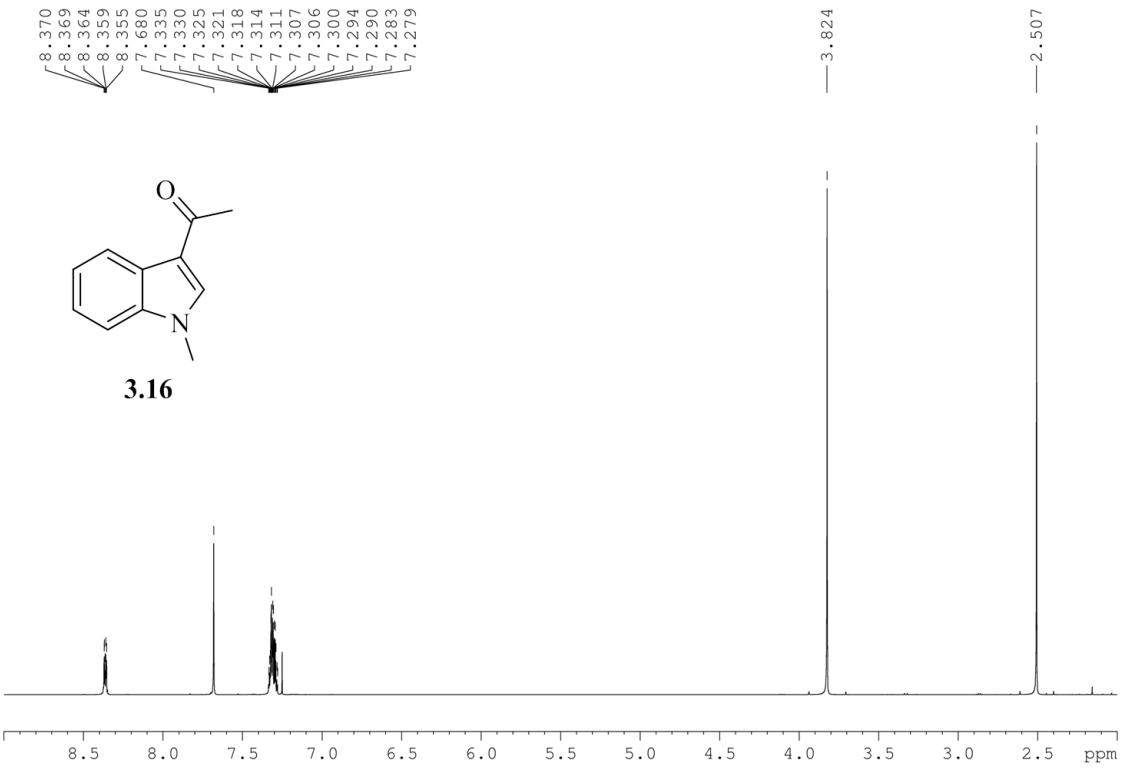


**Figure 3.3**: $^{1}$H NMR spectrum (300 MHz, $CDCl_3$) for compound **3.16**

### 3.2.4 Synthesis of α-brominated 3-acetylindoles

Following the successful acetylation of indoles to form the 3-acetylindoles (see section **3.3.2**) and *N*-modification of **3.15** (see section **3.3.3**), we proceeded on to the bromination step to access the desired key α-bromo carbonyl intermediates (**3.18 – 3.26**). As previously mentioned, we opted for this synthetic approach as direct acylation of indoles yielded mixed results. We opted to utilise a selective bromination method originally published by King *et al*.[103] where $CuBr_2$ is used as the brominating agent (**Scheme 3.5**).

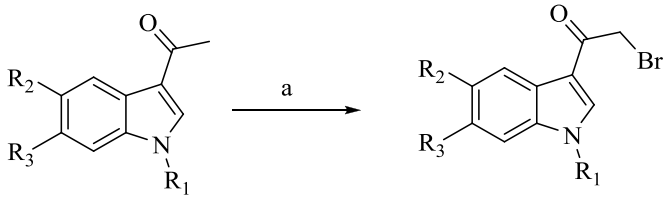


**3.9:** $R_1$ = H, $R_2$ = F, $R_3$ = Cl
**3.10:** $R_1$ = H, $R_2$ = F, $R_3$ = Br
**3.11:** $R_1$ = H, $R_2$ = H, $R_3$ = F
**3.12:** $R_1$ = H, $R_2$ = Cl, $R_3$ = H
**3.13:** $R_1$ = H, $R_2$ = H, $R_3$ = Cl
**3.14:** $R_1$ = H, $R_2$ = Br, $R_3$ = H
**3.15:** $R_1$ = $R_2$ = $R_3$ = H
**3.16:** $R_1$ = Me, $R_2$ = $R_3$ = H
**3.17:** $R_1$ = Bn, $R_2$ = $R_3$ = H

**3.18:** $R_1$ = H, $R_2$ = F, $R_3$ = Cl 32%
**3.19:** $R_1$ = H, $R_2$ = F, $R_3$ = Br 26%
**3.20:** $R_1$ = H, $R_2$ = H, $R_3$ = F 25%
**3.21:** $R_1$ = H, $R_2$ = Cl, $R_3$ = H 35%
**3.22:** $R_1$ = H, $R_2$ = H, $R_3$ = Cl 28%
**3.23:** $R_1$ = H, $R_2$ = Br, $R_3$ = H 39%
**3.24:** $R_1$ = $R_2$ = $R_3$ = H 41%
**3.25:** $R_1$ = Me, $R_2$ = $R_3$ = H 24%
**3.26:** $R_1$ = Bn, $R_2$ = $R_3$ = H 55%

**Scheme 3.5** Selective α-bromination of substituted 3-acetylindoles

a) $CuBr_2$, $CHCl_3$, EtOAc, reflux

Thus, the alpha bromination of 3-acetylindoles with $CuBr_2$ led to our desired α-bromo carbonyl compounds, albeit in low yields. Our group had previously conducted an in-depth study of this bromination reaction, and found that when applied to compound **3.15**, a second bromination readily occurs after roughly 50% conversion to **3.24**, resulting in a dibrominated compound, and consequently reduced yields. This effect was further enhanced when applied to C-6 halogenated compounds.[100] Therefore in order to avoid obtaining even lower yields due to formation of the dibrominated side product, each of these reactions were constantly monitored by TLC. This was in addition to monitoring colour change of the reaction suspension from green to amber. By this method, we could recover unreacted 3-acetyl indole and repeat the reaction if necessary.

### 3.2.4.1 Characterisation of compounds 3.18 – 3.26

To illustrate the successful formation of our target α-bromoketones, the $^{1}$H-NMR spectrum of compound **3.21** is shown below (**Figure 3.4**). Here we a observed a new chemical shift at δ 4.66 ppm integrating for 2 protons, which correlates to a conversion of the $CH_3$ group to a $CH_2$ following successful bromination.

Furthermore, the $^{13}$C NMR spectrum featured the characteristic signals of the $CH_2$ (δ 33.4 ppm) functionality and carbonyl carbon (δ 186.5 ppm) after successful synthesis of α-bromo carbonyl compounds.

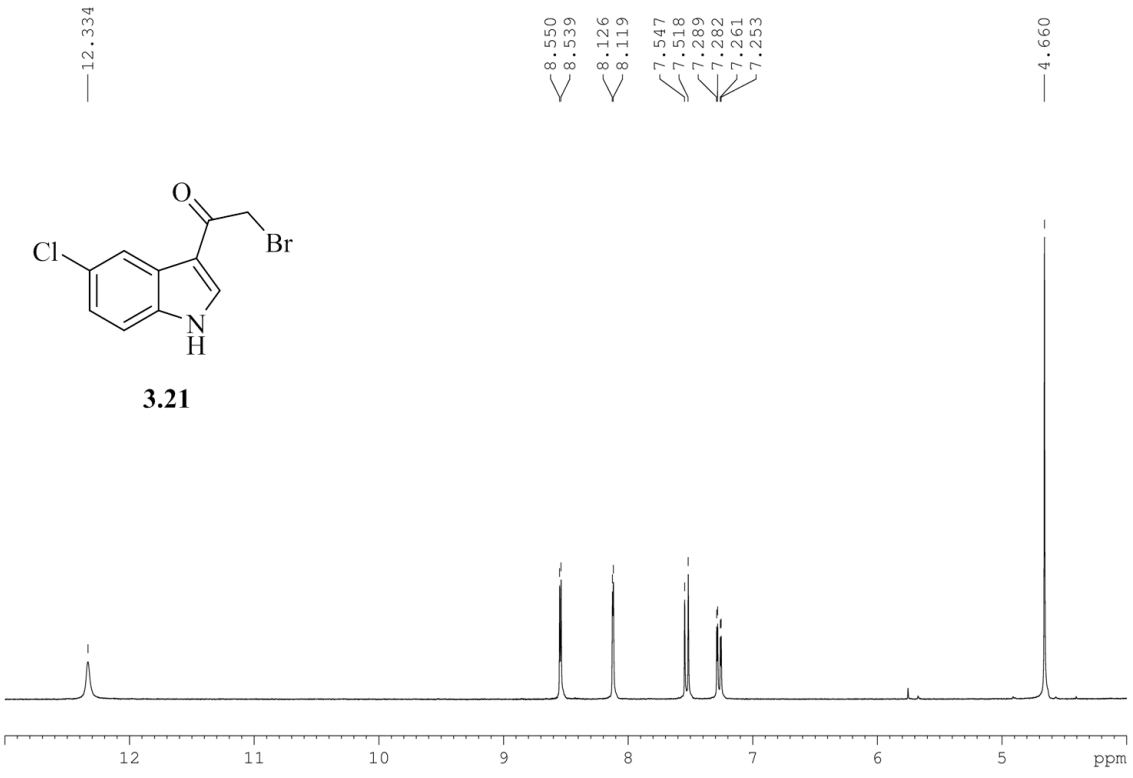


**Figure 3.4**: $^{1}$H NMR spectrum (300 MHz, DMSO-$d_6$) for compound **3.21**

### 3.2.5 Nucleophilic coupling reaction to generate α-aryl substituted 3-indolylethanones

#### 3.2.5.1 Overview of nucleophilic displacement of α-bromoketones

The specific nucleophilic substitution of the α-bromine was identified as the critical step to afford our desired final compounds. Accordingly, we reviewed many of the reported methods used to nucleophilically substitute halogens with either an amine, hydroxyl or thiol functionality.

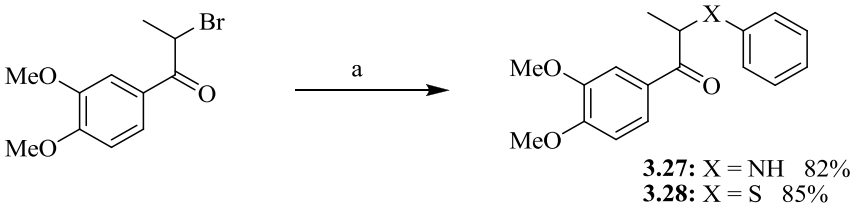


**Scheme 3.6** Barata *et al*.`s synthesis of **3.27** and **3.28**[104]

a) Aniline/ Thiophenol, $NaHCO_3$/ $K_2CO_3$, butanone, 3-8 hr, 80 $^oC$

Barata *et al.*[104] prepared the *β*-ketoamine **3.27** and *β*-ketosulfide **3.28** as intermediates in the synthesis of Surinamensin analogues, an active antileishmanial agent (**Scheme 3.6**). In this procedure, $NaHCO_3$ or $K_2CO_3$ were used as a coupling agent to assist nucleophilic displacement, with the unusual solvent butanone.

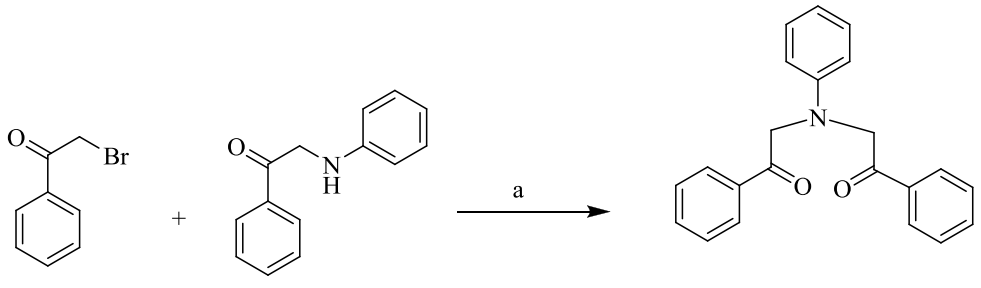


**Scheme 3.7** Fourrey`s synthesis of **3.30**[105]

a) $KHCO_3$, tetrabutylammonium hydrogen sulphate, 1 hr, 80 $^oC$

Fourrey[105] and co-workers performed the nucleophilic substitution of compound **3.29** with *N*-phenacylaniline under phase-transfer catalysis conditions in the presence of $KHCO_3$ to afford their synthetic intermediate **3.30** (**Scheme 3.7**). For the purposes of our study, we were keen to avoid a second halogen substitution as observed here, and therefore resolved to use an excess of the relevant nucleophile.

Pal *et al*.,[106] Rao *et al*.[107] and Chen *et al*.[108] all successfully synthesized anilinoacetophenone (**3.31**) from **3.29** with the aid of $NaHCO_3$ in ethanol (**Scheme 3.8**). Interestingly, in their method, they were able to avoid competition for **3.29** from nucleophilic ethanol, which was present in excess. A similar reaction was observed by Gupta *et al*.[109], where they also treated **3.29** with aniline in the presence of $Na_2CO_3$/ $K_2CO_3$ to obtain **3.31**.

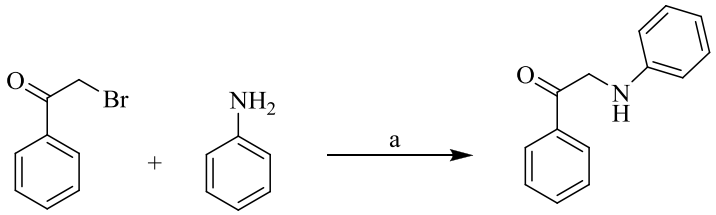


**3.29** **3.31**

**Scheme 3.8** General synthesis of **3.31**

a) $NaHCO_3$, ethanol, $N_2$, 6 hr, 25°C

He *et al*.[110] reported the synthesis of thioether **3.32** (87%) through nucleophilic substitution of the α-bromine with the assistance of $K_2CO_3$ in ethanol (**Scheme 3.9**). In a related synthesis, Fatunsin *et al*.[111] obtained **3.32** (95%) as a precipitate after adding the mixture into ice-water. Loghmani-Khouzani *et al*.[112] generated **3.32** in 95% yield after stirring the

starting materials together for 10 min in ethanol. Remarkably, the base used in this reaction, sodium ethanolate, did not compete in the reaction.

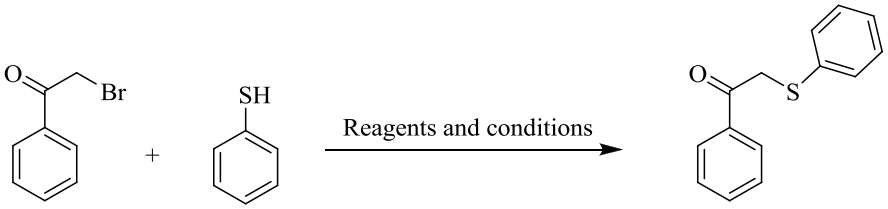


**3.29** **3.32**

**Scheme 3.9** General synthesis of **3.32**

Aveniente *et al*.[113] prepared the thioether **3.32** (**Scheme 3.9**) and ether **3.33** (**Scheme 3.10**) in butanone using $K_2CO_3$ as a coupling agent. Refluxing the mixture for 3 – 6 hr afforded **3.32** and **3.33** in yields of 79% and 75%, respectively. Similarly, Strassberger *et al*.[114] utilised KOH as a base in DMF for their nucleophilic synthesis of **3.33** (86%).

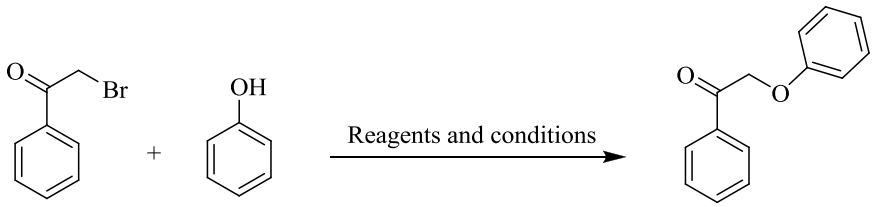


**3.29** **3.33**

**Scheme 3.10** General synthesis of **3.33**

He *et al*.[110] coupled alpha and beta naphthol with **3.29** by employing $K_2CO_3$ under reflux in acetone for 2 hr to form **3.34** and **3.35** (**Scheme 3.11**).

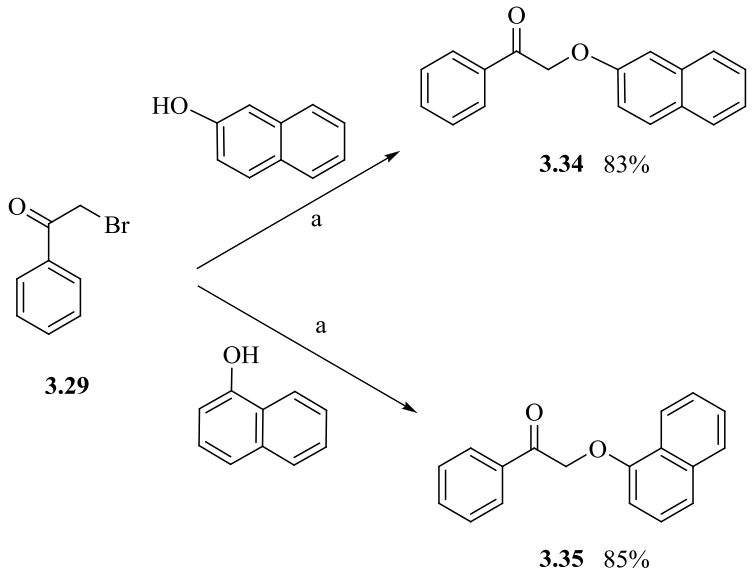


**Scheme 3.11** He`s synthesis of **3.34** and **3.35**[110]

a) $K_2CO_3$, acetone, 2 hr, reflux

While most procedures present in the literature utilised some manner of base, in a polar solvent, Spiteri *et al*.[115] and Ritson *et al*.[116] were interested in using the halophilic nature of cationic silver to aid the initial nucleophilic displacement of bromine in their Hantzsch oxazole synthesis **3.29** (**Scheme 3.12**). Here they showed that various silver salts could be incorporated to improve the yield of their reaction where they obtained oxazole **3.36** in 81% yield.

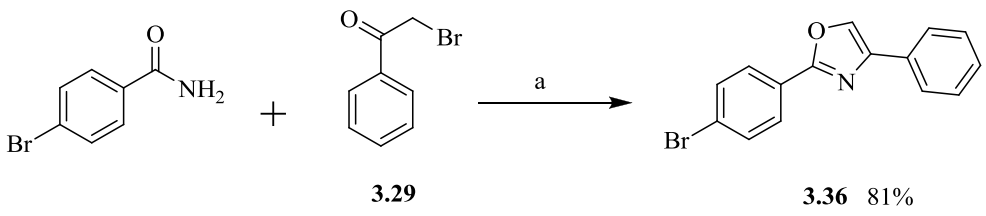


**Scheme 3.12** Spiteri`s synthesis of **3.36**[115]

a) $AgSbF_6$, DCE, 2 hr, 90 $^oC$

Having considered various reaction conditions discussed above, we opted to avoid any possible side reactions from nucleophilic solvents or bases such as ethanol or ethoxide. Due to the relative ease of access of acetone over butanone, we opted for the former for our study. As a coupling agent, we decided to compare several available silver salts to the readily available $K_2CO_3$ in order to possibly improve our procedure.

### 3.2.5.2 Optimisation of nucleophilic coupling reaction to generate indolyl-3-ethanone-α-amines, ethers and thioethers

In light of the work of Ritson *et al*.,[116] who proposed that a silver cation formed from salt dissociation, coordinates to an α-bromine, thereby activating it toward nucleophilic attack, we hypothesized that the coordination of silver to the bromine atom of **3.24** would activate the halogenated carbon atom toward nucleophilic attack to obtain our desired compounds (**Scheme 3.13**).

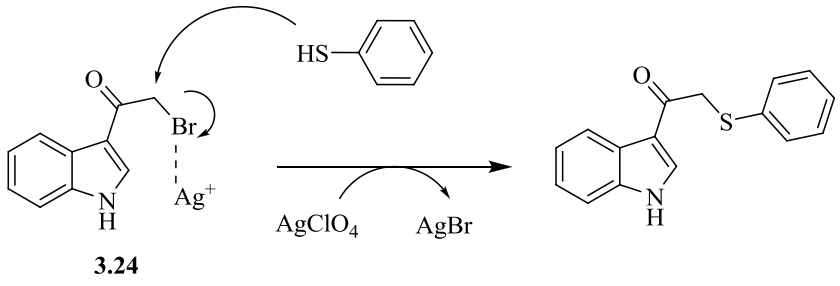


**Scheme 3.13** Proposed silver-mediated coupling, adapted from Ritson *et al*.[116]

Accordingly, we compared the isolated yields of an indolyl-3-α-amine (**3.37**), thioether (**3.38**) and an ether (**3.39**) formed with the assistance of either a silver salt or $K_2CO_3$ as well as the formation of an additional thioether (**3.40**) formed through the combined use of a silver salt and $K_2CO_3$ (**Scheme 3.14, Table 3.1**).[104,109,110,113]

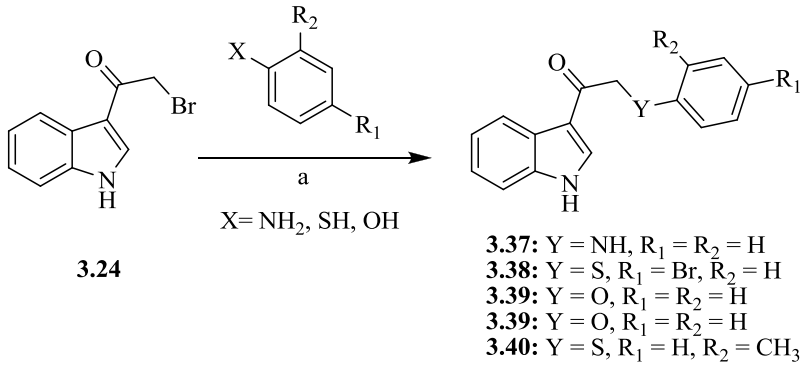


**Scheme 3.14** Sythesis of α-aryl substituted 3-indolylethanones

a) Acetone, 5 hr, reflux

As an initial control to determine the necessity of a base for the coupling reaction, we attempted the synthesis of compound **3.37** (**Table 3.1**) in the absence of base, resulting in no reaction occurring. The use of various silver salts resulted in the formation of **3.37**, at low yield, while the $K_2CO_3$ assisted the formation of **3.37** in a moderate yield. A similar trend was observed upon application of these reactions toward the formation of **3.38** and **3.39**, confirming the superiority of $K_2CO_3$ for this particular reaction. Out of interest, we attempted the synthesis of **3.40** though the combined use of 1 eq. each of $AgClO_4$ and $K_2CO_3$. Intriguingly, this combination performed marginally better than $K_2CO_3$ on its own. However, we decided that a small increase in yield, did not justify the use of an additional reagent. We therefore proceeded with the synthesis of our desired cohort of compounds

using the method described by He *et al.*[110], which involves the use of $K_2CO_3$ in acetone under reflux conditions (**Scheme 3.15**). The target compounds were isolated as either yellow or white crystalline solids ranging between 12 – 96 % yields.

**Table 3.1:** Optimisation of the coupling reactions

| Compound formed | Coupling agent | Isolated Yield |
|---|---|---|
| **3.37** | No base | 0% |
| | $AgClO_4$ | 25% |
| | $AgBF_4$ | 15% |
| | $AgNO_3$ | 25% |
| | $K_2CO_3$ | 57% |
| **3.38** | $AgClO_4$ | 49% |
| | $AgBF_4$ | 44% |
| | $AgNO_3$ | 34% |
| | $K_2CO_3$ | 92% |
| **3.39** | $AgClO_4$ | 7% |
| | $AgBF_4$ | 6% |
| | $AgNO_3$ | 15% |
| | $K_2CO_3$ | 39% |
| **3.40** | $K_2CO_3$: $AgClO_4$ (1:1) | 44% |
| | $K_2CO_3$ | 34% |

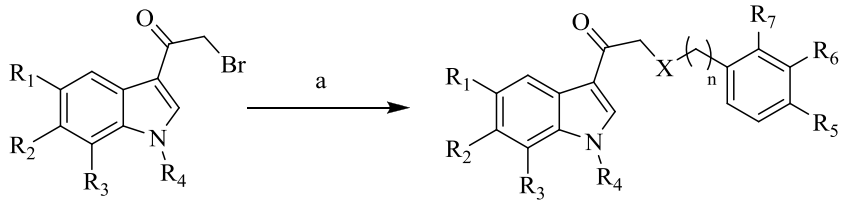


**3.37 - 3.73** See tables **4.1**, **4.2**, **4.3**, **4.4** and **4.5**
X = NH, O or S

**Scheme 3.15** Synthesis of **3.37 - 3.73**

a) NH, O, S nucleophile, $K_2CO_3$ (2 eq), acetone, reflux, 5 hr

### 3.2.5.3 Characterisation of compounds 3.37 – 3.73

Compounds **3.37 – 3.73** were characterised by common analytical techniques. The $^{1}$H-NMR spectra of all compounds showed the presence of new aromatic protons through the introduction of variously substituted anilines, phenols and thiophenols. For example, in the $^{1}$H-NMR spectrum of **3.54** the *para*-nitro thiophenyl protons present as a set of correlating doublets in addition to indole signals in the aromatic region of the spectrum (**Figure 3.5**). The full structural elucidation of each compound (i.e. **3.37 – 3.73**) was carried out using 2D NMR spectroscopic data sets consisting of COSY, HSQC and HMBC spectra. In addition, high resolution mass spectra were obtained for all final compounds.

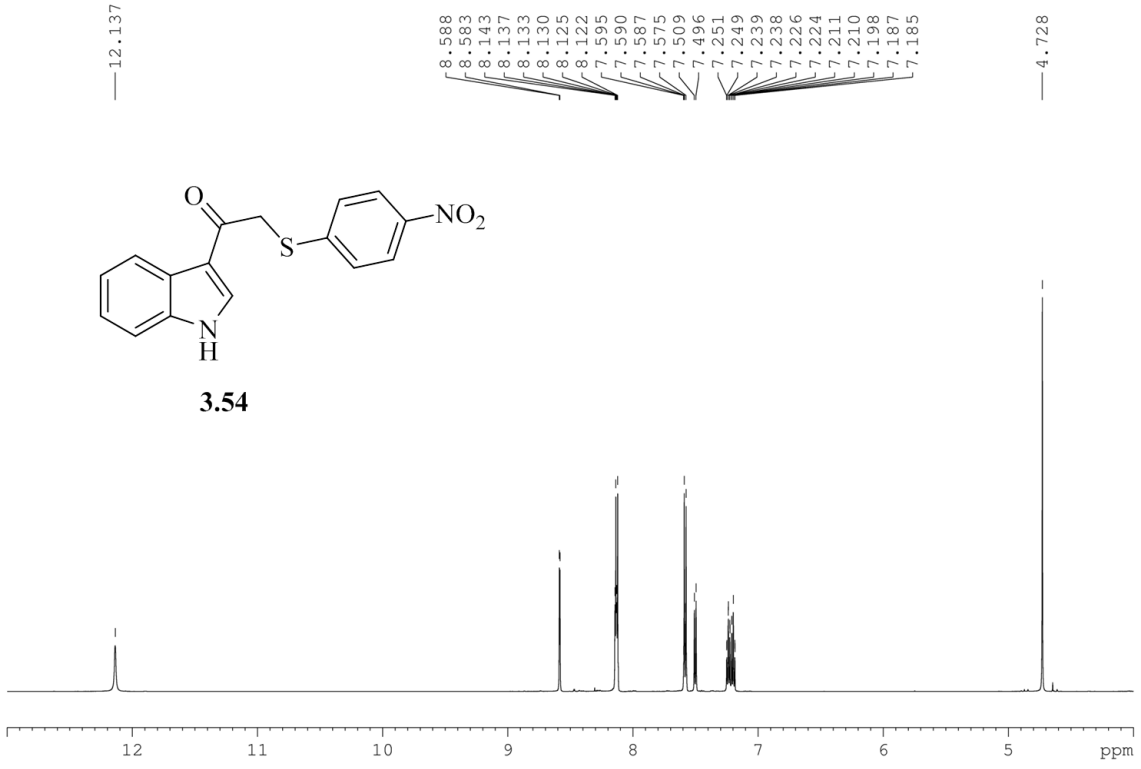


**3.54**

**Figure 3.5**: $^{1}$H NMR spectrum (300 MHz, DMSO-$d_6$) for compound **3.54**

### 3.3 Conclusions

In conclusion, we were able to successfully synthesise our desired compounds in low to moderate yields. We opted to synthesise our target compounds *via* a three-step method beginning with acetylation of indole, when 3-acetylindoles were not already available (**section 3.2.2**) followed by selective bromination (**section 3.2.4**). The rationale for this workflow being that direct formation of α-haloketones (**3.8a** and **b**) from indole has been unsuccessful in our laboratory previously.

Finally, we were able to couple our α-bromoketones with an amine, phenol or thiophenol with the assistance of a either a silver salt, or $K_2CO_3$. A comparative study of these coupling agents, revealed that $K_2CO_3$ was superior to the three silver salts used in this study, therefore we synthesized the remainder of our final desired compounds (**3.37 – 3.73**) with $K_2CO_3$ in acetone.

# Chapter Four

## Biological evaluation and docking study of indolyl-3-ethanone-α-amines, ethers and thioethers

### 4.1 Introduction: Brief overview of phenotypic vs. target based assays

Target-based and phenotypic screening are the two major strategies currently used in early drug discovery.[117] Phenotypic screens look at the phenotypic changes that compounds induce in tissues or cell-based assays whereas target-based screens measures the *in vitro* effects of a compound on a purified target protein.[118,119]

Several eminent opinions in modern drug discovery consider phenotypic screening superior to that of target based screening for discovering new classes of drugs, particularly against novel targets.[120] Hypothetically, phenotypic screens will select for compounds with built in preferential properties like cell wall penetration, whilst providing a more realistic physiological-like environment in which a drug and target might encounter each other.[120]

However, in phenotypic screening, a compound of interest could be acting on one or possibly more undescribed target/s simultaneously.[117,118] Therefore target deconvolution has been stated as one of the major drawbacks of phenotypic screening.[118] The knock on effect of slow target deconvolution and subsequent lack of mechanistic understanding of the hit compound slows down the progression of a drug candidate through the drug discovery pipeline[117], except occasionally in desperate instances where the knowledge of the target may not hinder the drug approval process.[119] Conversely, the mechanistic hypothesis in a target-based approach allows for a rapid proof of a biological mechanism, but is best utilised for monogenic disease conditions[117] and may in some instances require

more than one candidate target to find a potent lead.[118] Additionally, this approach suffers from a lack of information about the utility of a hit compound in a more biologically accurate system best utilised for monogenic disease conditions.[117,118]

Accordingly, since our goal in this study was to discover new antimalarials with possibly new mechanisms of action, we opted to screen new compounds in a whole cell phenotypic screen against a chloroquine-sensitive strain of *P. falciparum* (3D7). As a control measure, all compounds were screened for cytotoxicity using the human derived HeLa cell line.

## 4.2 Biological evaluation of α-aryl substituted 3-indolylethanones

### 4.2.1 Phenyl modification

Consistent with the objective of this project we sought out, in the first instance, to probe the differences in biological activity between a small cohort of related indolyl-3-ethanone-α-amines, indolyl-3-ethanone-α-ethers and indolyl-3-ethanone-α-thioethers **3.37**, **3.39** and **3.41 – 3.44** (**Table 4.1**). The clogP values were obtained using the computer free online software package pkCSM.[121]

Compound **3.37**, whose α-amino carbonyl motif resembles that of the amino acid glycine, was found to be poorly active against 3D7, but with an encouraging lack of cytotoxicity against HeLa cells. Substitution of aniline with para-chloro aniline (**3.41**) resulted in a moderate increase in antimalarial activity, coupled to a significant increase in cytotoxicity.

Replacing the aniline moiety with a phenolic group severely reduced the activity with compound **3.39** showing no activity at maximum tested concentration. Pleasingly, moderate antiplasmodial activity was re-gained upon introduction of a sulfur atom of thiophenol

(**3.42)** which showed a similar $IC_{50}$ value to **3.41** with a significant reduction in HeLa cytotoxicity. Activity and selectivity were further enhanced, with the introduction of a chlorine atom at the para position for both thiophenol and phenol compounds **3.43** and **3.44** respectively.

**Table 4.1:** *In vitro* antiplasmodial and cytotoxicity inhibitory activities of compounds **3.37**, **3.39** and **3.41 – 3.44**.

| Compound no. | Structure | $IC_{50}$ (μM) | | clogP |
|---|---|---|---|---|
| | | 3D7 | HeLa | |
| **3.37** | 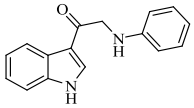 | 73 | > 500 | 2.9 |
| **3.41** | 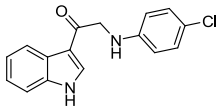 | 29 | 16 | 3.6 |
| **3.39** | 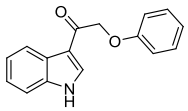 | > 500 | > 500 | 2.9 |
| **3.42** | 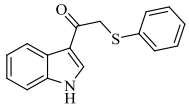 | 29 | 284 | 3.6 |
| **3.43** | 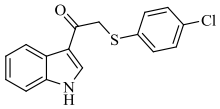 | 1.4 | > 500 | 4.3 |
| **3.44** | 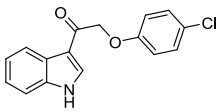 | 1.8 | > 500 | 3.6 |
| **CQ** | | 0.028 | | |
| **Emetine** | | | 0.37 | |

Tentatively, these results suggested that a clogP less than 3 significantly hampered activity, while a para chloro substituent on the aryl ring significantly improved activity. Moreover, an α-sulfur atom appeared more important for activity than the corresponding NH and O bioisosteres. Following the identification of active compound **3.43** (**Table 4.1**), we resolved to retain the α-sulfur atom while exploring further the influence of different substituents on the phenyl ring of the indolyl-3-ethanone-α-thioether scaffold. Additionally, we investigated substitution at the *ortho*, *meta* and *para* positions of the phenyl ring. These results are summarised below (**Table 4.2**).

**Table 4.2:** *In vitro* antiplasmodial and cytotoxicity inhibitory activities of compounds **3.38**, **3.40** and **3.45 – 3.54**.

| Compound no. | Structure | $IC_{50}$ (μM) | | clogP |
|---|---|---|---|---|
| | | 3D7 | HeLa | |
| **3.45** | 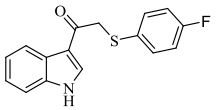 | 1.7 | > 500 | 3.8 |
| **3.38** | 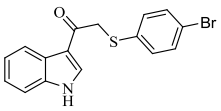 | 1.3 | > 500 | 4.4 |
| **3.46** | 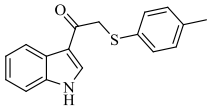 | 19 | > 500 | 3.9 |
| **3.47** | 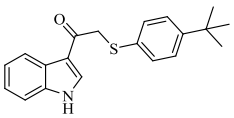 | 8.9 | > 500 | 4.9 |
| **3.48** | 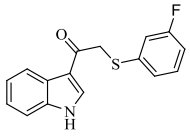 | 3.9 | > 500 | 3.8 |

**Table 4.2: Continued**

| Compound no. | Structure | $IC_{50}$ (μM) | | clogP |
|---|---|---|---|---|
| | | 3D7 | HeLa | |
| **3.49** | 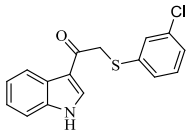 | 44 | > 500 | 4.3 |
| **3.50** | 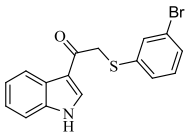 | 106 | > 500 | 4.4 |
| **3.51** | 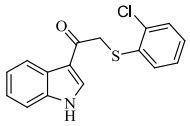 | > 500 | > 500 | 4.3 |
| **3.40** | 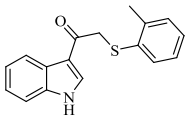 | 12 | > 500 | 3.9 |
| **3.52** | 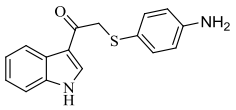 | 20 | 36 | 3.2 |
| **3.53** | 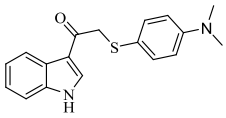 | 105 | 60 | 3.7 |
| **3.54** | 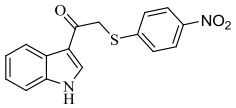 | 0.24 | > 500 | 3.4 |
| **CQ** | | 0.028 | | |
| **Emetine** | | | 0.37 | |

Bioisosteric replacement of the chlorine atom of **3.43** to yield fluorinated and brominated analogues **3.45** and **3.38** respectively, resulted in no significant changes in activity against 3D7 or HeLa. In order to investigate whether improved activity of compounds **3.43**, **3.45** and **3.38** over **3.42** was a function of a possible hydrophobic interaction, with a putative

receptor, we evaluated the effect of both the hydrophobic *para* methyl (**3.46**) and *tert*-butyl (**3.47**) functionality, both of which resulted in a decrease in antiplasmodial activity. This result suggests that the interaction between the para phenyl of these ligands and the unknown receptor is not purely hydrophobic, and is possibly due to halogen bonding. Shifting of the small fluorine to the *meta*-position (**3.48)** had a negligible effect on activity, while the chloro and bromo analogues (**3.49** and **3.50**) lost significant activity in comparison to the *para*-substituted analogues (i.e. **3.38**, **3.43** and **3.45**). However, compound **3.48** – **3.50** still showed no noticeable cytotoxicity against the HeLa cell line (**Table 4.2**). Finally, compounds **3.51** and **3.40** suggested that *ortho*-substitution was poorly tolerated in this system, especially considering that **3.51** was ineffective against the 3D7 cell line. This data suggested that the halogens at the *para*-position are important for antiplasmodial activity of this series.

Having observed the superior antiplasmodial activity of para halogenated analogues (**3.43, 3.45** and **3.38**) over para alkyl substituted compounds (**3.46** and **3.47**), we were curious as to the effect of different ionisable moieties at the *para*-position. Significant drops in antiplasmodial activity were observed for the primary amino (**3.52**) and tertiary amino (**3.53**) substituted compounds, coupled to significant loss of selectivity over HeLa cells. A remarkable improvement in activity into the mid to low nanomolar range was observed upon the introduction of a nitro functionality at the *para*-position (**3.54**) and importantly, this hit compound maintained high selectivity for the plasmodial cells over HeLa cells. This observation also supported our previous observation about the interactions between this portion of the ligands and the unknown receptor.

### 4.2.2 Chain length modification

Having established a trend for the nature and position of thiophenyl substitution, we turned our focus to the effect of chain length between the sulfur atom and the aryl moiety. The results are summarised below (**Table 4.3**).

**Table 4.3:** Growth inhibitory assays of compounds **3.55 – 3.61**.

| Compound no. | Structure | $IC_{50}$ (μM) | | clogP |
|---|---|---|---|---|
| | | 3D7 | HeLa | |
| **3.55** | 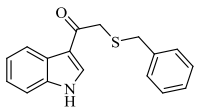 | 131 | > 500 | 3.7 |
| **3.56** | 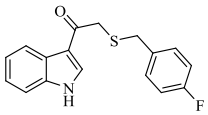 | 58 | > 500 | 3.8 |
| **3.57** | 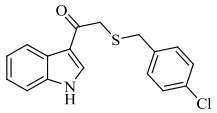 | > 500 | > 500 | 4.3 |
| **3.58** | 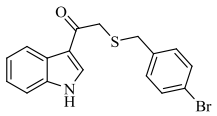 | > 500 | > 500 | 4.4 |
| **3.59** | 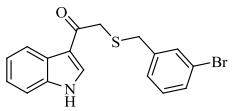 | 13 | 35 | 4.4 |
| **3.60** | 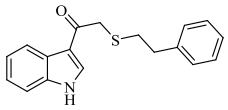 | 7.8 | 14 | 3.8 |
| **3.61** | 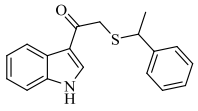 | 122 | 76 | 4 |
| **CQ** | | 0.028 | | |
| **Emetine** | | | 0.37 | |

Generally, extending the chain by one carbon atom (**3.55** – **3.58**) resulted in a significant loss in overall activity, particularly in the case of the *para*-chlorinated (**3.57**) and *para*-brominated (**3.58**) analogues, where antiplasmodial activity was completely lost. Interestingly, the introduction of a bromine atom at the thiophenyl *meta*-position (**3.59**) only resulted in a moderate drop off in activity, but introduced a dramatic increase in cytotoxicity.

A further increase in chain length to generate phenylethyl analogue (**3.60**), did not mirror the antiplasmodial trend observed for **3.55**, displaying moderate activity, coupled to the greatest HeLa cytotoxicity observed in this series. The final racemate analogue in this series **3.61** which features a methyl substituent protruding off the extended chain, was also found to have no reasonable activity.

### 4.2.3 Indole modification

Having narrowed the SAR parameters of the thiophenyl portion of our scaffold (see section **4.2.2**) and observing that lengthening of the chain was not tolerated, we turned our attention to the effect of variable substitution on the indole ring system. Due to availability of chemical substrate, we opted in this portion of the study, to compare any effect to the para brominated compound **3.38**, which had shown moderate, yet encouraging activity. The results are summarised below (**Table 4.4**).

C-6 fluorination and chlorination (**3.62** and **3.63**) resulted in negligible changes to activity, while interestingly, C-6 functionalisation with a larger C-6 bromine decimated antiplasmodial activity. Upon shifting the position of the halogen atom to C-5, we noticed a

dramatic improvement in antiplasmodial activity again into the low nanomolar range, with a high degree of selectivity.

**Table 4.4:** Growth inhibitory assays of compounds **3.62 – 3.68**.

| Compound no. | Structure | $IC_{50}$ (μM) | | clogP |
|---|---|---|---|---|
| | | 3D7 | HeLa | |
| **3.62** | 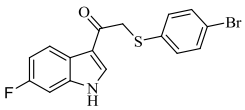 | 1.3 | > 500 | 4.5 |
| **3.63** | 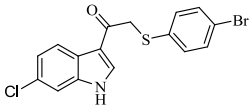 | 2.8 | > 500 | 5.1 |
| **3.64** | 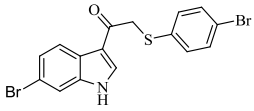 | 279 | > 500 | 5.2 |
| **3.65** | 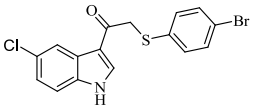 | 0.09 | > 500 | 5.1 |
| **3.66** | 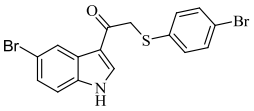 | 0.12 | > 500 | 5.2 |
| **3.67** | 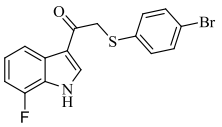 | 2.4 | > 500 | 4.6 |
| **3.68** | 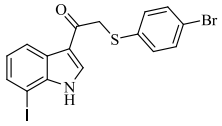 | 45 | 56 | 5 |
| **CQ** | | 0.028 | | |
| **Emetine** | | | 0.37 | |

The C-7 indole position was explored through a small fluorine (**3.67**) and large iodine (**3.68**) containing analogue. While **3.67** offered no change in terms of antiplasmodial activity, compound **3.68** displayed significantly reduced antiplasmodial activity coupled to a re-emergence of cytotoxicity.

**Table 4.5:** Growth inhibitory assays of compounds **3.69 – 3.73**.

| Compound no. | Structure | $IC_{50}$ / µM | | clogP |
|---|---|---|---|---|
| | | 3D7 | HeLa | |
| **3.69** | 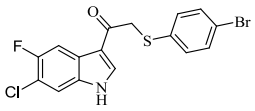 | 12 | > 500 | 5.2 |
| **3.70** | 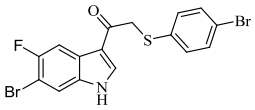 | 19 | > 500 | 5.3 |
| **3.71** | 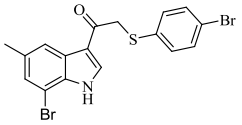 | 1.8 | 224 | 5.5 |
| **3.72** | 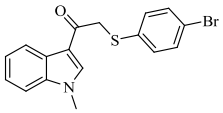 | 15 | > 500 | 4.9 |
| **3.73** | 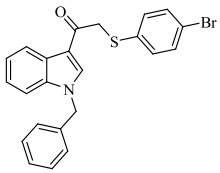 | 2.7 | > 500 | 6.4 |
| **CQ** | | 0.028 | | |
| **Emetine** | | | 0.37 | |

Inspired by NITD609, a compound currently in phase 1 clinical trials as an antimalarial drug, which features both a C-5 fluoro and C-6 chloro substitution on the indole ring, we prepared

dihalogenated compounds **3.69** and **3.70**, both of which displayed unremarkable activity (**Table 4.5**).

The first in this series to feature an indole alkyl substituent, compound **3.71**, also featured a large C-7 bromine. While a measure of cytotoxicity was recorded, mirroring the observation of **3.67**, **3.71** still maintained moderate activity.

Finally, the importance of the indole NH was assessed through compounds **3.72** and **3.73**. While the methylation resulted in a decline in activity, benzylation had limited effect, when compared to **3.38**. This suggests that while the NH is important for activity, the loss of this H-bond donating effect is off-set by the binding interactions of the benzyl group.

## 4.3 *In silico* docking studies

### 4.3.1 Overview: *In silico* design

The time and resource consuming processes of drug discovery and development has led to the incorporation of computational power into the drug discovery pipeline.[122,123] Computer aided or *in silico* design can be utilised to model and observe interactions between a putative drug (ligand) and its biological target (receptor).[122–124] *In silico* design can also be used alongside experimentally derived *in vitro* data in order to help interpret structure activity relationships.[122–124] Molecular docking provides an approximate insight into the expected conformation and orientation of the ligand within a given receptor.[122–125] Furthermore, scoring functions can be used to estimate the binding affinity of a given ligand to a receptor.[122–124]

However, while docking studies can be useful tools particularly in target based drug design, these techniques still suffer from a number of drawbacks.[125,126] Receptors which are used for docking studies are a static representation of a dynamic system, where a ligand influences the conformation of a biological receptor.[125,126] Therefore, docking may not predict favourable binding interactions for a ligand, since this technique can only take into account limited changes in protein conformation. In some instances, the scoring function could rank inactive compounds equal or better than active compounds thereby possibly leaving active compounds undetected.[125] Furthermore, the role of biological solvent (water) is difficult to fully ascertain. These molecules are electrostatically associated to the receptor and play a major role in serving as hydrogen bond bridges between the ligand and receptor protein site.[126] However, knowing which waters to retain for a docking experiment is often problematic.

### 4.3.2 *In silico* assessment

As part of their campaign to identify novel targets for the development of new antimicrobial agents, Dennis *et al*.[127] isolated 6-hydroxymethyl-7,8-dihydropterin pyrophosphokinase (HPPK), which is involved in the folate biosynthetic pathway of *S. aureus* and directly precedes dihydropteroate synthase (DHPS), a common and validated target for sulfonamide antimicrobials.[127] HPPK catalyses pyrophosphoryl transfer from a magnesium-bound ATP cofactor to 6-hydroxymethyl-7,8-dihydro-pterin (HMDP) in the folate pathway.

Folate is a precursor for purine biosynthesis which is required for DNA replication. Disruption of *de novo* folate biosynthesis is therefore lethal to microorganisms. Mammals obtain folates from diets, rendering this pathway selectively toxic to microorganisms.

Importantly for us, folate biosynthesis is also a validated antimalarial pathway. Furthermore, the HPPK enzyme shares 34 – 39% structure homology with other HPPK enzymes which sequences are known and is also present in *P. falciparum*, whilst being absent in humans suggesting that this could be a promising new target for antimalarial development.[128–131] To the best of our knowledge, HPPK is yet to be fully explored in the design of antimalarial agents.[132]

In their study, Dennis *et al*.[127] identified compound **4.1** as an inhibitor of *S. aureus* HPPK. Since this compound shares the α-thioketone moiety present in our series of antimalarials **3.37** – **3.73**, we were interested to see whether this enzyme might shed some light on their possible mechanism of action. Aiding to our speculations is the fact that the HPPK enzyme is absent in human beings and our compounds generally displayed negligible cytotoxicity against human HeLa. Furthermore, some recent unpublished data showed that several of our most active compounds tested here, were found to be inactive against a trypanosome strain, an organism which seemingly lacks HPPK, and is able to bypass certain enzymes used in folate biosynthesis. Accordingly, we conducted a speculative *in silico* docking study using our compounds on *S. aureus* HPPK which was retrieved from the protein data bank, co-crystallised with compound **4.1** (PDB ID: 4CRJ).[127] Proteins and ligands were prepared for docking using AutoDock 4[133] and docking experiments were performed using AutoDock Vina[134]. Discovery Studio 3.5 Visualiser[135] was used for ligand and receptor visualisations.

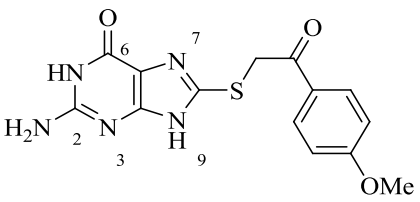


**4.1**

The analysis of the binding mode of **4.1** (**Figure 4.1**) revealed that the guanine moiety occupied a narrow binding region formed by π-stacking interaction between Phe54 and Phe123. In addition, cation-π interactions of the guanine scaffold with Val46 were observed including the H-bonds interactions.

The amine at position 2 had two H-bond interactions with Pro45 and Ala44, respectively. While the N and NH functionalities at position 3 and 1 interacted with Val46 through H-bonds. The carbonyl moiety at 6-position also interacted with Asn56 through the H-bonding interaction. Hydrophobic interactions between the adjoined aromatic ring and Arg88 were noted. Arg88 also interacted with the methoxy functionality through H-bonds.

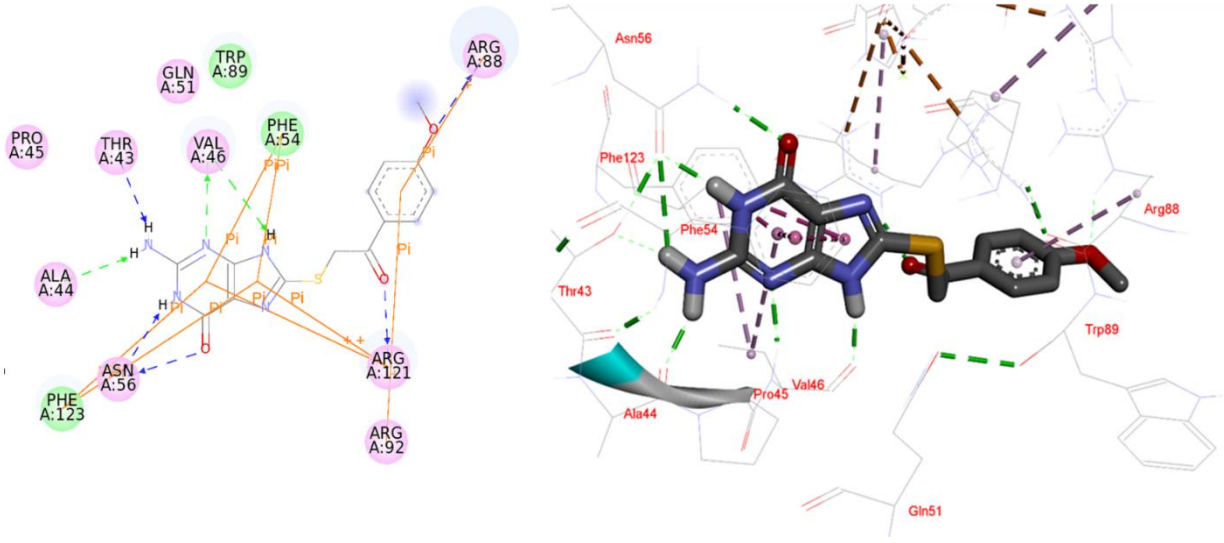


**Figure 4.1:** Left: A 2D representation of electrostatic interactions between compound **4.1** and HPPK. Right: Compound **4.1** occupying a binding pocket of *S. aureus* HPPK PDB ID:4CRJ.

The docking results of compounds **3.37 – 3.54**, revealed many similar binding interactions with HPPK. In our docking studies we observed that the indole moiety (**Figure 4.2**) occupied the same region of the pocket originally occupied by the guanine moiety of compound **4.1**

where the indole moiety was wedged between Phe54 and Phe123 through π-stacking interactions and hydrophobic interaction with Thr43, Val46 and Pro45. Additionally, our docking suggested a further interaction between the phenyl substituent and Arg88. Interestingly, while docking suggested that the *para* methyl (**3.46**) and *tert*-butyl (**3.47**) containing compounds had no interactions with the binding site, it was suggested that the *para*-halogenated compounds are able to form an electrostatic bond with Arg88, which seemingly supports our previous binding site hypothesis. Additionally, the para nitro containing compound **3.54** which showed potent antiplasmodial activity was also found to interact with Arg88 through hydrogen bonding (**Figure 4.2**).

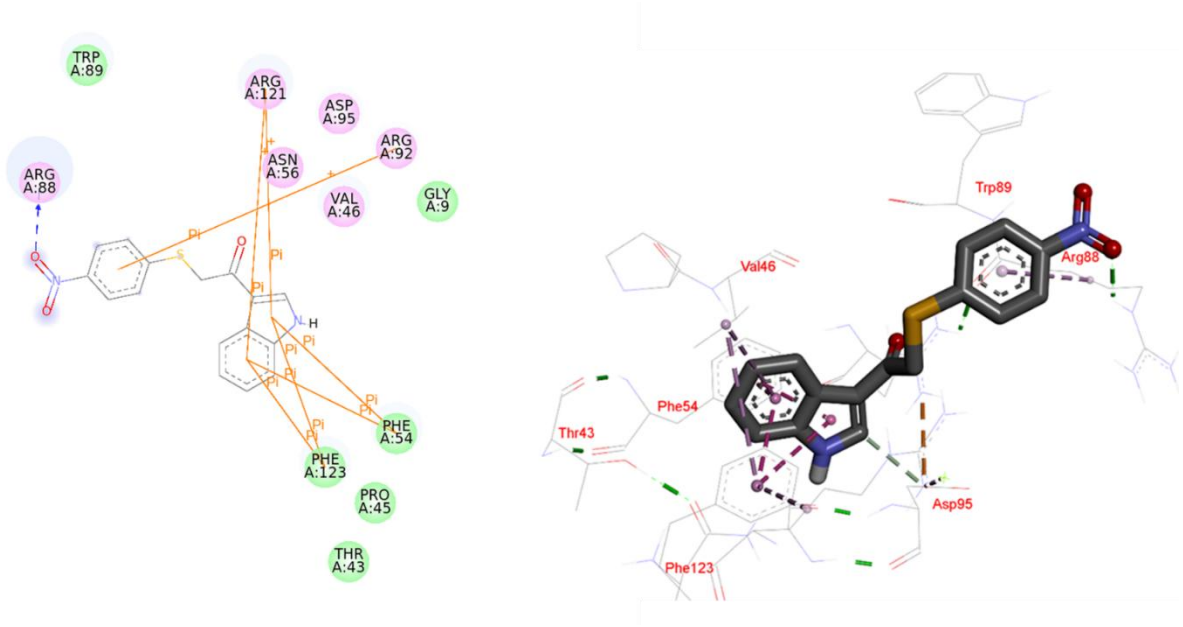


**Figure 4.2:** Compound **3.54** occupying the HPPK binding site featuring the additional hydrogen bonding interactions of the para-nitro substituent with Arg88.

Docking of the benzyl and phenylethyl analogues (**3.55 – 3.61**), placed the indole moiety in the same position as other docked analogues again as a result of π-stacking interactions with Phe54 and Phe123 as well as the hydrophobic interactions with Val46. However, the

extended chain seemingly upset the interaction between the *para* chloro substituent and Arg88, which we hypothesise is critical for activity. (**Figure 4.3**).

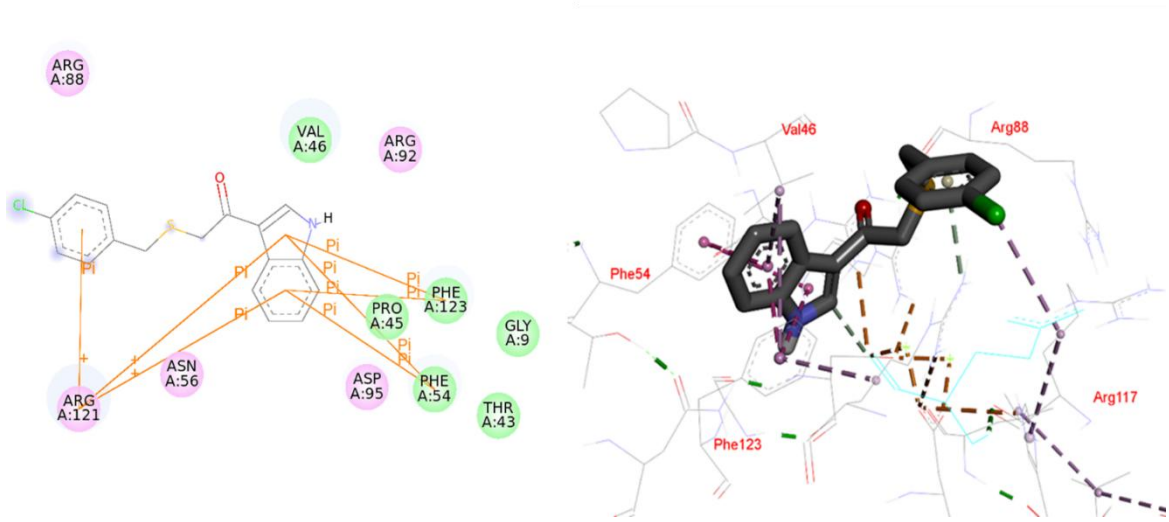


**Figure 4.3:** Compound **3.57** occupying the HPPK binding site featuring no interaction of the para-chlorine substituent with Arg88.

The docking of substituted indole analogues (**3.62** – **3.73**) again revealed the same π-stacking interactions of Phe54 and Phe123, and hydrophobic interactions of the valine pocket. What was of greatest significance to us however, was the C-5 substituted compounds such as **3.65**. In addition to the similar hydrophobic interactions, the chlorine group was placed in an additional hydrophobic pocket, which forced an altered binding pose leading to an additional new H-bond interaction between the indoles-NH functionality and Asp95 (**Figure 4.4**), which is the amino acid responsible for binding catalytic magnesium in HPPK.

We then docked compound **3.73** in order to test our hypothesis of the additional binding pocket which compensates for the lack of indole NH functionality. In addition to the normally encountered interactions of Phe54 and Phe123 through the hydrophobic π-

stacking and hydrophobic interactions with the indole moiety, we also observed that the benzyl portion of **3.73** occupied a previously unexplored region of HPPK, forming a π-edge stacking interaction with Phe123 (**Figure 4.5**) as well as an electrostatic interaction with Asp95. This provides a potential area for further optimisation in the search for new antimalarial agents.

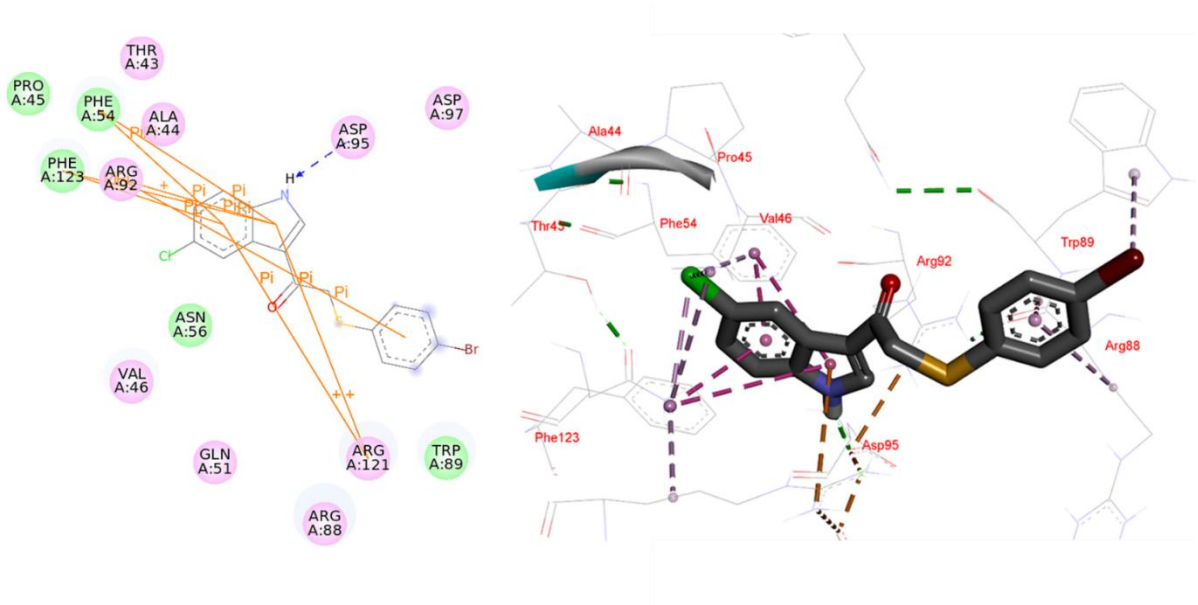


**Figure 4.4:** Compound **3.65** occupying the HPPK binding site featuring the additional H-bond interaction of the indole-NH functionality with Asp95.

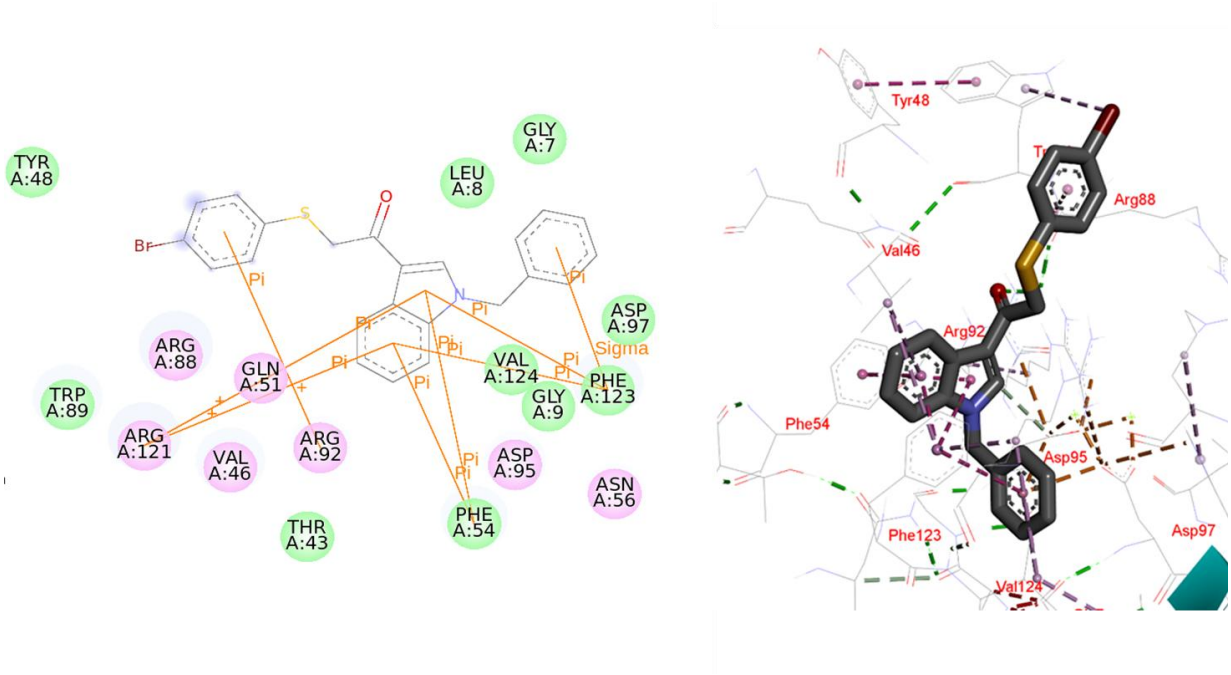


**Figure 4.5:** The benzyl portion of compound **3.73** occupying a previously unexplored region of the binding pocket allowing for additional π-edge stacking interaction with Phe123.

### 4.4 Conclusions

In this chapter we described a series of indolyl-3-ethanone-α- amines, ethers and thioethers and their *in vitro* activity as potential antimalarial agents against *P. falciparum* and their respective cytotoxicity against a HeLa cell line.

Our initial investigation showed that the thioether compounds showed a subtle, but important superiority over the corresponding amine and ether analogues, whilst also suggesting that a clogP below 3 resulted in weak plasmodial inhibition. No other trends relating to clogP were observed in the rest of the study. Deeper investigation suggested that the position and nature of the phenyl substitution had an important influence on antimalarial activity as well as the selectivity of these compounds. The general trend suggested that the *para* position was optimal for activity (i.e. **3.38** and **3.50**), whilst further

showing that a hydrophobic interaction (**3.46** and **3.47**) was not responsible for binding of this region, but rather a moiety capable of forming electrostatic interactions was preferred (**3.54**, $IC_{50}$ = 0.24 μM, **Table 4.2**). Extension of the chain length through replacement of the thiophenol moiety on the indolyl-α-thioether scaffold with the benzyl and phenylethyl functionalities was not tolerated (**Table 4.3**).

Exploring the space provided on the indole scaffold revealed substitution at the C-5 position to be critical, resulting in our most potent compounds **3.65** ($IC_{50}$ = 0.09 μM) and **3.66** ($IC_{50}$ = 0.12 μM) respectively. Di-substitutions on the indole scaffold did not result in any potent analogues being obtained. Also the probing of the indoles-NH functionality with both the methyl and benzyl groups did not result in improved antimalarial activity. However, in the case of the benzyl analogue the relative retention of activity was surprising.

Based on the fact that our compounds selectively inhibit malaria, do not inhibit trypanosomes and shared structure similarity to compound **4.1**, we conducted a series of docking experiments, in an attempt to support our hypothesis that our compounds potentially bind to HPPK. Docking at this site, supported our experimentally observed data, in a number of ways, including the reason for improved activity with the para halogenated and para nitro substituted compounds, as well as the reason for significantly improved activity of C-5 halogenated compounds **3.65** and **3.66** and the curious maintenance of activity with the benzylated analogue **3.73**.

# Chapter Five

## Experimental Section

### 5.1 Chemistry

#### 5.1.1 General chemistry

NMR spectra were acquired on either a Bruker Fourier 300 MHz, or a 600 MHz Avance II spectrometer. Chemical shifts are reported in ppm, referenced to residual solvent resonances ($CDCl_3$ $\delta_H$ 7.26, $\delta_C$ 77.0; DMSO-$d_6$ $\delta_H$ 2.50, $\delta_C$ 39.50 ppm).[136] High resolution mass spectrometry was performed on a Waters Synapt G2 TOF instrument with an ESI source. Flash chromatography was performed using Kieselgel 60 (230–400 mesh) silica gel. Anhydrous solvents were prepared by standard procedures outlined by Perrin and Amerego[137] as well as Casey, Leonard, Lygo and Procter.[138] Melting points were determined using a Reichert hot stage microscope (Protea Holdings Ltd.).

#### 5.1.2 General procedure for the synthesis of 3-acetylindoles (3.9 and 3.10)

$SnCl_4$ (520 µL, 1.2 eq.) was added to a stirred solution of indole (200 mg, 1 eq.) in dry DCM (7.5 mL) under argon at 0 °C after which the ice bath was removed. After stirring for 30 minutes acetyl chloride (1 eq.) was added dropwise to the reaction suspension, followed by nitromethane (4.5 mL). The reaction was quenched with ice and water after 4 hours and extracted with EtOAc (100 mL), washed with water (2 $\times$ 20 mL), sat. brine (2 $\times$ 30 mL) and dried over anhydrous $MgSO_4$. *In vacuo* solvent removal afforded a brown tarry solid which was dissolved in cold acetone and allowed to evaporate slowly. The resultant crystals were washed with cold chloroform to yield the desired compounds.[42]

**1-(6-chloro-5-fluoro-1H-indol-3-yl)ethanone (3.9):**

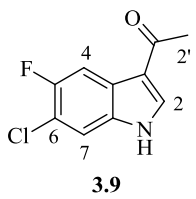

**3.9**

Yield = 68%; $^{1}$H NMR (DMSO, 300 MHz): $\delta_H$ 12.13 (s, 1H, NH-1), 8.42 (1H, s, H-2), 7.98 (1H, d, *J* = 10.2 Hz, H-4), 7.66 (1H, d, *J* = 6.4 Hz, H-7), 2.44 (3H, s, H-2′); $^{13}$C NMR (DMSO, 75 MHz): $\delta_C$ 192.8 ($q_c$, C-1′), 153.4 ($q_c$, d, $J_{F.C}$ = 220.3 Hz, C-5), 136.6 (CH, C-2), 131.1 ($q_c$, C-7a), 124.5 ($q_c$, d, $J_{F.C}$ = 10.0 Hz, C-3a), 116.9 ($q_c$, d, $J_{F.C}$ = 4.5 Hz, C-3), 114.9 ($q_c$, d, $J_{F.C}$ = 21.0 Hz, C-6), 113.6 (CH, C-7), 107.4 (CH, d, $J_{F.C}$ = 24.0 Hz, C-4), 27.2 ($CH_3$, C-2′) ppm.

**1-(6-bromo-5-fluoro-1H-indol-3-yl)ethanone (3.10):**

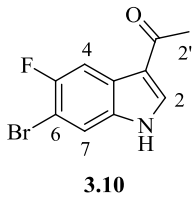

**3.10**

Yield = 55%; $^{1}$H NMR (DMSO, 300 MHz): $\delta_H$ 12.12 (s, 1H, NH-1), 8.40 (1H, s, H-2), 7.96 (1H, d, *J* = 9.6 Hz, H-4), 7.78 (1H, d, *J* = 5.9 Hz, H-7), 2.44 (3H, s, H-2′); $^{13}$C NMR (DMSO, 75 MHz): $\delta_C$ 192.9 ($q_c$, C-1′), 159.6 ($q_c$, d, $J_{F.C}$ = 220.3 Hz, C-5), 136.7 (CH, C-2), 133.7 ($q_c$, C-7a), 125.2 ($q_c$, d, $J_{F.C}$ = 9.1 Hz, C-3a), 116.8 ($q_c$, d, $J_{F.C}$ = 4.1 Hz, C-3), 116.3 (CH, C-7), 107.3 (CH, d, $J_{F.C}$ = 26.0 Hz, C-4), 103.0 ($q_c$, d, $J_{F.C}$ = 25.0 Hz, C-6), 27.2 ($CH_3$, C-2′) ppm.

### 5.1.3 General procedure for the synthesis of *N*-substituted 3-acetylindoles (3.16 and 3.17)

To a stirred solution of 3-acetylindole (200 mg, 1.26 mmol, 1 eq.) in DMF (4 mL) at 0 °C, was added NaH (60% in oil, 252 mg). After 15 minutes either iodomethane or benzyl bromide (1.88 mmol, 1.5 eq.) were added dropwise and allowed to react for 1 hour after which time the reaction was quenched with sat. aq. $NaHCO_3$. The reaction was extracted with EtOAc (15 mL) and concentrated *in vacuo*, followed by purification using normal phase flash chromatography (DCM: Hex 2:1).[102]

**1-(1-methyl-1H-indol-3-yl)ethanone (3.16):**[139]

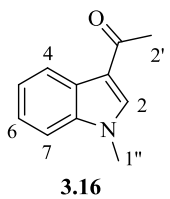

**3.16**

Yield = 30%; $^{1}$H NMR ($CDCl_3$, 400 MHz): $\delta_H$ 8.38-8.36 (1H, m, H-4), 7.70 (1H, s, H-2), 7.34-7.29 (3H, m, H-5, H-6, H-7), 3.84 (3H, s, H-1$''$); 2.52 (3H, s, 2$'$), $^{13}$C NMR ($CDCl_3$, 100 MHz): $\delta_C$ 193.0 ($q_c$, C-1$'$), 136.8 ($q_c$, C-7a), 134.9 (CH, C-2), 126.4 ($q_c$, C-3a), 124.3 (CH, C-6), 123.5 (CH, C-5), 121.9 (CH, C-4), 117.1 ($q_c$, C-3), 110.6 (CH, C-7), 34.3 ($CH_3$, C-1$''$), 27.1 ($CH_3$, C-2$'$) ppm.

**1-(1-benzyl-1H-indol-3-yl)ethanone (3.17):**[140]

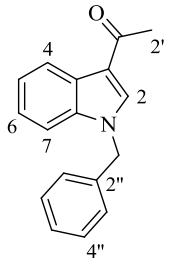

**3.17**

Yield = 24%; $^{1}$H NMR ($CDCl_3$, 400 MHz): $\delta_H$ 8.41-8.39 (1H, m, H-4), 7.76 (1H, s, H-2), 7.35-7.26 (6H, m, H-5, H-6, H-7, H-4$''$, H-5$''$), 7.17-7.15 (2H, m, H-3$''$), 5.36 (2H, s, 1$''$), 2.52 (3H, s, H-2$'$), $^{13}$C NMR ($CDCl_3$, 100 MHz): $\delta_C$ 193.2 ($q_c$, C-1$'$), 135.9 ($q_c$, C-7a), 134.1 ($q_c$, C-2$''$), 130.1 (CH, C-2), 130.0 (CH, C-4$''$), 129.8, (CH, C-5$''$), 129.2 (CH, C-3$''$), 126.3 ($q_c$, C-3a), 124.5 (CH, C-6), 123.7 (CH, C-5), 122.0 (CH, C-4), 117.7 ($q_c$, C-3), 111.0 (CH, C-7), 50.9 ($CH_2$, C-1$''$), 27.2 ($CH_3$, C-2$'$) ppm.

### 5.1.4 General procedure for the synthesis of 2-bromo-1-(1*H*-indol-3-yl)-ethanones (3.18 – 3.26)

A solution of 3-acetylindole (**3.9 – 3.17**, 0.63 mmol, 1 eq.) in hot $CHCl_3$ (20 mL) was added to a vigorously stirred suspension of $CuBr_2$ (252 mg, 1.13 mmol, 1.8 eq.) in EtOAc (15 mL) and heated to reflux, with constant monitoring by TLC. After reacting for various times,[100] the reaction mixture was allowed to cool, washed with water (2 × 20 mL), sat. brine (2 × 20 mL) and dried over anhydrous $MgSO_4$.Solvent was removed *in vacuo* followed by purification *via* normal phase flash chromatography (100% $CH_2Cl_2$) to afford compounds **3.18 – 3.26**. Two

dimensional NMR spectroscopic data was not obtained for compounds **3.18 – 3.20, 3.25** and **3.26**.

**2-bromo-1-(5-chloro-6-fluoro-1*H*-indol-3-yl)-ethanone (3.18):**

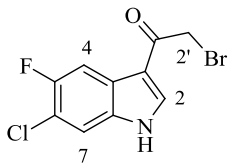

**3.18**

Yield = 32%; $^{1}$H NMR (DMSO, 300 MHz): $\delta_H$ 12.36 (1H, s), 8.58 (1H, d, *J* = 3.2 Hz), 8.00 (1H, d, *J* = 9 Hz), 7.24 (1H, d, *J* = 6.5 Hz), 4.67 (2H, s); $^{13}$C NMR (DMSO, 75 MHz): $\delta_c$ 186.3, 151.8 (d, $J_{F,C}$ = 241 Hz), 137.2, 132.5, 124.5 (d, $J_{F,C}$ = 10.0 Hz), 115.9 (d, $J_{F,C}$ = 4.7 Hz), 114.7 (d, $J_{F,C}$ = 20 Hz), 113.9, 107.2 (d, $J_{F,C}$ = 25 Hz), 33.3 ppm.

**2-bromo-1-(6-bromo-5-fluoro-1*H*-indol-3-yl)-ethanone (3.19):**

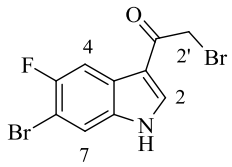

**3.19**

Yield = 26%; $^{1}$H NMR (DMSO, 300 MHz): $\delta_H$ 12.35 (1H, s), 8.57 (1H, d, *J* = 3.3 Hz), 7.98 (1H, d, *J* = 9.5 Hz), 7.84 (1H, d, *J* = 5.9 Hz), 4.66 (2H, s); $^{13}$C NMR (DMSO, 75 MHz): $\delta_C$ 186.8, 155.0 (d, $J_{F,C}$ = 245 Hz), 136.7, 134.2, 125.9 (d, $J_{F,C}$ = 9.2 Hz), 117.3, 116.9, 107.3 (d, $J_{F,C}$ = 24 Hz), 103.2 (d, $J_{F,C}$ = 25 Hz), 33.6 ppm.

**2-bromo-1-(6-fluoro-1*H*-indol-3-yl)-ethanone (3.20):**[100]

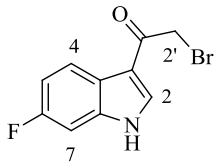

**3.20**

Yield = 25%; $^{1}$H NMR (MeOD, 600 MHz): $\delta_H$ 8.27 (1H, s), 8.19 (1H, dd, *J* = 8.8, 5.5 Hz), 7.17 (1H, dd, *J* = 9.4, 2.2 Hz), 7.01 (1H, m), 4.48 (2H, s). $^{13}$C NMR (MeOD, 150 MHz): $\delta_c$ 189.4, 161.9 (d, $J_{F,C}$ = 238.6 Hz), 138.7 (d, $J_{F,C}$ = 12.0 Hz), 136.4, 124.0 (d, $J_{F,C}$ = 9.9 Hz), 123.7, 115.4, 111.8 (d, $J_{F,C}$ = 24.1 Hz), 99.2 (d, $J_{F,C}$ = 26.2 Hz), 32.3 ppm.

**2-bromo-1-(5-chloro-1*H*-indol-3-yl)ethanone (3.21):**

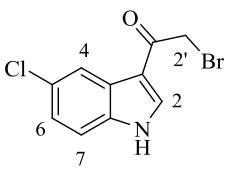


**3.21**

Yield = 35%; $^{1}$H NMR (DMSO, 300 MHz): $\delta_H$ 12.33 (s, 1H, NH-1), 8.54 (1H, d, *J* = 3.2 Hz,H-2), 8.12 (1H, d, *J* = 2.0 Hz, H-4), 7.53 (1H, d, *J* = 8.6 Hz, H-7), 7.29-7.25 (1H, m, H-6), 4.66 (2H, s, H-2′); $^{13}$C NMR (DMSO, 75 MHz): $\delta_C$ 186.6 ($q_c$, C-1′), 136.6 (CH, C-2), 135.3 ($q_c$, C-7a), 126.9 ($q_c$, C-3a), 126.7 ($q_c$, C-5), 123.3 (CH, C-6), 120.3 (CH, C-4), 114.1 (CH, C-7), 113.1 ($q_c$, C-3), 33.4 ($CH_2$, C-2′) ppm.

**2-bromo-1-(6-chloro-1*H*-indol-3-yl)ethanone (3.22):**[100]

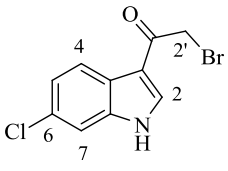


**3.22**

Yield = 28%; $^{1}$H NMR (DMSO, 300 MHz): $\delta_H$ 12.25 (s, 1H, NH-1), 8.52 (1H, d, *J* = 3.2 Hz,H-2), 8.13 (1H, d, *J* = 8.5 Hz, H-4), 7.57-7.56 (1H, m, H-7), 7.27-7.23 (1H, m, H-5), 4.66 (2H, s, H-2′); $^{13}$C NMR (DMSO, 75 MHz): δ 186.5 ($q_c$, C-1′), 137.2 ($q_c$, C-7a), 136.2 (CH, C-2), 127.8 ($q_c$, C-6), 124.2 ($q_c$, C-3a), 122.5 (CH, C-4), 122.5 (CH, C-5), 113.5 (CH, C-7), 112.2 ($q_c$, C-3), 33.5 ($CH_2$, C-2′) ppm.

**2-bromo-1-(5-bromo-1*H*-indol-3-yl)ethanone (3.23):**

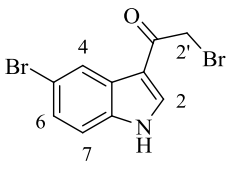


**3.23**

Yield = 39%; $^{1}$H NMR (DMSO, 300 MHz): δ 12.34 (s, 1H, NH-1), 8.52 (1H, d, *J* = 3.2 Hz,H-2), 8.28 (1H, d, *J* = 2.0 Hz, H-4), 7.50-7.47 (1H, m, H-7), 7.40-7.37 (1H, m, H-6), 4.65 (2H, s, H-2′); $^{13}$C NMR (DMSO, 75 MHz): δ 186.6 ($q_c$, C-1′), 136.4 (CH, C-2), 135.5 ($q_c$, C-7a), 127.3 ($q_c$, C-3a), 125.9 (CH, C-6), 123.3 (CH, C-4), 115.0 (CH, C-7), 114.6 ($q_c$, C-5), 113.0 ($q_c$, C-3), 33.4 ($CH_2$, C-2′) ppm.

**2-bromo-1-(1*H*-indol-3-yl)ethanone (3.24):**[100]

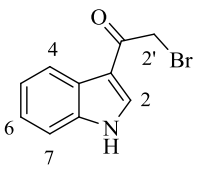


**3.24**

Yield = 41%; $^{1}$H NMR (DMSO, 300 MHz): $\delta_H$ 12.13 (s, 1H, NH-1), 8.47 (1H, d, *J* = 3.1 Hz,H-2), 8.15 (1H, d, *J* = 8.2 Hz, H-4), 7.50 (1H, d, *J* = 7.7 Hz, H-

7), 7.26-7.20 (2H, m, H-5, H-6), 4.64 (2H, s, H-2′); $^{13}$C NMR (DMSO, 75 MHz): $\delta_C$ 186.5 ($q_c$, C-1′), 136.8 ($q_c$, C-7a), 136.3 (CH, C-2), 125.5 ($q_c$, C-3a), 123.3 (CH, C-4), 122.3 (CH, C-6), 121.3 (CH, C-5), 113.6 ($q_c$, C-3), 112.4 (CH, C-7), 33.7 ($CH_2$, C-2′) ppm.

**2-bromo-1-(*N*-methyl-indol-3-yl)-ethanone (3.25):**[141]

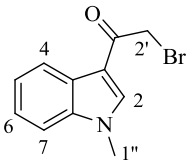


**3.25**

Yield = 24 %; $^1$H NMR ($CDCl_3$, 600 MHz): $\delta_H$ 8.35 – 8.33 (1H, m), 7.81 (1H, s), 7.36 – 7.32 (3H, m), 4.28 (2H, s), 3.86 (3H, s); $^{13}$C NMR ($CDCl_3$, 150 MHz): $\delta_C$ 186.1, 137.5, 136.2, 126.4, 123.4, 123.1, 122.6, 113.5, 109.8, 33.7, 31.7 ppm.

**2-bromo-1-(*N*-benzyl-indol-3-yl)-ethanone (3.26):**[142]

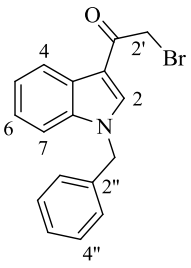


**3.26**

Yield = 55%; $^1$H NMR ($CDCl_3$, 600 MHz): $\delta_H$ 8.37 – 8.36 (1H, m), 7.86 (1H, s), 7.35 – 7.28 (6H, m), 7.17 – 7.16 (2H, m), 5.36 (2H, s), 4.29 (3H, s); $^{13}$C NMR ($CDCl_3$, 150 MHz): $\delta_C$ 186.3, 137.1, 135.5, 135.3, 129.1, 128.4, 127.0, 126.6, 123.9, 123.2, 122.7, 114.0, 110.4, 50.9, 31.8 ppm.

### 5.1.5 General procedure for the synthesis of α-substituted-indolyl-3-ethanones (3.37 – 3.73)

To a stirred suspension of 2-bromo-1-(1*H*-indol-3-yl)-ethanone (1 eq.) and $K_2CO_3$ (2 eq.) in acetone was added a relevant nucleophile (2 eq.). The reaction mixture was heated to reflux and after 5 hours it was cooled and extracted with EtOAc. This EtOAc layer was further washed with water and sat. brine respectively. The organic layers were combined and dried over $MgSO_4$/$Na_2SO_4$. After filtration, the solvent was removed under reduced pressure to

give semi-solid crude products. The crude products were purified by normal phase flash chromatography (DCM: Hex 2:1), followed by recrystallisation in EtOAc to afford compounds **3.37 – 3.73**.

**1-(1*H*-indol-3-yl)-2-(phenylamino)-ethanone (3.37):**[143]

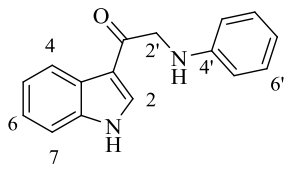


**3.37**

Yellow crystalline solid (57%); m. p: 168- 170 °C; $^{1}$H NMR (DMSO, 600 MHz): $\delta_H$ 12.04 (1H, s, NH-1), 8.55 (1H, s, H-2), 8.18 (1H, d, *J* = 7.2 Hz, H-4), 7.49 (1H, d, *J* = 7.5 Hz, H-7), 7.23-7.18 (2H, m, H-5, H-6), 7.08-7.06 (2H, m, H-6′), 6.68 (2H, d, *J* = 7.8 Hz, H-5′), 6.55 (1H, t, *J* = 7.43 Hz, H-7′), 5.85 (1H, t, *J* = 5.47 Hz, NH-3′), 4.46 (2H, d, *J* = 5.5 Hz, H-2′); $^{13}$C NMR (DMSO, 150 MHz): $\delta_C$ 191.9 ($q_c$, C-1′), 148.4 ($q_c$, C-4′), 136.4 ($q_c$, C-7a), 133.7 (CH, C-2), 128.8 (CH, C-6′), 125.4 ($q_c$, C-3a), 122.9 (CH, C-6), 121.9 (CH, C-5), 121.2 (CH, C-4), 116.0 (CH, C-7′), 114.3 ($q_c$, C-3), 112.4 (CH, C-5′), 112.2 (CH, C-7), 49.8 (CH, C-2′) ppm; EIMS *m/z* (rel. int.) 130 $[M+H]^+$ (100), 117 (15), 106 (25) 77 (7); HREIMS *m/z* 251.1182 (calcd for $C_{16}H_{15}N_2O$ $[M+H]^+$ 251.1184); Elem. Anal. Found: C, 76.85; H, 6.34; N, 11.08%; Calcd for $C_{16}H_{15}N_2O$: C, 76.78; H, 5.64; N, 11.19%.

**1-(1*H*-indol-3-yl)-2-[(4-bromophenyl)thio]-ethanone (3.38):**

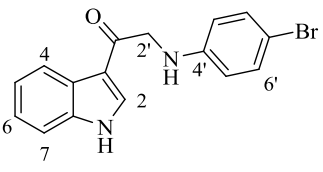


**3.38**

White crystalline solid (92%); m. p: 159- 161 °C; $^{1}$H NMR (DMSO, 600 MHz): $\delta_H$ 12.08 (1H, s, NH-1), 8.50 (1H, s, H-2), 8.13 (1H, d, *J* = 7.6 Hz, H-4), 7.49-7.46 (3H, m, H7, H-6′), 7.34 (2H, d, *J* = 8.7 Hz, H-5′), 7.24-7.20 (2H, m, H-5, H-6), 4.49 (2H, s, H-2′); $^{13}$C NMR (DMSO, 150 MHz): $\delta_C$ 188.8 ($q_c$, C-1′), 136.6 ($q_c$, C-7a), 136.2 ($q_c$, C-4′), 135.0 (CH, C-2), 131.6 (CH, C-6′), 129.8 (CH, C-5′), 125.4 ($q_c$, C-3a), 123.0 (CH, C-6), 122.0 (CH, C-5), 121.2 (CH, C-4), 118.4 ($q_c$, C-7′), 115.0 ($q_c$, C-3), 112.3 (CH, C-7), 40.1 ($CH_2$, C-2′) ppm; EIMS *m/z* (rel. int.) 202 $[M+H]^+$ (6), 159 (24), 144 (47), 130 (25), 122 (100), 117 (25); HREIMS *m/z* 345.9908 (calcd for $C_{16}H_{13}{}^{79}BrNOS$ $[M+H]^+$

345.9901). *resolved by HSQC; Elem. Anal. Found: C, 55.75; H, 3.75; N, 3.99; S, 8.86%; Calcd for $C_{16}H_{13}BrNOS$: C, 55.5; H, 3.49; N, 4.05; S, 9.26%.

**1-(1*H*-indol-3-yl)-2-(phenoxy)-ethanone (3.39):**

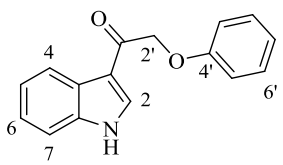


**3.39**

White crystalline solid (33%) ; m. p: 192- 193 °C; $^1$H NMR (DMSO, 600 MHz): $\delta_H$ 12.07 (1H, s, NH-1), 8.51 (1H, s, H-2), 8.16 (1H, d, *J* = 7.4 Hz, H-4), 7.50 (1H, d, *J* = 7.9 Hz, H-7), 7.29-7.27 (2H, m, H-6′), 7.25-7.19 (2H, m, H-5, H-6), 6.98-6.96 (2H, m, H-5′), 6.94-6.92 (1H. m, H-7′), 5.27 (2H, s, H-2′); $^{13}$C NMR (DMSO, 150 MHz): $\delta_C$ 189.7 ($q_c$, C-1′), 158.2 ($q_c$, C-4′),136.3 ($q_c$, C-7a), 134.0 (CH, C-2), 129.4 (CH, C-6′), 125.4 ($q_c$, C-3a), 123.0 (CH, C-6), 122.0 (CH, C-5), 121.2 (CH, C-4), 120.7 ($q_c$, C-7′), 114.5 (CH, C-5′), 113.4 ($q_c$, C-3), 112.2 (CH, C-7), 70.0 ($CH_2$, C-2′) ppm; EIMS *m/z* (rel. int.) 159 $[M+H]^+$ (15), 144 (55), 130 (100), 117 (32), 103 (10), 90 (6), 77 (4); HREIMS *m/z* 252.1023 (calcd for $C_{16}H_{14}NO_2$ $[M+H]^+$ 252.1025); Elem. Anal. Found: C, 77.1; H, 6.14; N, 5.81%; Calcd for $C_{16}H_{14}NO_2$; C, 76.48; H, 5.21; N, 5.57%.

**1-(1*H*-indol-3-yl)-2-[(2-methylphenyl)thio]-ethanone (3.40):**

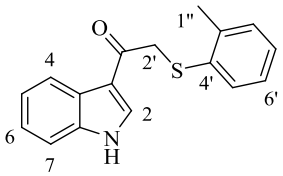


**3.40**

Yellow crystalline solid (34%); m. p: 157- 158 °C; $^1$H NMR (600 MHz, $d_6$-DMSO): $\delta_H$ 12.08 (1H, s, NH-1), 8.49 (1H, d, *J* = 3.1 Hz, H-2), 8.14 (1H, d, *J* = 7.7 Hz, H-4), 7.48 (1H, d, *J* = 8.0 Hz, H-7), 7.38 (1H, d, *J* = 7.7 Hz, H-8′), 7.24-7.18 (3H, m, H-5′, H-6′, H-7′), 7.16-7.14 (1H, m, H-5), 7.09-7.07 (1H, m, H-6), 4.42 (2H, s, H-2′), 2.30 (3H, s, H1″); $^{13}$C NMR (DMSO, 150 MHz): $\delta_C$ 189.1 ($q_c$, C-1′), 136.6 ($q_c$, C-7a), 135.9 ($q_c$, C-4′), 135.6 (CH, C-2), 134.9 ($q_c$, C-9′), 129.8 (CH, C-8′), 127.3 (CH, C-5′), 126.6 (CH, C-6′), 125.5 (CH, C-7′), 125.4 ($q_c$, C-3a), 123.0 (CH, C-6), 122.0 (CH, C-5), 121.1 (CH, C-4), 115.0 ($_{qc}$, C-3), 112.2 (CH, C-7), 40.1 ($CH_2$, C-2′), 19.8 ($CH_3$, C-1″) ppm; EIMS *m/z* (rel. int.) 159 $[M+H]^+$ (32), 148 (10), 144 (100), 137 (35), 130 (65), 117 (50), 91 (7); HREIMS *m/z*

282.0958 (calcd for $C_{17}H_{16}NOS$ $[M+H]^+$ 282.0953).*resolved by HSQC; Elem. Anal. Found: C, 72.64; H, 6.29; N, 5.14; S, 11.42%; Calcd for $C_{17}H_{16}NOS$: C, 72.57; H, 5.37; N, 4.98; S, 11.4%.

**1-(1*H*-indol-3-yl)-2-[(4-chlorophenyl)amino]-ethanone (3.41):**

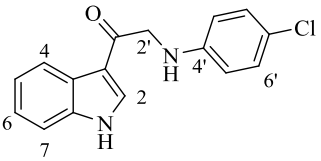


**3.41**

White crystalline solid (55%); m. p: 210- 212 °C; $^1$HNMR (DMSO, 600 MHz): $\delta_H$ 12.04 (1H, s, NH-1), 8.54 (1H, s, H-2), 8.18 (1H, d, *J* = 7.6 Hz, H-4), 7.49 (1H, d, *J* = 7.6 Hz, H-7), 7.24 – 7.18 (2H, m, H-5, H-6), 7.11-7.08 (2H, m, H-6′), 6.70-6.68 (2H, m, H-5′), 6.11 (1H, t, *J* = 5.6 Hz, H-3′), 4.47 (2H, d, *J* = 5.6 Hz, H-2′); $^{13}$C NMR (DMSO, 150 MHz): $\delta_C$ 191.5 ($q_c$, C-1′), 147.4 ($q_c$, C-4′), 136.4 ($q_c$, C-7a), 133.7 (CH, C-2), 128.5 (CH, C-6′), 125.4 ($q_c$, C-3a), 122.9 (CH, C-6), 121.9 (CH, C-5), 121.2 (CH, C-4), 119.1 (CH, C-7′), 114.2 ($q_c$, C-3), 113.8 (CH, C-5′), 112.2 (CH, C-7), 49.7 ($CH_2$, C-2′) ppm; EIMS *m/z* (rel. int.) 231 $[M+H]^+$ (20), 140 (65), 130 (100), 117 (5), 111 (6), 103 (7), 77 (3); HREIMS *m/z* 285.0788 (calcd for $C_{16}H_{14}{}^{35}ClN_2O$ $[M+H]^+$285.0795).

**1-(1*H*-indol-3-yl)-2-(phenylthio)-ethanone (3.42):**

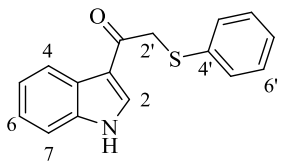


**3.42**

White crystalline solid (66%); m. p: 150- 151 °C; $^1$H NMR (DMSO, 600 MHz): $\delta_H$ 12.06 (1H, s, NH-1), 8.48 (1H, s,H-2), 8.14 (1H, d, *J* = 7.6 Hz, H-4), 7.48 (1H, d, *J* = 7.8 Hz, H-7), 7.39 (2H, d, *J* = 7.3 Hz, H-5′), 7.29 (2H, t, *J* = 7.7 Hz, H-6′), 7.24-7.15 (3H, m, H-5, H-6, H-7′), 4.45 (2H, s, H-2′); $^{13}$C NMR (DMSO, 150 MHz): $\delta_C$ 189.2 ($q_c$, C-1′), 136.6 ($q_c$, C-7a), 136.4 ($q_c$, C-4′), 134.9 (CH, C-2), 128.9 (CH, C-5′), 127.9 (CH, C-6′), 125.6 (CH, C-7′), 125.5 ($q_c$, C-3a), 123.0 (CH, C-6), 122.0 (CH, C-5), 121.3 (CH, C-4), 115.0 ($q_c$, C-3), 112.2 (CH, C-7), 40.1 ($CH_2$, C-2′) ppm; EIMS *m/z* (rel. int.) 159 $[M+H]^+$ (30), 144 (30), 130 (34), 123 (100), 117 (20);

HREIMS *m/z* 268.0789 (calcd for $C_{16}H_{14}NOS$ $[M+H]^+$ 268.0796).*resolved by HSQC; Elem. Anal. Found: C, 71.68; H, 5.23; N, 5.18; S, 11.92%; Calcd for $C_{16}H_{14}NOS$: C, 71.88; H, 4.9; N, 5.24; S, 11.99%.

**1-(1*H*-indol-3-yl)-2-[(4-chlorophenyl)thio]-ethanone (3.43):**

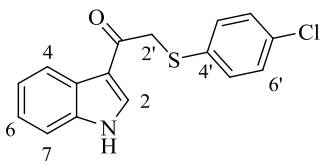


**3.43**

White crystalline solid (74%); m. p: 170- 171 °C; $^1$H NMR (DMSO, 600 MHz): $\delta_H$ 12.07 (1H, s, NH-1), 8.49 (1H, s, H-2), 8.13 (1H, d, *J* = 7.4 Hz, H-4), 7.48 (1H, d, *J* = 7.9 Hz, H-7), 7.42-7.39 (2H, m, H-6′), 7.36-7.34 (2H, m, H-5′), 7.24-7.14 (2H, m, H-5, H-6), 4.48 (2H, s, H-2′); $^{13}$C NMR (DMSO, 150 MHz): $\delta_C$ 188.9 ($q_c$, C-1′), 136.6 ($q_c$, C-7a), 135.6 ($q_c$, C-4′), 135.0 (CH, C-2), 130.2 (CH, C-5′), 129.6 (CH, C-6′), 128.8 ($q_c$, C-7′), 125.5 ($q_c$, C-3a), 123.1 (CH, C-6), 122.0 (CH, C-5), 121.3 (CH, C-4), 115.0 ($q_c$, C-3), 112.3 (CH, C-7), 40.1 ($CH_2$, C-2′) ppm; EIMS *m/z* (rel. int.) 159 $[M+H]^+$ (35), 144 (100), 130 (45), 117 (45), 103 (5); HREIMS *m/z* 302.0409 (calcd for $C_{16}H_{13}{}^{35}ClNOS$ $[M+H]^+$ 302.0406). *resolved by HSQC; Elem. Anal. Found: C, 63.54; H, 4.28; N, 4.62; S, 9.98%; Calcd for $C_{16}H_{13}ClNOS$: C, 63.68; H, 4.01; N, 4.64; S, 10.62%.

**1-(1*H*-indol-3-yl)-2-(4-chlorophenyloxy)-ethanone (3.44):**

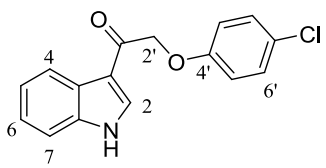


**3.44**

White crystalline solid (31%); m. p: 196- 197 °C; $^1$H NMR (DMSO, 600 MHz): $\delta_H$ 12.08 (1H, s, NH-1), 8.47 (1H, s, H-2), 8.14 (1H, d, *J* = 7.7 Hz, H-4), 7.50 (1H, d, *J* = 7.9 Hz, H-7), 7.32-7.30 (2H, m, H-6′), 7.25-7.19 (2H, m, H-5, H-6), 7.00-6.97 (2H, m, H-5′), 5.30 (2H, s, H-2′); $^{13}$C NMR (DMSO, 150 MHz): $\delta_C$ 189.3 ($q_c$, C-1′), 157.2 ($q_c$, C-4′),136.4 ($q_c$, C-7a), 132.0 (CH, C-2), 129.2 (CH, C-6′), 125.4 ($q_c$, C-3a), 124.4 ($q_c$, C-7′), 123.1 (CH, C-6), 122.1 (CH, C-5), 121.2 (CH, C-4), 116.4 (CH, C-5′), 113.3 ($q_c$, C-3), 112.3 (CH, C-7), 70.1 ($CH_2$, C-2′) ppm; EIMS *m/z* (rel. int.) 159 $[M+H]^+$ (25), 144 (100), 130 (60), 117 (50), 89 (5); HREIMS *m/z* 286.0635 (calcd for

$C_{16}H_{13}{}^{35}ClNO_2$ $[M+H]^+$ 286.0629); Elem. Anal. Found: C, 66.95; H, 4.44; N, 5.08%; Calcd for $C_{16}H_{13}ClNO_2$: C, 67.26; H, 4.23; N, 4.9%.

**1-(1*H*-indol-3-yl)-2-[(4-fluorophenyl)thio]-ethanone (3.45):**

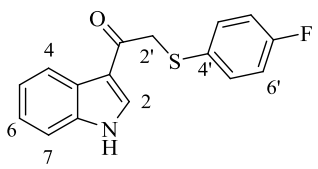


**3.45**

White crystalline solid (78%); m. p: 210- 211 °C; $^1$H NMR (DMSO, 600 MHz): $\delta_H$ 12.04 (1H, s, NH-1), 8.44 (1H, d, *J* = 3.2 Hz, H-2), 8.14 (1H, d, *J* = 7.7 Hz, H-4), 7.48-7.44 (3H, m, H-7, H-5′), 7.24-7.14 (4H, m, H-5, H-6, H-6′), 4.41 (2H, s, H-2′); $^{13}$C NMR (DMSO, 150 MHz): $\delta_C$ 189.1 ($q_c$, C-1′), 160.8 ($q_c$, d, $J_{F.C}$ = 237.9 Hz, C-7′), 136.6 ($q_c$, C-7a), 134.9 (CH, C-2), 131.6 ($q_c$, d, $J_{F.C}$ = 2.9 Hz, C-4′), 131.0 (CH, d, $J_{F.C}$ = 2.9 Hz, C-5′), 125.5 ($q_c$, C-3a), 123.0 (CH, C-6), 122.0 (CH, C-5), 121.3 (CH, C-4), 116.0 (CH, d, $J_{F.C}$ = 12.5 Hz, C-6′), 115.0 ($q_c$, C-3), 112.2 (CH, C-7), 40.8 ($CH_2$, C-2′) ppm; EIMS *m/z* (rel. int.) 159 $[M+H]^+$ (30), 144 (100), 130 (50), 117 (45), 103 (5), 89 (10), 77 (3); HREIMS *m/z* 286.0697 (calcd for $C_{16}H_{13}FNOS$ $[M+H]^+$ 286.0702). *resolved by HSQC; Elem. Anal. Found: C, 66.53; H, 4.26; N, 4.86; S, 10.68%; Calcd for $C_{16}H_{13}FNOS$: C, 67.35; H, 4.24; N, 4.91; S, 11.24%.

**1-(1*H*-indol-3-yl)-2-[(4-methylphenyl)thio]-ethanone (3.46):**

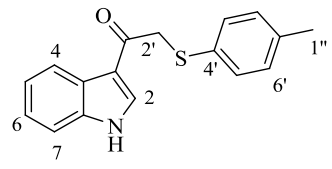


**3.46**

White crystalline solid (47%); m. p: 170- 171 °C; $^1$H NMR (DMSO, 600 MHz): $\delta_H$ 12.06 (1H, s, NH-1), 8.45 (1H, d, *J* = 1.4 Hz, H-2), 8.13 (1H, d, *J* = 7.6 Hz, H-4), 7.48-7.47 (1H, m, H-7), 7.29-7.27 (2H, m, H-5′), 7.23-7.17 (2H, m, H-5, H-6), 7.10 (2H, d, *J* = 8.0 Hz, H-6′), 4.37 (2H, s, H-2′), 2.24 (3H, s, H-1″); $^{13}$C NMR (DMSO, 150 MHz): $\delta_C$ 189.4 ($q_c$, C-1′), 136.7 ($q_c$, C-7a), 135.4 ($q_c$, C-7′), 135.0 (CH, C-2), 132.6 ($q_c$, C-4′), 129.7 (CH, C-5′), 128.7 (CH, C-6′), 125.6 ($q_c$, C-3a), 123.1 (CH, C-6), 122.1 (CH, C-5), 121.3 (CH, C-4), 115.1 ($q_c$, C-3), 112.3 (CH, C-7), 40.4 ($CH_2$, C-

2′), 20.6 ($q_c$, C-1″) ppm; EIMS *m/z* (rel. int.) 159 $[M+H]^+$ (50), 144 (90), 137 (100), 130 (60), 117 (50), 103 (5), 89 (5); HREIMS *m/z* 282.0946 (calcd for $C_{17}H_{16}NOS$ $[M+H]^+$ 282.0953).

**1-(1*H*-indol-3-yl)-2-[(4-*tert*-butylphenyl)thio]-ethanone (3.47):**

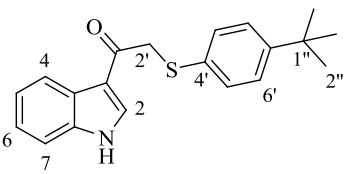


**3.47**

White crystalline solid (35%); m. p: 189- 190 °C; $^1$H NMR (DMSO, 600 MHz): $\delta_H$ 12.05 (1H, s, NH-1), 8.45 (1H, d, *J* = 3.0 Hz, H-2), 8.14 (1H, d, *J* = 7.6 Hz, H-4), 7.48-7.47 (1H, m, H-7), 7.31 (4H, s, H-5′, H-6′), 7.23-7.17 (2H, m, H-5, H-6), 4.39 (2H, s, H-2′), 1.24 (9H, s, H-2″); $^{13}$C NMR (DMSO, 150 MHz): $\delta_C$ 189.4 ($q_c$, C-1′), 148.5 ($q_c$, C-7′), 136.6 ($q_c$, C-7a), 134.8 (CH, C-2), 132.8 ($q_c$, C-4′), 128.2 (CH, C-5′), 125.8 (CH, C-6′), 125.5 ($q_c$, C-3a), 123.0 (CH, C-6), 122.0 (CH, C-5), 121.3 (CH, C-4), 115.1 ($q_c$, C-3), 112.3 (CH, C-7), 40.3 ($CH_2$, C-2′), 34.2 ($q_c$, C-1″), 31.1 (CH, C-2″) ppm; EIMS *m/z* (rel. int.) 179 $[M+H]^+$ (7), 159 (75), 151 (35), 144 (100), 130 (60), 123 (80), 117 (55), 103 (4), 89 (4); HREIMS *m/z* 324.1423 (calcd for $C_{20}H_{22}NOS$ $[M+H]^+$ 324.1422).

**1-(1*H*-indol-3-yl)-2-[(3-fluorophenyl)thio]-ethanone (3.48):**

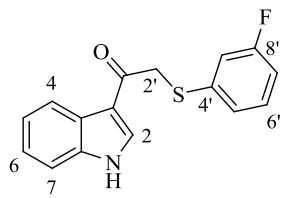


**3.48**

White crystalline solid (92%); m. p: 185- 186 °C; $^1$H NMR (DMSO, 600 MHz): $\delta_H$ 12.09 (1H, s, NH-1), 8.54 (1H, d, *J* = 3.2 Hz, H-2), 8.15-8.14 (1H, m, H-4), 7.61-7.60 (1H, m, H-7′), 7.50-7.48 (1H, m, H-7), 7.38-7.34 (2H, m, H-5′, H-9′), 7.25-7.18 (3H, m, H-5, H-6, H-5′), 4.54 (2H, s, H-2′); $^{13}$C NMR (DMSO, 150 MHz): $\delta_C$ 188.8 ($q_c$, C-1′), 162.3 ($q_c$, d, $J_{F.C}$ = 245.4 Hz, C-8′), 139.5 ($q_c$, d, $J_{F.C}$ = 7.9 Hz, C-4′), 136.6 ($q_c$, C-7a), 135.0 (CH, C-2), 130.6 (CH, d, $J_{F.C}$ = 8.7 Hz, C-6′), 125.4 ($q_c$, C-3a), 123.3 (CH, C-5′), 123.0 (CH, C-6), 122.0 (CH, C-5), 121.2 (CH, C-4), 115.0 ($q_c$, C-3), 113.8 (CH, C-7′), 112.2 (CH, C-7), 112.0 (CH, C-9′), 40.1 ($CH_2$, C-2′) ppm; EIMS *m/z* (rel. int.) 159 $[M+H]^+$ (40), 144 (100), 141 (38), 130 (65), 117 (55), 103 (5), 89 (5); HREIMS

*m/z* 286.0696 (calcd for $C_{16}H_{13}FNOS$ $[M+H]^+$ 286.0702). *resolved by HSQC; Elem. Anal. Found: C, 61.72; H, 3.48; N, 4.58; S, 9.84%; Calcd for $C_{16}H_{13}FNOS$: C, 67.35; H, 4.24; N, 4.91; S, 11.24%.

**1-(1*H*-indol-3-yl)-2-[(3-chlorophenyl)thio]-ethanone (3.49):**

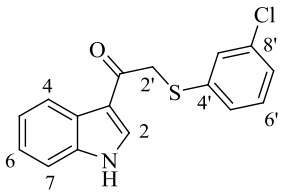


**3.49**

White crystalline solid (96%); m. p: 186- 188 °C; $^1$H NMR (DMSO, 600 MHz): $\delta_H$ 12.09 (1H, s, NH-1), 8.54 (1H, d, *J* = 3.1 Hz, H-2), 8.15-8.14 (1H, m, H-4), 7.50-7.48 (2H, m, H-7, H-9), 7.48-7.29 (2H, m, H-5′, H-6′), 7.24-7.18 (3H, m, H-5, H-6, H-7′), 4.54 (2H, s, H-2′); $^{13}$C NMR (DMSO, 150 MHz): $\delta_C$ 188.8 ($q_c$, C-1′), 139.2 ($q_c$, C-4′), 136.6 ($q_c$, C-7a), 135.0 (CH, C-2), 133.5 ($q_c$, C-8′), 130.4 (CH, C-6′), 126.6 ($q_c$, C-9′), 126.0 (CH, C-5′), 125.4 ($q_c$, C-3a), 125.3 (CH, C-7′), 123.0 (CH, C-6), 122.0 (CH, C-5), 121.2 (CH, C-4), 115.0 ($q_c$, C-3), 112.2 (CH, C-7), 40.1 ($CH_2$, C-2′) ppm; EIMS *m/z* (rel. int.) 159 $[M+H]^+$ (40), 144 (100), 130 (90), 122 (7), 117 (50), 103 (3), 89 (6), 78 (3); HREIMS *m/z* 302.0399 (calcd for $C_{16}H_{13}{}^{35}ClNOS$ $[M+H]^+$ 302.0406). *resolved by HSQC; Elem. Anal. Found: C, 62.44; H, 3.70; N, 4.56; S, 9.76%; Calcd for $C_{16}H_{13}ClNOS$: C, 63.68; H, 4.01; N, 4.64; S, 10.62%.

**1-(1*H*-indol-3-yl)-2-[(3-bromophenyl)thio]-ethanone (3.50):**

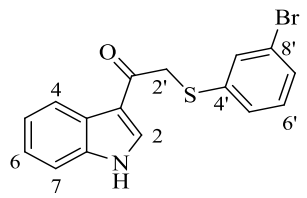


**3.50**

White crystalline solid (91%); m. p: 194- 195 °C; $^1$H NMR (DMSO, 600 MHz): $\delta_H$ 12.09 (1H, s, NH-1), 8.54 (1H, d, *J* = 3.2 Hz, H-2), 8.15-8.14 (1H, m, H-4), 7.61-7.60 (1H, m, H-7′), 7.50-7.48 (1H, m, H-7), 7.38-7.34 (2H, m, H-5′, H-9′), 7.25-7.18 (3H, m, H-5, H-6, H-5′), 4.54 (2H, s, H-2′); $^{13}$C NMR (DMSO, 150 MHz): $\delta_C$ 188.8 ($q_c$, C-1′), 139.5 ($q_c$, C-4′), 136.6 ($q_c$, C-7a), 135.0 (CH, C-2), 130.7 (CH, C-6′), 129.4 ($q_c$, C-7′), 128.2 (CH, C-5′), 126.4 (CH, C-9′), 125.4 ($q_c$, C-3a), 123.0 (CH, C-6), 122.1 (CH, C-5), 122.0 ($q_c$, C-8′), 121.2 (CH, C-4), 115.0 ($q_c$,

C-3), 112.2 (CH, C-7), 40.1 ($CH_2$, C-2′) ppm; EIMS *m/z* (rel. int.) 202 $[M+H]^+$ (25), 159 (22), 144 (25), 130 (25), 122 (100), 117 (15), 103 (3), 78 (3); HREIMS *m/z* 345.9895 (calcd for $C_{16}H_{13}{}^{79}BrNOS$ $[M+H]^+$ 345.9901). *resolved by HSQC; Elem. Anal. Found: C, 52.62; H, 2.74; N, 3.95; S, 8.21%; Calcd for $C_{16}H_{13}BrNOS$: C, 55.5; H, 3.49; N, 4.05; S, 9.26%.

**1-(1*H*-indol-3-yl)-2-[(2-chlorophenyl)thio]-ethanone (3.51):**

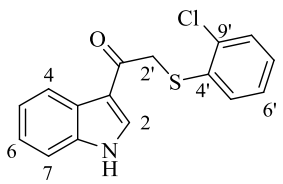


**3.51**

White crystalline solid (42%); m. p: 210- 212 °C; $^1H$ NMR (DMSO, 600 MHz): $\delta_H$ 12.11 (1H, s, NH-1), 8.58 (1H, s, H-2), 8.14 (1H, d, *J* = 7.6 Hz, H-4), 7.50-7.44 (3H, m, H-7, H-5′, H-8′), 7.32-7.29 (1H, m, H-6′), 7.25-7.16 (3H, m, H-5, H-6, H-7′), 4.57 (2H, s, H-2′); $^{13}C$ NMR (DMSO, 150 MHz): $\delta_C$ 188.5 ($q_c$, C-1′), 136.6 ($q_c$, C-7a), 136.0 ($q_c$, C-4′), 135.1 (CH, C-2), 130.6 ($q_c$, C-9′), 129.8 (CH, C-8′), 127.7 (CH, C-5′), 127.4 (CH, C-6′), 126.3 (CH, C-7′), 125.4 ($q_c$, C-3a), 123.1 (CH, C-6), 122.1 (CH, C-5), 121.2 (CH, C-4), 115.0 ($q_c$, C-3), 112.3 (CH, C-7), 40.1 ($CH_2$, C-2′) ppm; EIMS *m/z* (rel. int.) 159 $[M+H]^+$ (75), 156 (100), 144 (85), 130 (60), 117 (40), 103 (5), 89 (7), 77 (3); HREIMS *m/z* 302.0401 (calcd for $C_{16}H_{13}{}^{35}ClNOS$ $[M+H]^+$ 302.0406).*resolved by HSQC; Elem. Anal. Found: C, 62.33; H, 3.91; N, 4.94; S, 10.11%; Calcd for $C_{16}H_{13}ClNOS$: C, 63.68; H, 4.01; N, 4.64; S, 10.62%.

**1-(1*H*-indol-3-yl)-2-[(4-aminophenyl)thio]-ethanone (3.52):**

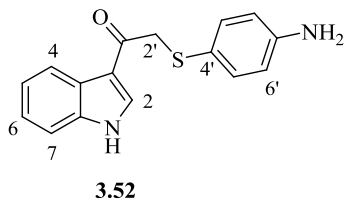


**3.52**

White crystalline solid (62%); m. p: 145- 146 °C; $^1H$ NMR (DMSO, 600 MHz): $\delta_H$ 11.95 (1H, s, NH-1), 8.21 (1H, d, *J* = 2.9 Hz, H-2), 8.14 (1H, d, *J* = 7.4 Hz, H-4), 7.45 (1H, d, *J* = 7.8 Hz, H-7), 7.22-7.16 (2H, m, H-5′), 7.11-7.09 (2H, m, H-5, H-6), 6.49-6.47 (2H, m, H-6′), 5.24 (2H, s, NH-1″), 4.04 (2H, s, H-2′); $^{13}C$ NMR (DMSO, 150 MHz): $\delta_C$ 190.1 ($q_c$, C-1′), 148.6 ($q_c$, C-7′), 136.6 ($q_c$, C-7a), 134.6 (CH, C-2), 133.8 (CH, C-6), 125.6 ($q_c$, C-3a), 122.9 (CH, C-5′), 121.9 (CH,

C-5), 121.3 (CH, C-4), 118.8 ($q_c$, C-4′), 115.2 ($q_c$, C-3), 114.3 ($q_c$, C-6′), 112.2 (CH, C-7), 43.8 ($CH_2$, C-2′) ppm; EIMS *m/z* (rel. int.) 159 $[M+H]^+$ (15), 144 (15), 138 (20), 124 (100), 117 (8), 94 (7), 80 (5); HREIMS *m/z* 283.0903 (calcd for $C_{16}H_{15}N_2OS$ $[M+H]^+$ 283.0905).

**1-(1*H*-indol-3-yl)-2-[(4-dimethylaminophenyl)thio]-ethanone (3.53):**

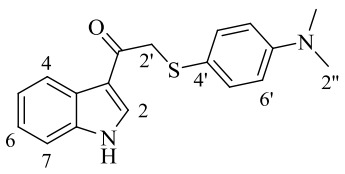


3.53

Yellow crystalline solid (56%); m. p: 205- 206 °C; $^1$H NMR (DMSO, 600 MHz): $\delta_H$ 11.96 (1H, s, NH-1), 8.5 (1H, s, H-2), 8.14 (1H, d, *J* = 7.5 Hz, H-4), 7.46 (1H, d, *J* = 7.9 Hz, H-7), 7.26-7.24 (2H, m, H-5′), 7.22-7.16 (2H, m, H-5, H-6), 6.65-6.62 (2H, m, H-6′), 4.11 (2H, s, H-2′), 2.87 (6H, s, H-1″); $^{13}$C NMR (DMSO, 150 MHz): $\delta_C$ 190.0 ($q_c$, C-1′), 149.8 ($q_c$, C-7′), 136.6 ($q_c$, C-7a), 134.6 (CH, C-2), 133.2 ($q_c$, C-5′), 125.6 ($q_c$, C-3a), 122.9 (CH, C-6), 121.9 (CH, C-5), 121.3 (CH, C-4), 119.8 ($q_c$, C-4′), 115.1 ($q_c$, C-3), 112.8 (CH, C-6′), 112.2 (CH, C-7), 43.0 ($CH_2$, C-2′), 34.2 ($CH_3$, C-1″ *) ppm; EIMS *m/z* (rel. int.) 152 $[M+H]^+$ (100), 144 (100), 136 (8), 116 (10), 108 (5), 89 (5); HREIMS *m/z* 311.1217 (calcd for $C_{18}H_{19}N_2OS$ $[M+H]^+$ 311.1218). *resolved by HSQC.

**1-(1*H*-indol-3-yl)-2-[(4-nitroaminophenyl)thio]-ethanone (3.54):**

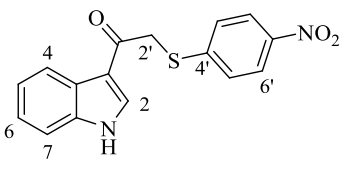


3.54

Yellow crystalline solid (40%); m. p: 230- 232 °C; $^1$H NMR (DMSO, 600 MHz): $\delta_H$ 12.14 (1H, s, NH-1), 8.59 (1H, d, *J* = 3.2 Hz, H-2), 8.14-8.12 (3H, m, H-4, H-6′), 7.60-7.58 (2H, m, H-5′), 7.50 (1H, d, *J* = 8.0 Hz, H-7), 7.25-7.19 (2H, m, H-5, H-6), 4.73 (2H, s, H-2′); $^{13}$C NMR (DMSO, 150 MHz): $\delta_C$ 188.0 ($q_c$, C-1′), 147.6 ($q_c$, C-7′), 144.4 ($q_c$, C-4′), 136.6 ($q_c$, C-7a), 135.2 (CH, C-2), 126.4 (CH, C-5′), 125.4 ($q_c$, C-3a), 123.8 (CH, C-6′), 123.1 (CH, C-6), 122.1 (CH, C-5), 121.2 (CH, C-4), 114.8 ($q_c$, C-3), 112.3 (CH, C-7), 40.1 ($CH_2$, C-2′ *) ppm; EIMS *m/z* (rel. int.) 223 $[M+H]^+$ (5), 212 (4), 168 (20), 159 (50), 151 (20), 144 (100), 138 (10), 130 (90), 122 (100), 117 (35), 89 (10), 77 (5); HREIMS *m/z* 313.0645 (calcd for $C_{16}H_{13}N_2O_3S$ $[M+H]^+$ 313.0647).

*resolved by HSQC; Elem. Anal. Found: C, 60.14; H, 3.47; N, 8.76; S, 9.34%; Calcd for $C_{16}H_{13}N_2O_3S$: C, 61.53; H, 3.87; N, 8.97; S, 10.27%.

**1-(1*H*-indol-3-yl)-2-[(phenylmethyl)thio]-ethanone (3.55):**

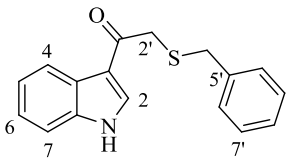


**3.55**

Yellow crystalline solid (80%); m. p: 81- 82 °C; $^1$H NMR (DMSO, 600 MHz): $\delta_H$ 12.02 (1H, s, NH-1), 8.34 (1H, d, *J* = 3.2 Hz, H-2), 8.19-8.17 (1H, m, H-4), 7.48-7.47 (1H, m, H-7), 7.36-7.30 (4H, m, H-6′, H-7′), 7.26-7.18 (3H, m, H-5, H-6, H-8′), 3.83 (2H, s, H-4′), 3.71 (2H, s, H-2′); $^{13}$C NMR (DMSO, 150 MHz): $\delta_C$ 190.6 ($q_c$, C-1′), 138.2 ($q_c$, C-5′), 136.7 ($q_c$, C-7a), 134.8 (CH, C-2), 129.1 (CH, C-6′), 128.5 (CH, C-7′), 127.0 (CH, C-8′), 125.7 ($q_c$, C-3a), 123.0 (CH, C-6), 122.0 (CH, C-5), 121.4 (CH, C-4), 115.0 ($q_c$, C-3), 112.3 (CH, C-7), 36.9 ($CH_2$, C-2′), 35.6 ($CH_2$, C-4′) ppm; EIMS *m/z* (rel. int.) 137 $[M+H]^+$ (15), 118 (5), 91 (100); HREIMS *m/z* 282.0950 (calcd for $C_{17}H_{16}NOS$ $[M+H]^+$ 282.0953).

**1-(1*H*-indol-3-yl)-2-[(4-fluorophenylmethyl)thio]-ethanone (3.56):**

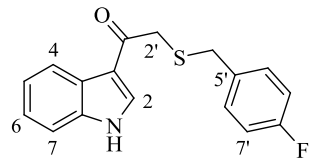


**3.56**

Yellow crystalline solid (26%); m. p: 178- 180 °C; $^1$H NMR (DMSO, 600 MHz): $\delta_H$ 12.02 (1H, s, NH-1), 8.35 (1H, d, *J* = 3.1 Hz, H-2), 8.18 (1H, d, *J* = 7.3 Hz, H-4), 7.48 (1H, d, *J* = 7.5 Hz, H-7), 7.40 (2H, m, H-6′), 7.24-7.18 (2H, m, H-5, H-6), 7.16-7.13 (2H, m, H-7′), 3.82 (2H, s, H-4′), 3.71 (2H, s, H-2′); $^{13}$C NMR (DMSO, 150 MHz): $\delta_C$ 190.4 ($q_c$, C-1′), 161.2 ($q_c$, d, $J_{F.C}$ = 242.9 Hz, C-8′), 136.7 ($q_c$, C-7a), 134.7 (CH, C-2), 134.4 ($q_c$, d, $J_{F.C}$ = 3.0 Hz, C-5′), 130.9 (CH, d, $J_{F.C}$ = 8.4 Hz, C-6′), 125.6 ($q_c$, C-3a), 122.9 (CH, C-6), 121.9 (CH, C-5), 121.3 (CH, C-4), 115.1 (CH, d, $J_{F.C}$ = 12.5 Hz, C-7′), 114.9 ($q_c$, C-3), 112.2 (CH, C-7), 36.9 ($CH_2$, C-2′), 34.7 ($CH_2$, C-4′) ppm; EIMS *m/z* (rel. int.) 130 $[M+H]^+$ (5), 109 (100), 83 (4); HREIMS *m/z* 300.0849 (calcd for $C_{17}H_{15}FNOS$ $[M+H]^+$ 300.0858).

**1-(1*H*-indol-3-yl)-2-[(4-chlorophenylmethyl)thio]-ethanone (3.57):**

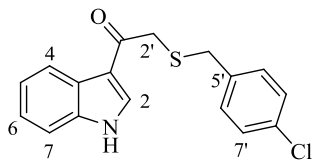


**3.57**

White crystalline solid (25%); m. p: 202- 204 °C; $^{1}$H NMR (DMSO, 600 MHz): $\delta_H$ 12.00 (1H, s, NH-1), 8.34 (1H, d, *J* = 3.2 Hz, H-2), 8.17 (1H, d, *J* = 6.7 Hz, H-4), 7.48-7.47 (1H, m, H-7), 7.39-7.36 (4H, m, H-6′, H-7′), 7.24-7.18 (2H, m, H-5, H-6), 3.82 (2H, s, H-4′), 3.71 (2H, s, H-2′); $^{13}$C NMR (DMSO, 150 MHz): $\delta_C$ 190.4 ($q_c$, C-1′), 137.3 ($q_c$, C-5′), 136.7 ($q_c$, C-7a), 134.7 (CH, C-2), 131.5 ($q_c$, C-8′), 130.9 (CH, C-6′), 128.3 (CH, C-7′), 125.6 ($q_c$, C-3a), 122.9 (CH, C-6), 121.9 (CH, C-5), 121.3 (CH, C-4), 114.9 ($q_c$, C-3), 112.2 (CH, C-7), 36.8 ($CH_2$, C-2′), 34.7 ($CH_2$, C-4′) ppm; EIMS *m/z* (rel. int.) 130 $[M+H]^+$ (5), 125 (100), 99 (4), 89 (5); HREIMS *m/z* 316.0562 (calcd for $C_{17}H_{15}{}^{35}ClNOS$ $[M+H]^+$ 316.0563).

**1-(1*H*-indol-3-yl)-2-[(4-bromophenylmethyl)thio]-ethanone (3.58):**

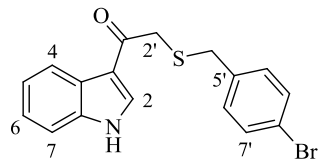


**3.58**

Yellow crystalline solid (21%); m. p: 219- 220 °C; $^{1}$H NMR (DMSO, 600 MHz): $\delta_H$ 12.00 (1H, s, NH-1), 8.35 (1H, d, *J* = 3.2 Hz, H-2), 8.17-8.16 (1H, m, H-4), 7.52-7.49 (1H, m, H-7′), 7.48-7.47 (2H, m, H-7'), 7.24-7.22 (2H, m, H-6′), 7.21-7.18 (2H, m, H-5, H-6), 3.80 (2H, s, H-4′), 3.71 (2H, s, H-2′); $^{13}$C NMR (DMSO, 150 MHz): $\delta_C$ 190.3 ($q_c$, C-1′), 137.8 ($q_c$, C-5′), 136.7 ($q_c$, C-7a), 134.7 (CH, C-2), 131.2 (CH, C-6′), 131.2 (CH, C-7′), 125.6 ($q_c$, C-3a), 122.9 (CH, C-6), 121.9 (CH, C-5), 121.3 (CH, C-4), 120.0 ($q_c$, C-8′), 114.9 ($q_c$, C-3), 112.2 (CH, C-7), 36.8 ($CH_2$, C-2′), 34.8 ($CH_2$, C-4′) ppm; EIMS *m/z* (rel. int.) 170 $[M+H]^+$ (100), 168 (98), 130 (5), 90 (10); HREIMS *m/z* 360.0050 (calcd for $C_{17}H_{15}{}^{79}BrNOS$ $[M+H]^+$ 360.0053).

**1-(1*H*-indol-3-yl)-2-[(3-bromophenylmethyl)thio]-ethanone (3.59):**

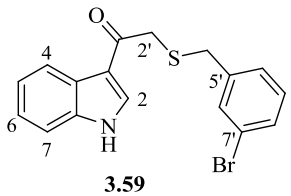


**3.59**

White crystalline solid (20%); m. p: 140- 141 °C; $^{1}$H NMR (DMSO, 600 MHz): $\delta_H$ 12.00 (1H, s, NH-1), 8.34 (1H, d, *J* = 3.1 Hz, H-2), 8.17 (1H, d, *J* = 7.1 Hz, H-4), 7.57-7.56 (1H, m, H-8′), 7.48-7.47 (1H, m, H-7), 7.45-7.43 (1H, m, H-6′), 7.37 (1H, d, *J* = 7.7 Hz, H-10′), 7.28 (1H, t, *J* = 7.8 Hz, H-9′), 7.24-7.18 (2H, m, H-5, H-6), 3.82 (2H, s, H-4′), 3.72 (2H, s, H-2′); $^{13}$C NMR (DMSO, 150 MHz): $\delta_C$ 190.3 ($q_c$, C-1′), 141.2 ($q_c$, C-5′), 136.7 ($q_c$, C-7a), 134.7 (CH, C-2), 131.7 ($q_c$, C-8′), 130.5 ($q_c$, C-7′), 129.7 (CH, C-6′), 128.1 (CH, C-10′),125.6 ($q_c$, C-3a), 122.9 (CH, C-6), 121.9 (CH, C-5), 121.5 (CH, C-9′), 121.3 (CH, C-4), 114.6 ($q_c$, C-3), 112.2 (CH, C-7), 36.8 ($CH_2$, C-2′), 34.8 ($CH_2$, C-4′) ppm; EIMS *m/z* (rel. int.) 214 $[M+H]^+$ (10), 168 (100), 130 (12), 90 (5); HREIMS *m/z* 360.0055 (calcd for $C_{17}H_{15}{}^{79}BrNOS$ $[M+H]^+$ 360.0058).

**1-(1*H*-indol-3-yl)-1-[(phenylethyl)thio]-ethanone (3.60):**

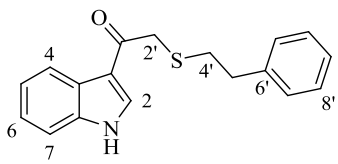


**3.60**

Yellow crystalline solid (27%); m. p: 101- 102 °C; $^{1}$H NMR (DMSO, 600 MHz): $\delta_H$ 12.00 (1H, s, NH-1), 8.40 (1H, d, *J* = 3.1 Hz, H-2), 8.17 (1H, d, *J* = 7.5 Hz, H-4), 7.48-7.47 (1H, m, H-7), 7.28-7.26 (2H, m, H-8′), 7.23-7.17 (5H, m, H-5, H-6, H-7′, H-9′), 3.84 (2H, s, H-2′), 2.87-2.81 (4H, m, H-4′, H-5′); $^{13}$C NMR (DMSO, 150 MHz): $\delta_C$ 190.8 ($q_c$, C-1′), 140.5 ($q_c$, C-6′), 136.7 ($q_c$, C-7a), 134.7 (CH, C-2), 128.5 (CH, C-8′), 128.3 (CH, C-7′), 126.1 (CH, C-9′), 125.6 ($q_c$, C-3a), 122.9 (CH, C-6), 121.8 (CH, C-5), 121.3 (CH, C-4), 115.0 ($q_c$, C-3), 112.2 (CH, C-7), 37.4 ($CH_2$, C-2′), 35.1 ($CH_2$, C-5′), 33.2 ($CH_2$, C-4′) ppm; EIMS *m/z* (rel. int.) 151 $[M+H]^+$ (30), 130 (25), 117 (30), 105 (100), 91 (10), 79 (5); HREIMS *m/z* 296.1106 (calcd for $C_{18}H_{18}NOS$ $[M+H]^+$ 296.1109).

**1-(1*H*-indol-3-yl)-2-[(*iso*-phenylethyl)thio]-ethanone (3.61):**

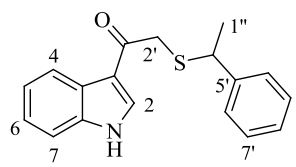

**3.61**

White crystalline solid (56%); m. p: 154- 155 °C; $^{1}$H NMR (DMSO, 600 MHz): $\delta_H$ 12.00 (1H, s, NH-1), 8.24 (1H, s, H-2), 8.16 (1H, d, *J* = 7.3 Hz,, H-4), 7.47 (1H, d, *J* = 7.9 Hz, H-7), 7.37 (2H, d, *J* = 7.2 Hz, H-6′), 7.34-7.31 (2H, m, H-7′), 7.25-7.18 (3H, m, H-5, H-6, H-8′), 4.19-4.15 (1H, m, H-4′), 3.78 (1H, d, *J* = 14.0 Hz, H-2′), 3.50 (1H, d, *J* = 14.1 Hz, H-2′), 1.53 (3H, d, *J* = 7.0 Hz, H-1″); $^{13}$C NMR (DMSO, 150 MHz): $\delta_C$ 190.5 ($q_c$, C-1′), 143.3 ($q_c$, C-5′), 136.6 ($q_c$, C-7a), 134.5 (CH, C-2), 128.4 (CH, C-6′), 127.3 (CH, C-7′), 127.1 (CH, C-8′), 125.6 ($q_c$, C-3a), 122.9 (CH, C-6), 121.9 (CH, C-5), 121.3 (CH, C-4), 114.9 ($q_c$, C-3), 112.2 (CH, C-7), 43.4 (CH, C-4′), 37.2 ($CH_2$, C-2′), 21.8 ($CH_3$, C-1″) ppm; EIMS *m/z* (rel. int.) 192 $[M+H]^+$ (100), 105 (10); HREIMS *m/z* 296.1113 (calcd for $C_{18}H_{18}NOS$ $[M+H]^+$ 296.1109).

**1-(6-Fluoro-1*H*-indol-3-yl)-2-[(4-bromophenyl)thio]-ethanone (3.62):**

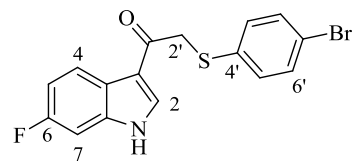

**3.62**

White crystalline solid (91%), $^{1}$H NMR (DMSO, 600 MHz): $\delta_H$ 12.02 (1H, s, NH-1), 8.49 (1H, s, H-2), 8.11-8.09 (1H, m, H-4), 7.48-7.46 (2H, m, H-6′), 7.34-7.32 (2H, m, H-5′), 7.30-7.27 (1H, m, H-7), 7.07-7.04 (1H, m, H-5), 4.48 (2H, s, H-2′); $^{13}$C NMR (DMSO, 150 MHz): $\delta_C$ 189.0 ($q_c$, C-1′), 169.5 ($q_c$, d, $J_{F.C}$ = 236.5 Hz, C-6), 136.8 ($q_c$, d, $J_{F.C}$ = 11.5 Hz, C-7a), 136.1 (CH, C-2), 135.7 ($q_c$, C-4′), 131.7 (CH, C-6′), 129.9 (CH, C-5′), 122.5 (CH, d, $J_{F.C}$ = 10.4 Hz, C-4), 122.2 ($q_c$, C-7′), 118.6 ($q_c$, C-3a), 115.0 ($q_c$, C-3), 110.5 (CH, d, $J_{F.C}$ = 23.5 Hz, C-7), 98.7 (CH, d, $J_{F.C}$ = 26.1 Hz, C-5), 40.1 ($CH_2$, C-2′*) ppm; EIMS *m/z* (rel. int.) 200 $[M+H]^+$ (18), 177 (30), 162 (45), 148 (30), 135 (30), 122 (100); HREIMS *m/z* 363.9811 (calcd for $C_{16}H_{12}{}^{79}BrFNOS$ $[M+H]^+$ 363.9807). *resolved by HSQC; Elem. Anal. Found: C, 52.71; H, 3.12; N, 3.86; S, 8.57%; Calcd for $C_{16}H_{12}BrFNOS$: C, 52.76; H, 3.04; N, 3.85; S, 8.8%.

**1-(6-Chloro-1*H*-indol-3-yl)-2-[(4-bromophenyl)thio]-ethanone (3.63):**

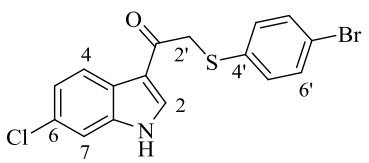


**3.63**

Yellow crystalline solid (59%); m. p: 198- 199 °C; $^{1}$H NMR (DMSO, 600 MHz): $\delta_H$ 12.18 (1H, s, NH-1), 8.53 (1H, s, H-2), 8.11 (1H, d, *J* = 8.5 Hz, H-4), 7.54 (1H, s, H-7), 7.48-7.46 (2H, m, H-6′), 7.34-7.32 (2H, m, H-5′), 7.22-7.21 (1H, m, H-5), 4.49 (2H, s, H-2′); $^{13}$C NMR (DMSO, 150 MHz): $\delta_C$ 188.9 ($q_c$, C-1′), 137.1 ($q_c$, C-4′), 136.0 (CH, C-2), 135.9 ($q_c$, C-7a), 131.7 (CH, C-6′), 129.8 (CH, C-5′), 127.6 (CH, C-6), 124.2 ($q_c$, C-3a), 122.5 (CH, C-4), 122.3 (CH, C-5), 118.5 ($q_c$, C-7′), 114.9 ($q_c$, C-3), 112.0 (CH, C-7), 40.1 (CH, C-2′ *) ppm; EIMS *m/z* (rel. int.) 299 $[M+H]^+$ (20), 202 (5), 193 (25), 178 (40), 164 (15), 151 (18), 122 (100); HREIMS *m/z* 379.9502 (calcd for $C_{16}H_{12}{}^{79}Br^{35}ClNOS$ $[M+H]^+$ 379.9512). *resolved by HSQC; Elem. Anal. Found: C, 50.47; H, 2.45; N, 3.85; S, 7.43%; Calcd for $C_{16}H_{12}{}^{79}BrClNOS$: C, 50.48; H, 2.91; N, 3.68; S, 8.42%.

**1-(6-Bromo-1*H*-indol-3-yl)-2-[(4-bromophenyl)thio]-ethanone (3.64):**

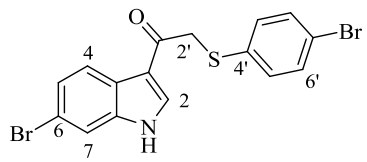


**3.64**

White crystalline solid (26%), $^{1}$H NMR (DMSO, 600 MHz): $\delta_H$ 12.18 (1H, s, NH-1), 8.52 (1H, s, H-2), 8.1 (1H, d, *J* = 8.5 Hz, H-4), 7.68 (1H, s, H-7), 7.49-7.46 (2H, m, H-6′), 7.34-7.32 (3H, m, H-5′, H-5), 4.49 (2H, s, H-2′); $^{13}$C NMR (DMSO, 150 MHz): $\delta_C$ 188.9 ($q_c$, C-1′), 137.5 ($q_c$, C-7a), 136.0 ($q_c$, C-4′), 135.8 (CH, C-2), 133.0 (CH, C-6′), 130.7 (CH, C-5′), 129.8 ($q_c$, C-6), 125.0 (CH, H-5), 124.5 ($q_c$, C-3a), 123.0 (CH, C-4), 118.5 ($q_c$, C-7′), 115.6 ( CH, C-7), 115.0 ($q_c$, C-3), 40.1 ($CH_2$, C-2′ *) ppm; EIMS *m/z* (rel. int.) 238 $[M+H]^+$ (10), 223 (17), 202 (30), 177 (12), 122 (100); HREIMS *m/z* 423.8994 (calcd for $C_{16}H_{12}{}^{79}Br_2NOS$ $[M+H]^+$ 423.0096). *resolved by HSQC; Elem. Anal. Found: C, 44.78; H, 1.24; N, 3.38; S, 7.54%; Calcd for $C_{16}H_{12}{}^{79}Br_2NOS$: C, 45.2; H, 2.61; N, 3.29; S, 7.54%.

**1-(5-Chloro-1*H*-indol-3-yl)-2-[(4-bromophenyl)thio]-ethanone (3.65):**

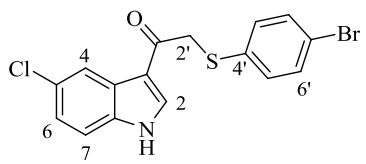


**3.65**

White crystalline solid (74%); m. p: 199- 200 °C; $^{1}$H NMR (DMSO, 600 MHz): $\delta_H$ 12.26 (1H, s, NH-1), 8.54 (1H, s, H-2), 8.10 (1H, s, H-4), 7.51 (1H, d, *J* = 8.4 Hz, H-7), 7.47 (2H, d, *J* = 8.9 Hz, H-6′), 7.33 (2H, d, *J* = 8.9 Hz, H-5′), 7.26-7.24 (1H, m, H-6), 4.47 (2H, s, H-2′); $^{13}$C NMR (DMSO, 150 MHz): $\delta_C$ 189.0 ($q_c$, C-1′), 136.3 ($q_c$, C-4′), 136.0 (CH, C-2), 135.1 ($q_c$, C-7a), 131.7 (CH, C-6′), 130.0 (CH, C-5′), 126.8 ($q_c$, C-3a), 126.6 (CH, C-5), 123.1 (CH, C-6), 120.3 (CH, C-4), 118.6 ($q_c$, C-7′), 114.5 ($q_c$, C-3), 114.0 (CH, C-7), 40.1 (CH, C-2′ *) ppm; EIMS *m/z* (rel. int.) 299 $[M+H]^+$ (10), 200 (8), 193 (20), 178 (23), 164 (15), 151 (16), 130 (5), 122 (100), 78 (3); HREIMS *m/z* 379.9494 (calcd for $C_{16}H_{12}{}^{79}Br^{35}ClNOS$ $[M+H]^+$ 379.9512). *resolved by HSQC; Elem. Anal. Found: C, 50.45; H, 2.45; N, 3.85; S, 7.43%; Calcd for $C_{16}H_{12}BrClNOS$: C, 50.48; H, 2.91; N, 3.68; S, 8.42%.

**1-(5-Bromo-1*H*-indol-3-yl)-2-[(4-bromophenyl)thio]-ethanone (3.66):**

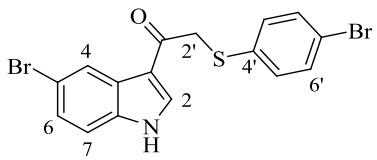


**3.66**

Yellow crystalline solid (55%); m. p: 214- 216 °C; $^{1}$H NMR (DMSO, 600 MHz): $\delta_H$ 12.26 (1H, s, NH-1), 8.54 (1H, s, H-2), 8.26 (1H, s, H-4), 7.49-7.46 (3H, m, H-7, H-6′), 7.37-7.35 (1H, m, H-6), 7.34-7.32 (2H, m, H-5′), 4.48 (2H, s, H-2′); $^{13}$C NMR (DMSO, 150 MHz): $\delta_C$ 189.0 ($q_c$, C-1′), 136.1 ($q_c$, C-4′), 135.9 (CH, C-2), 135.3 ($q_c$, C-7a), 131.7 (CH, C-6′), 130.0 (CH, C-5′), 127.2 ($q_c$, C-3a), 125.7 (CH, C-6), 123.4 (CH, C-4), 118.6 ($q_c$, C-7′), 114.8 ($q_c$, C-3), 114.4 (overlapping CH, C-7 and qc, C-5 ), 40.1 (CH, C-2′ *) ppm; EIMS *m/z* (rel. int.) 299 $[M+H]^+$ (15), 236 (7), 221 (10), 207 (8), 202 (10), 194 (7), 122 (100), 78 (3); HREIMS *m/z* 423.9002 (calcd for $C_{16}H_{12}{}^{79}Br_2NOS$ $[M+H]^+$ 423.9006). *resolved by HSQC; Elem. Anal. Found: C, 45.3; H, 2.53; N, 3.5; S, 6.98%; Calcd for $C_{16}H_{12}{}^{79}Br_2NOS$: C, 45.2; H, 2.61; N, 3.29; S, 7.54%.

**1-(7-Fluoro-1*H*-indol-3-yl)-2-[(4-bromophenyl)thio]-ethanone (3.67):**

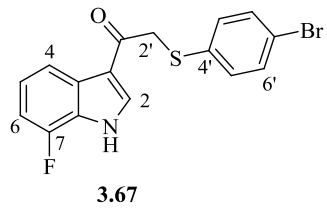


**3.67**

Yellow crystalline solid (63%); m. p: 172- 174 °C; $^{1}$H NMR (DMSO, 600 MHz): $\delta_H$ 12.61 (1H, s, NH-1), 8.57 (1H, d, *J* = 3.1 Hz, H-2), 7.94 (1H, d, *J* = 7.8 Hz, H-4), 7.49-7.46 (2H, m, H-6′), 7.35-7.32 (2H, m, H-5′), 7.18-7.15 (1H, m, H-5), 7.10-7.06 (1H, m, H-6), 4.52 (2H, s, H-2′); $^{13}$C NMR (DMSO, 150 MHz): $\delta_C$ 189.1 ($q_c$, C-1′), 149.1 ($q_c$, d, $J_{F.C}$ = 245.4 Hz, C-7), 136.0 (CH, C-2), 135.7 ($q_c$, C-4′), 131.7 (CH, C-6′), 129.8 (CH, C-5′), 129.1 ($q_c$, d, $J_{F.C}$ = 4.4 Hz, C-7a), 124.5 ($q_c$, d, $J_{F.C}$ = 13.2 Hz, C-3a), 122.7 (CH, d, $J_{F.C}$ = 6.4 Hz, C-5), 118.5 ($q_c$, C-7′), 117.4 (CH, d, $J_{F.C}$ = 3.7 Hz, C-4), 115.3 ($q_c$, C-3), 108.2 (CH, d, $J_{F.C}$ = 15.2 Hz, C-6), 40.1 ($CH_2$, C-2′ *) ppm; EIMS *m/z* (rel. int.) 299 $[M+H]^+$ (10), 202 (10), 177 (18), 162 (55), 148 (25), 135 (20), 122 (100), 107 (3); HREIMS *m/z* 363.9802 (calcd for $C_{16}H_{12}{}^{79}BrFNOS$ $[M+H]^+$ 363.9807). *resolved by HSQC; Elem. Anal. Found: C, 51.98; H, 2.95; N, 3.84; S, 8.51%; Calcd for $C_{16}H_{12}BrFNOS$: C, 52.76; H, 3.04; N, 3.85; S, 8.8%.

**1-(7-Iodo-1*H*-indol-3-yl)-2-[(4-bromophenyl)thio]-ethanone (3.68):**

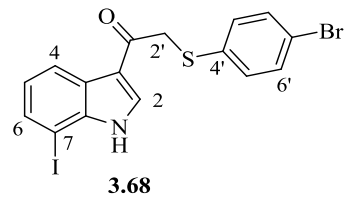


**3.68**

White crystalline solid (12%); m. p: 196- 197 °C; $^{1}$H NMR (DMSO, 600 MHz): $\delta_H$ 12.01 (1H, s, NH-1), 8.52 (1H, d, *J* = 3.2 Hz, H-2), 8.15 (1H, d, *J* = 7.9 Hz, H-4), 7.64-7.63 (1H, m, H-6), 7.48-7.46 (2H, m, H-6′), 7.35-7.32 (2H, m, H-5′), 7.00 (1H, t, *J* = 7.9 Hz, H-5), 4.53 (2H, s, H-2′); $^{13}$C NMR (DMSO, 150 MHz): $\delta_C$ 189.3 ($q_c$, C-1′), 138.5 ($q_c$, C-7a),136.0 (CH, C-2), 135.5 ($q_c$, C-4′), 132.1 (CH, C-6), 131.6 (CH, C-6′), 129.8 (CH, C-5′), 126.0 ($q_c$, C-3a), 123.8 (CH, C-5), 121.2 (CH, C-4), 118.5 ($q_c$, C-7′), 115.8 ($q_c$, C-3), 77.6 ($q_c$, C-7), 40.1 ($CH_2$, C-2′ *) ppm; EIMS *m/z* (rel. int.) 299 $[M+H]^+$ (40), 284 (20), 255 (15), 202 (45), 173 (18), 163 (15), 144 (10), 122 (100), 117 (4), 78 (3); HREIMS *m/z* 471.8854 (calcd for $C_{16}H_{12}{}^{79}BrINOS$ $[M+H]^+$ 471.8868). *resolved

by HSQC; Elem. Anal. Found: C, 39.93; H, 2.23; N, 3.31; S, 7.11%; Calcd for $C_{16}H_{12}BrINOS$: C, 40.7; H, 2.35; N, 2.97; S, 6.79%.

**1-(6-Chloro-5-fluoro-1*H*-indol-3-yl)-2-[(4-bromophenyl)thio]-ethanone (3.69):**

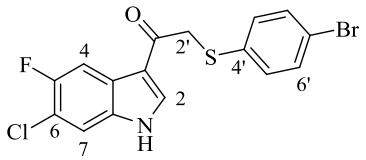


**3.69**

White crystalline solid (73%); m. p: 212- 213 °C; $^{1}$H NMR (DMSO, 600 MHz): $\delta_H$ 12.28 (1H, s, NH-1), 8.57 (1H, s, H-2), 7.94 (1H, d, *J* = 10.0 Hz, H-4), 7.70 (1H, d, *J* = 6.4 Hz, H-7), 7.47-7.45 (2H, m, H-6′), 7.33-7.31 (2H, m, H-5′), 4.47 (2H, s, H-2′); $^{13}$C NMR (DMSO, 150 MHz): $\delta_C$ 189.1 ($q_c$, C-1′), 153.7 ($q_c$, d, $J_{F.C}$ = 237.9 Hz, C-5), 137.1 (CH, C-2), 135.9 ($q_c$, C-4′), 132.8 ($q_c$, C-7a), 131.8 (CH, C-6′), 130.1 (CH, C-5′), 124.8 ($q_c$, d, $J_{F.C}$ = 9.6 Hz, C-3a), 118.8 ($q_c$, C-7′), 115.4 ($q_c$, C-3), 115.2 ($q_c$, d, $J_{F.C}$ = 29.3 Hz, C-6), 113.9 (CH, C-7), 107.5 (CH, d, $J_{F.C}$ = 24.2 Hz, C-4), 40.1 ($CH_2$, C-2′*) ppm; EIMS *m/z* (rel. int.) 211 $[M+H]^+$ (15), 202 (20), 196 (20), 182 (16), 169 (15), 148 (5), 140 (5), 122 (100), 95 (3), 78 (3); HREIMS *m/z* 397.9402 (calcd for $C_{16}H_{11}{}^{79}Br^{35}ClFNOS$ $[M+H]^+$ 397.9417). *resolved by HSQC; Elem. Anal. Found: C, 48.6; H, 1.57; N, 3.78; S, 7.54%; Calcd for $C_{16}H_{11}BrClFNOS$: C, 48.2; H, 2.53; N, 3.51; S, 8.04%.

**1-(6-Bromo-5-fluoro-1*H*-indol-3-yl)-2-[(4-bromophenyl)thio]-ethanone (3.70):**

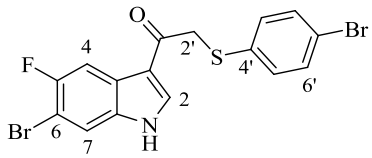


**3.70**

White crystalline solid (37%); m. p: 225- 226 °C; $^{1}$H NMR (DMSO, 600 MHz): $\delta_H$ 12.27 (1H, s, NH-1), 8.59 (1H, s, H-2), 7.93 (1H, d, *J* = 7.5 Hz, H-4), 7.81 (1H, d, *J* = 5.9 Hz, H-7), 7.48-7.46 (2H, m, H-6′), 7.34-7.32 (2H, m, H-5′), 4.49 (2H, s, H-2′); $^{13}$C NMR (DMSO, 150 MHz): $\delta_C$ 189.1 ($q_c$, C-1′), 154.3 ($q_c$, d, $J_{F.C}$ = 236.5 Hz, C-5), 137.0 (CH, C-2), 135.9 ($q_c$, C-4′), 133.6 ($q_c$, C-7a), 131.6 (CH, C-6′), 129.9 (CH, C-5′), 125.3 ($q_c$, d, $J_{F.C}$ = 10.0 Hz, C-3a), 118.6 ($q_c$, C-7′), 116.5 (CH, C-7), 114.9 ($q_c$, d, $J_{F.C}$ = 4.9 Hz, C-3), 107.1 (CH, d, $J_{F.C}$ = 25.9 Hz, C-4), 103.2 ($q_c$, d, $J_{F.C}$ = 24.6 Hz, C-6), 40.1 ($CH_2$, C-2′*) ppm; EIMS *m/z* (rel. int.) 256 $[M+H]^+$ (10), 241

(10), 227 (5), 214 (8), 202 (32), 147 (7), 122 (100), 107 (3), 78 (3); HREIMS *m/z* 441.8908 (calcd for $C_{16}H_{11}{}^{79}Br_2FNOS$ $[M+H]^+$ 441.8912).*resolved by HSQC; Elem. Anal. Found: C, 43.42; H, 1.71; N, 3.33; S, 6.6%; Calcd for $C_{16}H_{11}Br_2FNOS$: C, 43.37; H, 2.27; N, 3.16; S, 7.24%.

**1-(7-Bromo-5-methyl-1*H*-indol-3-yl)-2-[(4-bromophenyl)thio]-ethanone (3.71):**

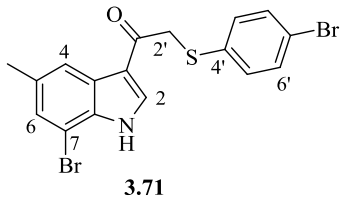

**3.71**

White crystalline solid (72%); m. p: 189- 190 °C; $^1$H NMR (DMSO, 600 MHz): $\delta_H$ 12.19 (1H, s, NH-1), 8.50 (1H, s, H-2), 7.94 (1H, s, H-4), 7.48-7.46 (2H, m, H-6′), 7.35-7.32 (2H, m, H-5′), 7.30 (1H, s, H-6), 4.50 (2H, s, H-2′), 2.39 (3H, s, H-1″); $^{13}$C NMR (DMSO, 150 MHz): $\delta_C$ 189.1 ($q_c$, C-1′), 136.0 ($q_c$, C-4′),135.8 (CH, C-2), 133.4 ($q_c$, C-5), 133.0 ($q_c$, C-7a), 131.6 (CH, C-6′), 129.9 (CH, C-5′), 127.3 (CH, C-6), 126.8 ($q_c$, C-3a), 120.5 (CH, C-4), 118.5 ($q_c$, C-7′), 115.4 ($q_c$, C-3), 104.3 (CH, C-7), 40.0 ($CH_2$, C-2′), 20.8 ($CH_3$, C-1″ *) ppm; EIMS *m/z* (rel. int.) 252 $[M+H]^+$ (12), 237 (25), 223 (10), 202 (20), 172 (5), 144 (10), 122 (100); HREIMS *m/z* 437.9154 (calcd for $C_{17}H_{14}{}^{79}Br_2NOS$ $[M+H]^+$ 437.9163). *resolved by HSQC; Elem. Anal. Found: C, 46.1; H, 2.6; N, 3.23; S, 7.0%; Calcd for $C_{17}H_{14}Br_2NOS$: C, 46.49; H, 2.98; N, 3.19; S, 7.3%.

**1-(1-Methyl-indol-3-yl)-2-(phenylthio)-ethanone (3.72):**

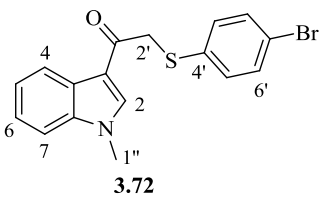

**3.72**

White crystalline solid (24%) ;m. p: 99- 100 °C; $^1$H NMR ($CDCl_3$, 600 MHz): $\delta_H$ 8.34-8.33 (1H, m, H-4), 7.68 (1H, s, H-2), 7.38-7.36 (2H, m, H-5′), 7.34-7.29 (3H, m, H-5, H-6, H-7), 7.29-7.27 (2H, m, H-6′), 4.10 (2H, s, 2′), 3.83 (3H, s, H-1″); $^{13}$C NMR ($CDCl_3$, 150 MHz): $\delta_C$ 188.7 ($q_c$, C-1′), 137.4 ($q_c$, C-7a), 135.8 (CH, C-2), 135.0 ($q_c$, C-4′), 132.0 (CH, C-5′), 131.6 (CH, C-6′), 126.5 ($q_c$, C-3a), 123.7 (CH, C-6), 122.9 (CH, C-5), 122.6 (CH, C-4), 120.7 ($q_c$, C-7′), 114.4 ($q_c$, C-3), 109.8 (CH, C-7), 41.9 ($CH_2$, C-2′), 33.7 ($CH_3$, C-1″) ppm; EIMS *m/z* (rel. int.) 200 $[M+H]^+$ (9), 173 (65), 158 (100), 144 (65), 131 (55), 122 (100), 103 (5); HREIMS *m/z* 360.0051 (calcd for $C_{17}H_{15}{}^{79}BrNOS$

$[M+H]^+$ 360.0058); Elem. Anal. Found: C, 56.17; H, 3.99; N, 3.73; S, 8.58%; Calcd for $C_{17}H_{15}BrNOS$: C, 56.67; H, 3.92; N, 3.89; S, 8.9%.

**1-(1-benzyl-indol-3-yl)-2-(phenylthio)-ethanone (3.73):**

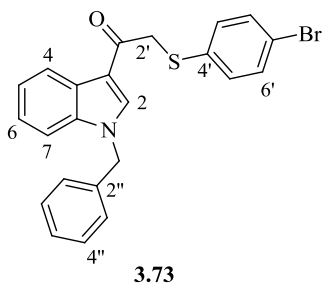


**3.73**

White crystalline solid (55%) ;m. p: 118- 119 °C; $^1$H NMR ($CDCl_3$, 600 MHz): $\delta_H$ 8.37-8.35 (1H, m, H-4), 7.73 (1H, s, H-2), 7.36-7.26 (10H, m, H-5, H-6, H-7, H-5′, H-6′, H-4″, H-5″), 7.14-7.13 (2H, m, H-3″), 5.32 (2H, s, 1″), 4.10 (2H, s, H-2′); $^{13}$C NMR ($CDCl_3$, 150 MHz): $\delta_C$ 188.9 ($q_c$, C-1′), 137.0 ($q_c$, C-7a), 135.4 ($q_c$, C-2″), 135.1 (CH, C-2), 134.9 ($q_c$, C-4′), 131.9 (CH, C-5′), 131.7 (CH, C-6′), 129.1 (CH, C-4″), 128.3, (CH, C-5″), 127.0 (CH, C-3″), 126.6 ($q_c$, C-3a), 123.8 (CH, C-6), 123.1 (CH, C-5), 122.7 (CH, C-4), 120.7 ($q_c$, C-7′), 115.4 ($q_c$, C-3), 110.3 (CH, C-7), 50.8 ($CH_2$, C-1″), 42.0 ($CH_2$, C-2′) ppm; EIMS *m/z* (rel. int.) 299 $[M+H]^+$ (5), 249 (45), 220 (18), 200 (15), 122 (100), 91 (30); HREIMS *m/z* 436.0367 (calcd for $C_{23}H_{19}{}^{79}BrNOS$ $[M+H]^+$ 436.0371); Elem. Anal. Found: C, 63.18; H, 3.7; N, 3.21; S, 7.73%; Calcd for $C_{23}H_{19}BrNOS$: C, 63.31; H, 4.16; N, 3.21; S, 7.35%.

## 5.2 Growth inhibition assays

### 5.2.1 *Plasmodium falciparum* growth inhibition assay

*P. falciparum* (3D7 strain) parasites were maintained in medium composed of RPMI 1640 supplemented with 2 mM L-glutamine, 25 mM Hepes, 5% (w/v) Albumax II, 20 mM glucose, 0.65 mM hypoxanthine, 60 µg/mL gentamicin sulfate and 2-4% (v/v) human red blood cells, in an atmosphere of 5% $O_2$, 5% $CO_2$, 90% $N_2$. For the growth inhibition assays, parasite cultures were adjusted to 2% parasitaemia and 1% haematocrit (final) and incubated with 3-

fold serial dilutions of compounds in 96-well plates (200 µL culture/well; two wells per compound dilution) for 48 hours. Following the incubation, parasite levels in the wells were determined by colorimetric determination of parasite lactate dehydrogenase activity.[144]

The $Abs_{620}$ values in experimental wells were converted to percentage parasite viability relative to wells containing untreated parasite cultures and $IC_{50}$ values derived from graphs of % parasite viability vs. log (compound concentration) using the non-linear regression function of GraphPad Prism v.5.02. These experiments were conducted by Michelle Isaacs.

### 5.2.2 HeLa cell growth inhibition assay

HeLa cells were plated in 96-well plates at 2 x $10^4$ cell per well in 150 µL culture medium composed of DMEM supplemented with 5 mM L-glutamine, 10% (v/v) fetal bovine serum and antibiotics (penicillin/streptopmycin/amphotericin B).[144] After an overnight incubation in a 5% $CO_2$ humidified incubator, 3-fold serial dilutions of compounds were added to the cultures (duplicate wells; 200 µL final culture volume) and incubation continued for an additional 24 hours. Cell viability in individual wells was assessed by adding 20 µL per well resazurin toxicology reagent (Sigma-Aldrich) and measuring fluorescence intensity (exc. 560 nm, em. 590 nm) in a Spectramax M3 plate reader after an incubation of 2-4 hours. Fluorescence readings in experimental wells were converted to % cell viability relative to control wells containing untreated cells and used to derive $IC_{50}$ values from dose-response plots of % cell viability vs. log (compound concentration) using the non-linear regression function of GraphPad Prism v.5.02. These experiments were conducted by Michelle Isaacs.

### 5.3 Molecular docking studies

All docking experiments were performed using AutoDock Vina[134] against the crystal structure of *S. aureus* HPPK (PDB ID: 4CRJ)[127] 4CRJ which was prepared for docking by removing the co-crystallised ligand from the active site, followed by the addition of polar-hydrogens in AutoDock tools. Electrostatic charges were calculated as Gasteiger charges and atoms were assigned by the AutoDock 4[133] typing rules. Coordinates for docking experiments were defined by X, Y and Z coordinates obtained from the originally co-crystallized ligand and the search space was restricted to a cube of 30 Å around this coordinate. Docking was repeated eight times except for compound **3.73** for which it was repeated 32 times.

**References**

(1) Greenwood, B. M.; Bojang, K.; Whitty, C. J. M.; Targett, G. A. T. *Lancet* **2005**, *365*, 1487–1498.

(2) Gkrania-Klotsas, E.; Lever, A. M. L. *Blood Rev.* **2007**, *21*, 73–87.

(3) Kalra, S. P.; Naithani, N.; Mehta, S. R.; Kumar, R. *Med. J. Armed Forces India* **2002**, *58*, 228–233.

(4) Hay, S. I.; Rogers, D. J.; Randolph, S. E.; Stern, D. I.; Cox, J.; Shanks, G. D.; Snow, R. W. *Trends Parasitol.* **2002**, *18*, 530–534.

(5) Pasvol, G. *Medicine (Baltimore).* **2005**, *33*, 39–43.

(6) Lim, P.; Wongsrichanalai, C.; Chim, P.; Khim, N.; Kim, S.; Chy, S.; Sem, R.; Nhem, S.; Yi, P.; Duong, S.; Bouth, D. M.; Genton, B.; Beck, H. P.; Gobert, J. G.; Rogers, W. O.; Coppee, J. Y.; Fandeur, T.; Mercereau-Puijalon, O.; Ringwald, P.; Le Bras, J.; Ariey, F. *Antimicrob. Agents Chemother.* **2010**, *54*, 2135–2142.

(7) Tiyong Ifoue, S. H.; Teugwa Mofor, C.; Gouado, I.; Teto, G.; Asonganyi, T.; Amvam Zollo, P. H. *Indian J. Clin. Biochem.* **2009**, *24*, 288–293.

(8) Walker, N. F.; Nadjm, B.; Whitty, C. J. M. *Medicine (Baltimore).* **2014**, *42*, 100–106.

(9) Page, K. R.; Jedlicka, A. E.; Fakheri, B.; Noland, G. S.; Kesavan, A. K.; Scott, A. L.; Kumar, N.; Manabe, Y. C. *Infect. Immun.* **2005**, *73*, 8369–8380.

(10) Hastings, I. M.; Watkins, W. M. *Acta Trop.* **2005**, *94*, 218–229.

(11) Swales, C. A.; Chiodini, P. L.; Bannister, B. A. *J. Infect. Dis.* **2007**, *54*, 107–110.

(12) Egan, T. J. *Targets* **2003**, *2*, 115–124.

(13) Crompton, P. D.; Moebius, J.; Portugal, S.; Waisberg, M.; Hart, G.; Garver, L. S.; Miller, L. H.; Barillas-Mury, C.; Pierce, S. K. *Ann. Rev. Immunol.* **2014**, *32*, 157–187.

(14) Greenwood, B. M.; Targett, G. A. T. *Clin. Microbiol. Infect.* **2011**, *17*, 1600–1607.

(15) Kelly-Hope, L.; Ranson, H.; Hemingway, J. *Lancet Infect. Dis.* **2008**, *8*, 387–389.

(16) Agnandji, S. T.; Lell, B.; Fernandes, F.; Abossolo, B. P. *N. Engl. J. Med.* **2012**, *367*, 2284–2295.

(17) Rafikov, M.; Bevilacqua, L.; Wyse, A. P. P. *J. Theor. Biol.* **2009**, *258*, 418–425.

(18) Singh, K.; Kaur, H.; Smith, P.; De Kock, C.; Chibale, K.; Balzarini, J. *J. Med. Chem.* **2014**, *57*, 435–448.

(19) Mjambili, F.; Njoroge, M.; Naran, K.; De Kock, C.; Smith, P. J.; Mizrahi, V.; Warner, D.; Chibale, K. *Bioorganic Med. Chem. Lett.* **2014**, *24*, 560–564.

(20) Njogu, P. M.; Gut, J.; Rosenthal, P. J.; Chibale, K. *ACS Med. Chem. Lett.* **2013**, *4*, 637–641.

(21) Ridley, R. G. *Nature* **2002**, *415*, 919–928.

(22) Pink, R.; Hudson, A.; Mouriès, M.-A.; Bendig, M. *Nat. Rev. Drug Discov.* **2005**, *4*, 727–740.

(23) Nwaka, S.; Ridley, R. G. *Nat. Rev. Drug Discov.* **2003**, *2*, 919–928.

(24) Noedl, H.; Se, Y.; Schaecher, K.; Smith, B. L.; Socheat, D.; Fukuda, M. M. *New Engl. J. Med.* **2008**, *359*, 2619–2620.

(25) Bandini, M. *Org. Biomol. Chem.* **2013**, *11*, 5206–5212.

(26) Lather, D.; Lather, V. *J. Nat. Prod. Sci.* **2012**, *1*, 133.

(27) Taber, D. F.; Tirunahari, P. K. *Tetrahedron.* **2011**, *67*, 7195–7210.

(28) Worthen, D. R.; Gibson, D. A.; Rogers, D. T.; Bence, A. K.; Fu, M.; Littleton, J. M.; Crooks, P. A. *Brain Res.* **2001**, *890*, 343–346.

(29) Sharma, V.; Kumar, P.; Pathak, D. *J. Heterocycl. Chem.* **2012**, *47*, 491–502.

(30) Vitaku, E.; Smith, D. T.; Njardarson, J. T. *J. Med. Chem.* **2014**, *57*, 10257–10274.

(31) Seefeld, M. A.; Miller, W. H.; Newlander, K. A.; Burgess, W. J.; Payne, D. J.; Rittenhouse, S. F.; Moore, T. D.; DeWolf, W. E.; Keller, P. M.; Qiu, X.; Janson, C. A.; Vaidya, K.; Fosberry, A. P.; Smyth, M. G.; Jaworski, D. D.; Slater-Radosti, C.; Huffman, W. F. *Bioorganic Med. Chem. Lett.* **2001**, *11*, 2241–2244.

(32) Fulco, A. J.; Press, P.; Angeles, L. *Prog. Lipid Res.* **1983**, *22*, 133–160.

(33) Fausta Palluotto, Angelo Carotti, Giovanni Casini, Marcello Ferappi, A. R.; Cesare Vitali, F. C. *Farm.* **1999**, *54*, 191–194.

(34) Daly, S.; Hayden, K.; Malik, I.; Porch, N.; Tang, H.; Rogelj, S.; Frolova, L. V.; Lepthien, K.; Kornienko, A.; Magedov, I. V. *Bioorganic Med. Chem. Lett.* **2011**, *21*, 4720–4723.

(35) Samosorn, S.; Bremner, J. B.; Ball, A.; Lewis, K. *Bioorganic Med. Chem.* **2006**, *14*, 857–865.

(36) Lewis, K. *J. Mol. Microbiol. Biotechnol.* **2001**, *3*, 247–254.

(37) Cinchana, N. V.; Sujan, G. P. S. S. *Res. J. Pharm. Biol. Chem. Sci.* **2011**, *2*, 353–362.

(38) Leboho, T. C.; Michael, J. P.; van Otterlo, W. A. L.; van Vuuren, S. F.; de Koning, C. B. *Bioorg Med. Chem. Lett.* **2009**, *19*, 4948–4951.

(39) Yamamoto, Y.; Kurazono, M. *Bioorg Med. Chem. Lett.* **2007**, *17*, 1626–1628.

(40) Singh, P.; Verma, P.; Yadav, B.; Komath, S. S. *Bioorg Med. Chem. Lett.* **2011**, *21*, 3367–3372.

(41) Zoraghi, R.; Worrall, L.; See, R. H.; Strangman, W.; Popplewell, W. L.; Gong, H.; Samaai, T.; Swayze, R. D.; Kaur, S.; Vuckovic, M.; Finlay, B. B.; Brunham, R. C.; McMaster, W. R.; Davies-Coleman, M. T.; Strynadka, N. C.; Andersen, R. J.; Reiner, N. E. *J. Biol. Chem.* **2011**, *286*, 44716–44725.

(42) Veale, C. G. L.; Zoraghi, R.; Young, R. M.; Morrison, J. P.; Pretheeban, M.; Lobb, K. A.; Reiner, N. E.; Andersen, R. J.; Davies-Coleman, M. T. *J. Nat. Prod.* **2015**, *78*, 355−362.

(43) Reddy, B. V. S.; Rajeswari, N.; Sarangapani, M.; Reddy, G. R.; Madan, C.; Kumar, K. P.; Rao, M. S. *Bioorg Med. Chem. Lett.* **2011**, *21*, 6510–6514.

(44) Pordel, M.; Abdollahi, A.; Razavi, B. *Russ. J. Bioorganic Chem.* **2013**, *39*, 211–214.

(45) Wang, G.; Li, C.; He, L.; Lei, K.; Wang, F.; Pu, Y.; Yang, Z.; Cao, D.; Ma, L.; Chen, J.; Sang, Y.; Liang, X.; Xiang, M.; Peng, A.; Wei, Y.; Chen, L. *Bioorg Med. Chem.* **2014**, *22*, 2060–2079.

(46) Tang, K.; Huang, J.; Pan, J.; Zhang, X.; Lu, W. *RSC Adv.* **2015**, *5*, 19620–19623.

(47) Wen, Z.; Xu, J.; Wang, Z.; Qi, H.; Xu, Q.; Bai, Z.; Zhang, Q.; Bao, K.; Wu, Y.; Zhang, W. *Eur. J. Med. Chem.* **2015**, *90*, 184–194.

(48) Quirante, J.; Dubar, F.; González, A.; Lopez, C.; Cascante, M.; Cortés, R.; Forfar, I.; Pradines, B.; Biot, C. *J. Organomet. Chem.* **2011**, *696*, 1011–1017.

(49) Baytas, S. N.; Inceler, N.; Yılmaz, A.; Olgac, A.; Menevse, S.; Banoglu, E.; Hamel, E.; Bortolozzi, R.; Viola, G. *Bioorg. Med. Chem.* **2014**, *22*, 3096–3104.

(50) Guan, Q.; Han, C.; Zuo, D.; Li, Z.; Zhang, Q.; Zhai, Y.; Jiang, X.; Bao, K.; Wu, Y.; Zhang, W. *Eur. J. Med. Chem.* **2014**, *87*, 306–315.

(51) van Staveren, D. R.; Metzler-Nolte, N. *Chem. Rev.* **2004**, *104*, 5931–5985.

(52) Kowalski, K.; Koceva-Chy, A.; Szczupak, L.; Hikisz, P.; Bernasińska, J.; Rajnisz, A.; Solecka, J.; Therrien, B. *J. Organomet. Chem.* **2013**, *741-742*, 153–161.

(53) Osella, D.; Ferrali, M.; Zanello, P.; Laschi, F.; Fontani, M.; Nervi, C.; G. Cavigiolio, G. *Inorg. Chim. Acta* **2000**, *306*, 42–48.

(54) Kumar, D.; Kumar, N. M.; Akamatsu, K.; Kusaka, E.; Harada, H.; Ito, T. *Bioorg Med. Chem. Lett.* **2010**, *20*, 3916–3919.

(55) Ke, S.; Yang, Z.; Zhang, Z.; Liang, Y.; Wang, K.; Liu, M.; Shi, L. *Bioorg Med. Chem. Lett.* **2014**, *24*, 1907–1911.

(56) Gali, R.; Banothu, J.; Gondru, R.; Bavantula, R.; Velivela, Y.; Crooks, P. A. *Bioorg. Med. Chem. Lett.* **2015**, *25*, 106–112.

(57) Lai, M. J.; Chang, J. Y.; Lee, H. Y.; Kuo, C. C.; Lin, M. H.; Hsieh, H. P.; Chang, C. Y.; Wu, J. S.; Wu, S. Y.; Shey, K. S.; Liou, J. P. *Eur. J. Med. Chem.* **2011**, *46*, 3623–3629.

(58) Singh, P.; Kaur, M.; Verma, P. *Bioorg Med. Chem. Lett.* **2009**, *19*, 3054–3058.

(59) Niemyjska, M.; MacIejewska, D.; Wolska, I.; Truszkowski, P. *J. Mol. Struct.* **2012**, *1026*, 30–35.

(60) Mazzei, M.; Miele, M.; Nieddu, E.; Barbieri, F.; Bruzzo, C.; Alama, A. *Eur. J. Med. Chem.* **2001**, *36*, 915–923.

(61) Singh, P.; Kaur, M.; Holzer, W. *Eur. J. Med. Chem.* **2010**, *45*, 4968–4982.

(62) Ziedan, N. I.; Stefanelli, F.; Fogli, S.; Westwell, A. D. *Eur. J. Med. Chem.* **2010**, *45*, 4523–4530.

(63) Md Tohid, S. F.; Ziedan, N. I.; Stefanelli, F.; Fogli, S.; Westwell, A. D. *Eur. J. Med. Chem.* **2012**, *56*, 263–270.

(64) MacDonough, M. T.; Strecker, T. E.; Hamel, E.; Hall, J. J.; Chaplin, D. J.; Trawick, M. L.; Pinney, K. G. *Bioorg Med. Chem.* **2013**, *21*, 6831–6843.

(65) Magedov, I. V.; Lefranc, F.; Frolova, L. V.; Banuls, L. M. Y.; Peretti, A. S.; Rogelj, S.; Mathieu, V.; Kiss, R.; Kornienko, A. *Bioorg. Med. Chem. Lett.* **2013**, *23*, 3277–3282.

(66) Tiwari, R. K.; Verma, A. K.; Chhillar, A. K.; Singh, D.; Singh, J.; Kasi Sankar, V.; Yadav, V.; Sharma, G. L.; Chandra, R. *Bioorg. Med. Chem.* **2006**, *14*, 2747–2752.

(67) Guillon, R.; Giraud, F.; Logé, C.; Le Borgne, M.; Picot, C.; Pagniez, F.; Le Pape, P. *Bioorg. Med. Chem. Lett.* **2009**, *19*, 5833–5836.

(68) Na, Y. M. *Bull. Korean Chem. Soc.* **2010**, *31*, 3467–3470.

(69) Siwek, A.; Stefanska, J.; Dzitko, K.; Ruszczak, A. *J. Mol. Model.* **2012**, *18*, 4159–4170.

(70) Zhang, L.; Hua, Z.; Song, Y.; Feng, C. *Fitoterapia* **2014**, *97*, 142–147.

(71) Song, Y.; Wu, F.; Zhang, C.; Liang, G.; Zhou, G.; Yu, J. *Bioorg. Med. Chem. Lett.* **2015**, *25*, 259–261.

(72) Blaising, J.; Polyak, S. J.; Pécheur, E. I. *Antiviral Res.* **2014**, *107*, 84–94.

(73) Zhang, M.-Z.; Chen, Q.; Yang, G.-F. *Eur. J. Med. Chem.* **2015**, *89*, 421–441.

(74) Yeung, K. S.; Qiu, Z.; Xue, Q.; Fang, H.; Yang, Z.; Zadjura, L.; D'Arienzo, C. J.; Eggers, B. J.; Riccardi, K.; Shi, P. Y.; Gong, Y. F.; Browning, M. R.; Gao, Q.; Hansel, S.; Santone, K.; Lin, P. F.; Meanwell, N. a.; Kadow, J. F. *Bioorg Med. Chem. Lett.* **2013**, *23*, 198–202.

(75) Wang, T.; Zhang, Z.; Wallace, O. B.; Deshpande, M.; Fang, H.; Yang, Z.; Zadjura, L. M.; Tweedie, D. L.; Huang, S.; Zhao, F.; Ranadive, S.; Robinson, B. S.; Gong, Y. F.; Ricarrdi, K.; Spicer, T. P.; Deminie, C.; Rose, R.; Wang, H. G. H.; Blair, W. S.; Shi, P. Y.; Lin, P. F.; Colonno, R. J.; Meanwell, N. a. *J. Med. Chem.* **2003**, *46*, 4236–4239.

(76) Wang, T.; Kadow, J. F.; Zhang, Z.; Yin, Z.; Gao, Q.; Wu, D.; Parker, D. D.; Yang, Z.; Zadjura, L.; Robinson, B. A.; Gong, Y. F.; Blair, W. S.; Shi, P. Y.; Yamanaka, G.; Lin, P. F.; Meanwell, N. A. *Bioorg Med. Chem. Lett.* **2009**, *19*, 5140–5145.

(77) Famiglini, V.; Regina, G. La; Coluccia, A.; Pelliccia, S.; Brancale, A.; Maga, G.; Crespan, E.; Badia, R.; Riveira-mun, E.; Este, J. A.; Ferretti, R.; Cirilli, R.; Zamperini, C.; Botta, M.; Schols, D.; Limongelli, V.; Agostino, B.; Novellino, E.; Silvestri, R. *J. Med. Chem.* **2014**, *57*, 9945−9957.

(78) Hassam, M.; Basson, A. E.; Liotta, D. C.; Morris, L.; van Otterlo, W. A. L.; Pelly, S. C. *ACS Med. Chem. Lett.* **2012**, *3*, 470–475.

(79) Müller, R.; Mulani, I.; Basson, A. E.; Pribut, N.; Hassam, M.; Morris, L.; van Otterlo, W. A. L.; Pelly, S. C. *Bioorg. Med. Chem. Lett.* **2014**, *24*, 4376–4380.

(80) Zhao, Z.; Wolkenberg, S. E.; Lu, M.; Munshi, V.; Moyer, G.; Feng, M.; Carella, A. V.; Ecto, L. T.; Gabryelski, L. J.; Lai, M. T.; Prasad, S. G.; Yan, Y.; McGaughey, G. B.; Miller, M. D.; Lindsley, C. W.; Hartman, G. D.; Vacca, J. P.; Williams, T. M. *Bioorganic Med. Chem. Lett.* **2008**, *18*, 554–559.

(81) De Luca, L.; Barreca, M. L.; Ferro, S.; Iraci, N.; Michiels, M.; Christ, F.; Debyser, Z.; Witvrouw, M.; Chimirri, A. *Bioorg Med. Chem. Lett.* **2008**, *18*, 2891–2895.

(82) Zhou, G.; Wu, D.; Hermel, E.; Balogh, E.; Gochin, M. *Bioorg Med. Chem. Lett.* **2010**, *20*, 1500–1503.

(83) Rottmann, M.; McNamara, C.; Yeung, B. K. S.; Lee, M. C. S.; Zou, B.; Russell, B.; Seitz, P.; Plouffe, D. M.; Dharia, N. V; Tan, J.; Cohen, S. B.; Spencer, K. R.; González-Páez, G. E.; Lakshminarayana, S. B.; Goh, A.; Suwanarusk, R.; Jegla, T.; Schmitt, E. K.; Beck, H.-P.; Brun, R.; Nosten, F.; Renia, L.; Dartois, V.; Keller, T. H.; Fidock, D. A.; Winzeler, E. A.; Diagana, T. T. *Science* **2010**, *329*, 1175–1180.

(84) Yeung, B. K. S.; Zou, B.; Rottmann, M.; Lakshminarayana, S. B.; Ang, S. H.; Leong, S. Y.; Tan, J.; Wong, J.; Keller-Maerki, S.; Fischli, C.; Goh, A.; Schmitt, E. K.; Krastel, P.; Francotte, E.; Kuhen, K.; Plouffe, D.; Henson, K.; Wagner, T.; Winzeler, E. A.; Petersen, F.; Brun, R.; Dartois, V.; Diagana, T. T.; Keller, T. H. *J. Med. Chem.* **2010**, *53*, 5155–5164.

(85) Schuck, D. C.; Jordão, A. K.; Nakabashi, M.; Cunha, A. C.; Ferreira, V. F.; Garcia, C. R. S. *Eur. J. Med. Chem.* **2014**, *78*, 375–382.

(86) Mbeunkui, F.; Grace, M. H.; Lategan, C.; Smith, P. J.; Raskin, I.; Lila, M. A. *J. Ethnopharmacol.* **2012**, *139*, 471–477.

(87) Nugroho, A. E.; Sugai, M.; Hirasawa, Y.; Hosoya, T.; Awang, K.; Hadi, A. H. A.; Ekasari, W.; Widyawaruyanti, A.; Morita, H. *Bioorganic Med. Chem. Lett.* **2011**, *21*, 3417–3419.

(88) Nugroho, A. E.; Hirasawa, Y.; Kawahara, N.; Goda, Y.; Awang, K.; Hadi, A. H. A. *J. Nat. Prod.* **2009**, *72*, 1502–1506.

(89) Colletti, S. L.; Li, C.; Fisher, M. H.; Wyvratt, M. J.; Meinke, P. T. *Tetrahedron Lett.* **2000**, *41*, 7825–7829.

(90) Stocks, P. A.; Raynes, K. J.; Bray, P. G.; Park, B. K.; O`Neil, P. M.; Ward, S. A. *J. Med. Chem.* **2002**, *45*, 4975–4983.

(91) Delarue, S.; Girault, S.; Maes, L.; Debreu-Fontaine, M. A.; Labaeid, M.; Grellier, P.; Sergheraert, C. *J.Med.Chem.* **2001**, *44*, 2827–2833.

(92) Agarwal, A.; Srivastava, K.; Puri, S. K.; Chauhan, P. M. S. *Bioorg. Med. Chem. Lett.* **2005**, *15*, 3133–3136.

(93) Kgokong, J. L.; Smith, P. P.; Matsabisa, G. M. *Bioorg Med. Chem.* **2005**, *13*, 2935–2942.

(94) van Schalkwyk, D. A.; Chan, X. W. A.; Misiano, P.; Gagliardi, S.; Farina, C.; Saliba, K. *J. Biochem. Pharmacol.* **2010**, *79*, 1291–1299.

(95) Davis, R. A.; Duffy, S.; Avery, V. M.; Camp, D.; Hooper, J. N. A.; Quinn, R. J. *Tetrahedron Lett.* **2010**, *51*, 583–585.

(96) Teguh, S. C.; Klonis, N.; Duffy, S.; Lucantoni, L.; Avery, V. M.; Hutton, C. A.; Baell, J. B.; Tilley, L. *J. Med. Chem.* **2013**, *56*, 6200–6215.

(97) Urgaonkar, S.; Cortese, J. F.; Barker, R. H.; Cromwell, M.; Serrano, A. E.; Wirth, D. F.; Clardy, J.; Mazitschek, R. *Org. Lett.* **2010**, *12*, 3998–4001.

(98) Veale, C. G. L.; Edkins, A. L.; de la Mare, J.-A.; de Kock, C.; Smith, P. J.; Khanye, S. D. *Tetrahedron Lett.* **2015**, *56*, 1860–1864.

(99) Ottoni, O.; Neder, A. V; Dias, A. K.; Cruz, R. P.; Aquino, L. B. *Org. Lett.* **2001**, *3*, 1005–1007.

(100) Veale, C. G. L.; Lobb, K. A.; Zoraghi, R.; Morrison, J. P.; Reiner, N. E.; Andersen, R. J.; Davies-Coleman, M. T. *Tetrahedron* **2014**, *70*, 7845–7853.

(101) Johansson, H.; Urruticoechea, A.; Larsen, I.; Pedersen, D. S. *J. Org. Chem.* **2015**, *80*, 471–481.

(102) Barreca, M. L.; Ferro, S.; Rao, A.; Luca, L. De; Zappala, M. *J. Med. Chem.* **2005**, *48*, 7084–7088.

(103) King, L. C.; Ostrum, G. K. *J. Org. Chem.* **1964**, *29*, 3459–3461.

(104) Barata, L. E. S.; Santos, L. S.; Ferri, P. H.; Phillipson, J. D.; Paine, A.; Croft, S. L. *Phytochemistry* **2000**, *55*, 589–595.

(105) Fourrey, J.-L.; Beauhaire, J.; Yuan, C. W. *J. Chem. Soc. Perkin Trans. 1* **1987**, *6*, 1841–1843.

(106) Pal, M.; Swamy, N. K.; Hameed, P. S.; Padakanti, S.; Yeleswarapu, K. R. *Tetrahedron* **2004**, *60*, 3987–3997.

(107) Mallikarjuna Rao, R.; Nagaraja Reddy, G.; Sreeramulu, J. *Der Pharma Chem.* **2011**, *3*, 301–309.

(108) Chen, Z.; Yan, Q.; Liu, Z.; Xu, Y.; Zhang, Y. *Angew. Chem. Int. Ed.* **2013**, *52*, 13324–13328.

(109) Gupta, G. K.; Saini, V.; Khare, R.; Kumar, V. *Med. Chem. Res.* **2014**, *23*, 4209–4220.

(110) He, M.; Yang, N.; Sun, C.; Yao, X.; Yang, M. *Med. Chem. Res.* **2011**, *20*, 200–209.

(111) Fatunsin, O.; Shkoor, M.; Riahi, A.; Hussain, M.; Villinger, A.; Fischer, C.; Langer, P. *Helv. Chim. Acta* **2010**, *93*, 1610–1621.

(112) Loghmani-Khouzani, H.; Poorheravi, M. R.; Sadeghi, M. M. M.; Caggiano, L.; Jackson, R. F. W. *Tetrahedron* **2008**, *64*, 7419–7425.

(113) Aveniente, M.; Pinto, E. F.; Santos, L. S.; Rossi-Bergmann, B.; Barata, L. E. S. *Bioorg Med. Chem.* **2007**, *15*, 7337–7343.

(114) Strassberger, Z.; Alberts, A. H.; Louwerse, M. J.; Tanase, S.; Rothenberg, G. *Green Chem.* **2013**, *15*, 768–774.

(115) Spiteri, C.; Ritson, D. J.; Awaad, A.; Moses, J. E. *J. Saudi Chem. Soc.* **2011**, *15*, 375–378.

(116) Ritson, D. J.; Spiteri, C.; Moses, J. E. *J. Org. Chem.* **2011**, *76*, 3519–3522.

(117) Swinney, D. C. *Clin. Pharmacol. Ther.* **2013**, *93*, 299–301.

(118) B. T. Priest, G. E. *Front. Pharmacol.* **2014**, *5*, 1–2.

(119) Kotz, J. *Sci. Exch.* **2012**, *5*, 1–3.

(120) Njoroge, M.; Njuguna, N. M.; Mutai, P.; Ongarora, D. S. B.; Smith, P. W.; Chibale, K. *Chem. Rev.* **2014**, *114*, 11138–11163.

(121) Pires, D. E. V.; Blundell, T. L.; Ascher, D. B. *J. Med. Chem.* **2015**, *58*, 4066–4072.

(122) Klebe, G. *Drug Discov. Today* **2006**, *11*, 580–594.

(123) Doman, T. N.; McGovern, S. L.; Witherbee, B. J.; Kasten, T. P.; Kurumbail, R.; Stallings, W. C.; Connolly, D. T.; Shoichet, B. K. *J. Med. Chem.* **2002**, *45*, 2213–2221.

(124) Kitchen, D. B.; Decornez, H.; Furr, J. R.; Bajorath, J. *Nat. Rev. Drug Discov.* **2004**, *3*, 935–949.

(125) Ekins, S.; Mestres, J.; Testa, B. *Br. J. Pharmacol.* **2007**, *152*, 9–20.

(126) Kapetanovic, I. M. *Chem Biol Interact.* **2008**, *171*, 165–176.

(127) Dennis, M. L.; Chhabra, S.; Wang, Z.; Debono, A.; Dolezal, O.; Newman, J.; Pitcher, N. P.; Rahmani, R.; Cleary, B.; Barlow, N.; Hattarki, M.; Graham, B.; Peat, T. S.; Baell, J. B.; Swarbrick, J. D. *J. Med. Chem.* **2014**, *57*, 9612−9626.

(128) Chhabra, S.; Dolezal, O.; Collins, B. M.; Newman, J.; Simpson, J. S.; Macreadie, I. G.; Fernley, R.; Peat, T. S.; Swarbrick, J. D. *PLoS One* **2012**, *7*, e29444.

(129) O'Cualain, R. D. M.; Hyde, J. E.; Sims, P. F. G. *Malar. J.* **2010**, *9*, 286–297.

(130) Wang, P.; Wang, Q.; Yang, Y.; Coward, J. K.; Nzila, A.; Sims, P. F. G.; Hyde, J. E. *Mol. Biochem. Parasitol.* **2010**, *172*, 41–51.

(131) Rattanachuen, W.; Jönsson, M.; Swedberg, G.; Sirawaraporn, W. *Mol. Biochem. Parasitol.* **2009**, *168*, 135–142.

(132) Salcedo-sora, J. E.; Ochong, E.; Beveridge, S.; Johnson, D.; Nzila, A.; Biagini, G. A.; Stocks, P. A.; O`Neil, P. M. O.; Krishna, S.; Bray, P. G.; Ward, S. A. *J. Biol. Chem.* **2011**, *286*, 44659–44668.

(133) Morris, G. M.; Huey, R.; Lindstrom, W.; Sanner, M. F.; Belew, R. K.; Goodsell, D. S.; Olson, A. J. *J Comput Chem.* **2009**, *30*, 2785–2791.

(134) Trott, O.; Olson, A. *J. Comput. Chem.* **2010**, *31*, 455–461.

(135) Accelrys Software Inc., D. S. M. E. No Title, 2013, Release 4.0, San Diego: Accelrys Software Inc.

(136) Gottlieb, H. E.; Kotlyar, V.; Nudelman, A. *J. Org. Chem.* **1997**, *62*, 7512–7515.

(137) Armarego, W. L. F.; Perrin, D. D. *Purification of Laboratory Chemicals*; 1998.

(138) Casey, M.; Leonard, J.; Lygo, B.; Procter, G. *Advanced Practical Organic Chemistry*.

(139) Depree, G. J.; Main, L.; Nicholson, B. K.; Robinson, N. P.; Jameson, G. B. *J. Organomet. Chem.* **2006**, *691*, 667–679.

(140) Sechi, M.; Derudas, M.; Dallocchio, R.; Dessı, A.; Bacchi, A.; Sannia, L. *J. Med. Chem.* **2004**, *47*, 5298–5310.

(141) Patrizia, D.; Carbone, A.; Barraja, P.; Parrino, B.; Lopergolo, A.; Pennati, M.; Cirrincione, G. *ChemMedChem.* **2011**, *6*, 1300–1309.

(142) El-Sawy, E. R.; Bassyouni, F. A.; Abu-Bark, S. H., Rady, H. M.; Abdlla, M. M. *Acta Pharm.* **2010**, *60*, 55–71.

(143) Thompson, M. J.; Louth, J. C.; Ferrara, S.; Sorrell, F. J.; Irving, B. J.; Cochrane, E. J.; Meijer, A. J. H. M.; Chen, B. *ChemMedChem.* **2011**, *6*, 115–130.

(144) Makler, M. T.; Ries, J. M.; Williams, J. A.; Bancroft, J. E.; Piper, R. C.; Gibbins, B. L.; Hinrichs, D. J. *Am. J. Trop. Med. Hyg* **1993**, *48*, 739–741.